U.PORTO

DOUTORAMENTO EM CIÊNCIAS BIOMÉDICAS

The peroxisomal matrix protein import machinery – a PEX5-centered perspective

Ana Filipa Dias

D

2017

U.PORTO

Ana Filipa Dias. The peroxisomal matrix protein import machinery – a PEX5-centered perspective

The peroxisomal matrix protein import machinery – a PEX5-centered perspective

Ana Filipa Dias

D.ICBAS **2017**

INSTITUTO DE CIÊNCIAS BIOMÉDICAS ABEL SALAZAR

ANA FILIPA CARVALHO MARQUES DIAS

The peroxisomal matrix protein import machinery – a PEX5-centered perspective

Tese de Candidatura ao grau de Doutor em Ciências Biomédicas submetida ao Instituto de Ciências Biomédicas Abel Salazar da Universidade do Porto.

Orientador – Doutor Jorge Eduardo da Silva Azevedo
Categoria – Professor catedrático
Afiliação – Instituto de Ciências Biomédicas Abel Salazar da Universidade do Porto

Coorientadora – Doutora Maria de Fátima Matos Almeida Henriques de Macedo
Categoria – Professora auxiliar convidada, investigadora auxiliar
Afiliação – Departamento de Ciências Médicas da Universidade de Aveiro, Instituto de Investigação e Inovação em Saúde da Universidade do Porto

TABLE OF CONTENTS

PRECEITOS LEGAIS

A autora desta tese declara que interveio na concepção e execução do trabalho experimental, na interpretação e redacção dos resultados que, além de incluídos nesta tese, culminaram numa publicação internacional (artigo abaixo indicado), sob o nome de "**Dias AF**". Para além deste artigo, a autora declara ter também participado na elaboração de um artigo de revisão, do qual é primeira autora.

The author of this thesis declares to have participated in the planning and execution of the experimental work, in the interpretation and preparation of the data which, besides being included in this thesis, were published in an international journal, under the name "**Dias AF**". Moreover, the author declares to have also participated in the elaboration of a review paper as first author.

Dias AF, Rodrigues TA, Pedrosa AG, Barros-Barbosa A, Francisco T, Azevedo JE. The peroxisomal matrix protein translocon is a large cavity-forming protein assembly into which PEX5 protein enters to release its cargo. J Biol Chem. 2017. pii: jbc.M117.805044. doi: 10.1074/jbc.M117.805044. [Epub ahead of print]

Dias AF, Francisco T, Rodrigues TA, Grou CP, Azevedo JE. The first minutes in the life of a peroxisomal matrix protein. Biochim Biophys Acta. 2016. 1863(5):814-820. doi: 10.1016/j.bbamcr.2015.09.025.

Este trabalho foi financiado pela FCT - Fundação para a Ciência e a Tecnologia/ Ministério da Ciência, Tecnologia e Ensino Superior, no contexto de uma bolsa de doutoramento (referência SFRH/BD/87352/2012), apoiada por financiamento do Programa Operacional Potencial Humano (POPH) do Quadro de Referência Estratégico Nacional (QREN), e do Fundo Social Europeu (FSE). Este trabalho foi também financiado pelo FEDER - Fundo Europeu de Desenvolvimento Regional, através do COMPETE 2020 - Programa Operacional Competitividade e Internacionalização (POCI), Portugal 2020, e por fundos Portugueses, através da FCT, no contexto dos projectos FCOMP-01-0124-FEDER-019731-PTDC/BIABCM/118577/2010, POCI-01-0145-FEDER-007274 e PTDC/BEX-BCM/2311/2014, e através do Norte 2020 - Programa Operacional Regional do Norte, no contexto da aplicação NORTE-01-0145-FEDER-000008.

This work was financed by FCT - Fundação para a Ciência e a Tecnologia/ Ministério da Ciência, Tecnologia e Ensino Superior, under a PhD fellowship (SFRH/BD/87352/2012), supported by funding from Programa Operacional Potencial Humano (POPH) from Quadro de Referência Estratégico Nacional (QREN), and from Fundo Social Europeu (FSE). This work was also financed by FEDER - Fundo Europeu de Desenvolvimento Regional, through the COMPETE 2020 - Programa Operacional Competitividade e Internacionalização (POCI), Portugal 2020, and by Portuguese funds, through the FCT, in the framework of the projects FCOMP-01-0124-FEDER-019731-PTDC/BIABCM/118577/2010, POCI-01-0145-FEDER-007274 and PTDC/BEX-BCM/2311/2014, and through Norte 2020 - Programa Operacional Regional do Norte, under the application NORTE-01-0145-FEDER-000008.

AGRADECIMENTOS

Em primeiro lugar, quero agradecer ao Prof. Doutor Jorge Azevedo, um enorme obrigado! Obrigado por me ter recebido no seu grupo de investigação, obrigado pela orientação de excelência, pela transmissão de conhecimentos, acompanhamento constante e dedicação a este projecto. O seu espírito crítico e rigor científico são um verdadeiro exemplo a seguir.

À Doutora Fátima Macedo, agradeço o que me ensinou.

A todos os "OBF´s", actuais e antigos, quero agradecer os dias que partilhámos no laboratório, o que aprendemos uns com os outros, a boa disposição. Em especial, agradeço à Tânia e ao Tony, que me ajudaram de forma particular na fase final deste projecto. À Tânia, a sua mão amiga sempre presente. Ao Tony, a sua calma no dia-a-dia e saídas inesperadas que nos deixam a rir. À Pedrosa, os nossos estados de espírito partilhados. À Aurora, por me incentivar e desejar sempre "muita inspiração" na fase de escrita. À Cláudia, por "descomplicar", porque afinal "é para isso que serve ter um *PhD*". Ao Manel, por me ensinar "*if you can see it, you can clone it*"; revelou-se verdade, mesmo quando muito mal se via. À Andreia e ao Ricardo, de quem inevitavelmente me lembro quando ouço a música "*Radioactive*".

Quero agradecer aos em tempo "vizinhos do lado". À Cátia, os muitos cafés extra que tomou para me fazer companhia nos dias em que já almoçava fora de horas ou precisava de um chocolate. Ao Paulo, as palhaçadas e boa disposição constantes.

Às grandes amizades que fiz no Porto: Cátia, Marisa, Marta, Tânia e Gaspar. Obrigado por me ajudarem a ultrapassar as dificuldades com que me deparei. Obrigado pelas jantaradas, por todos os alegres momentos de partilha e convívio.

Aos meus amigos de outros portos, obrigado pela força e motivação que me deram.

Ao Zequinha, obrigado por estares tão perto, apesar dos muitos km de distância. A tua companhia é preciosa. Obrigado pelo teu apoio, pelas muitas madrugadas, por me incentivares e alegrares cada dia.

E porque "os últimos são sempre os primeiros", um agradecimento muito especial aos meus pais e irmãos. Obrigado pelo vosso apoio e carinho constantes, obrigado por me ensinarem a "dar o pontapé no *im*", obrigado por acreditarem sempre.

RESUMO

As proteínas da matriz peroxissomal sintetizadas *de novo* são reconhecidas, no citosol, pelos receptores PEX5 ou PEX5.PEX7. O complexo receptor-proteína matricial interage com a membrana do peroxissoma e insere-se a nível do módulo de *docking* e translocação (DTM), resultando na translocação da proteína matricial para o interior do organelo. Após este evento, os receptores são extraídos da membrana peroxissomal em dois passos. Primeiro, a PEX5 é monoubiquitinada num resíduo de cisteína filogeneticamente conservado (Cys11 em seres humanos). Segundo, a PEX5 monoubiquitinada (Ub-PEX5) é removida para o citosol, pelo módulo de exportação do receptor (REM), o que também leva à libertação da PEX7 do DTM. A extracção dos receptores da membrana peroxissomal é o único processo da via de importação das proteínas matriciais que requer a hidrólise de ATP. Uma vez no citosol, a Ub-PEX5 é desubiquitinada e a PEX5 solúvel pode participar num novo ciclo de transporte proteico.

Foi recentemente proposto que a PEX5 actua também como uma holdase, evitando interacções prematuras ou inespecíficas, das proteínas destinadas à matriz peroxissomal, no citosol. Neste trabalho, foi explorada esta função da PEX5. O domínio N-terminal da PEX5 preveniu a agregação da malato desidrogenase, bem como a inactivação da citrato sintase, induzidas pela temperatura, sugerindo que a PEX5 consegue actuar como uma holdase.

Uma propriedade interessante dos peroxissomas é a sua capacidade de importar proteínas oligoméricas. Isto revela que a maquinaria de importação das proteínas da matriz peroxissomal (PIM) consegue aceitar como substrato proteínas já detentoras de uma estrutura terciária. Uma das questões mais importantes relativas à PIM é de que forma é que isto acontece. Neste trabalho, foi utilizado um sistema de importação *in vitro* e diversas versões truncadas da PEX5, com o intuito de caracterizar a arquitectura do DTM. Descobrimos que o DTM consegue acomodar mais moléculas de uma versão truncada da PEX5 contendo os primeiros 197 aminoácidos (PEX5(1-197)) do que moléculas de PEX5 *full-length*. Uma versão truncada da PEX5 ainda mais curta (PEX5(1-125)) é também capaz de interagir correctamente com o DTM, no entanto, esta molécula permanece acessível à proteinase K adicionada do lado citosólico, sugerindo que a protease consegue aceder ao DTM quando este está ocupado por uma pequena molécula de PEX5. Curiosamente, a interacção PEX5(1-125)-DTM é inibida por uma PEX5 truncada contendo os resíduos 138 a 639. Aparentemente, o DTM consegue recrutar a PEX5 solúvel através de interacções com diferentes domínios da PEX5, sugerindo que as interacções entre o DTM e a PEX5 são, em certa medida, *fuzzy*. Finalmente, mostrámos que a interacção entre a PEX5 e a PEX14, um componente maioritário do DTM, é estável a pH 11.5. Assim, não é necessário assumir que

a resistência à extracção alcalina da PEX5 associada ao peroxissoma reflecte um contacto directo da PEX5 com os lípidos presentes na membrana. No seu conjunto, os resultados sugerem que o DTM é um complexo proteico que forma uma grande cavidade, na qual a PEX5 citosólica entra para entregar as proteínas da matriz peroxissomal.

ABSTRACT

Newly synthesized peroxisomal matrix proteins are recognized in the cytosol by the shuttling receptors PEX5 or PEX5.PEX7. The receptor-cargo complex then docks and inserts into the peroxisomal membrane at the docking/translocation module (DTM), resulting in the translocation of the cargo protein into the organelle matrix. Following this event, the shuttling receptors are extracted from the peroxisomal membrane in two steps. First, DTM-embedded PEX5 is monoubiquitinated at a strictly conserved cysteine residue (Cys11 in humans). Subsequently, monoubiquitinated PEX5 (Ub-PEX5) is dislocated back into the cytosol by the receptor export module (REM), a step that also triggers the release of PEX7 from the DTM. Recycling of receptors is the only process of the peroxisomal matrix protein import pathway that requires ATP hydrolysis. Once in the cytosol, Ub-PEX5 is deubiquitinated, and the free soluble PEX5 can participate in a new protein transport cycle.

Recently, it was proposed that PEX5 acts also as a holdase-like protein, avoiding premature or unspecific interactions of its cargo proteins in the cytosol. In this work, this role of PEX5 was explored. The N-terminal half of PEX5 prevented the thermal-induced aggregation of malate dehydrogenase and inactivation of citrate synthase, suggesting that PEX5 can act as a holdase-like protein.

An interesting property of peroxisomes is their ability to import oligomerized proteins, indicating that the peroxisomal matrix protein import machinery (PIM) can accept already folded proteins as substrates. One of the most important questions about the PIM is how this happens. In this work, an established cell-free organelle-based *in vitro* system and several truncated versions of PEX5 were used to probe the DTM architecture. We found that the DTM can accommodate a larger number of truncated PEX5 molecules comprising amino acid residues 1-197 than full-length PEX5 molecules. A shorter PEX5 version (PEX5(1-125)) still interacted correctly with the DTM; however, this species was largely accessible to exogenously added proteinase K, suggesting that this protease can access the DTM when this is occupied by a small PEX5 protein. Interestingly, the PEX5(1-125)-DTM interaction was inhibited by an import-competent polypeptide comprising PEX5 residues 138-639. Apparently, the DTM can recruit soluble PEX5 through interactions with different PEX5 domains suggesting that the PEX5-DTM interactions are to some degree fuzzy. Finally, we found that the interaction between PEX5 and PEX14, a major DTM component, is stable at pH 11.5. Thus, there is no reason to assume that the hitherto intriguing resistance of DTM-bound PEX5 to alkaline extraction reflects its direct contact with the peroxisomal lipid bilayer. Collectively, these results suggest that the DTM is best described as a large cavity-forming protein assembly into which cytosolic PEX5 can enter to release its cargo.

LIST OF ABBREVIATIONS

AAA	ATPases associated with diverse cellular activities
ACOX	Acyl-CoA oxidase
AMP-PNP	Adenylyl-imidodiphosphate
ATP	Adenosine triphosphate
BSA	Bovine serum albumin
CS	Citrate synthase
DLP1	Dynamin-like protein 1
DNA	Deoxyribonucleic acid
DTM	Docking/translocation module
DTT	Dithiothreitol
E2	Ubiquitin-conjugating enzyme
ER	Endoplasmic reticulum
Fis1	Fission factor 1
GDAP1	Ganglioside induced differentiation associated protein 1
HS	Heimler syndrome
IRD	Infantile Refsum disease
MDH	Malate dehydrogenase
Mff	Mitochondrial fission factor
NALD	Neonatal adrenoleukodystrophy
NDPEX14	N-terminal domain of PEX14
PAGE	Polyacrylamide gel electrophoresis
PBD	Peroxisome biogenesis disorder
PCR	Polymerase chain reaction
PEX	Peroxin
PIM	Peroxisomal matrix protein import machinery
PK	Proteinase K
PMP	Peroxisomal membrane protein
PNS	Post-nuclear supernatant
PTS	Peroxisomal targeting signal
PTS1	PTS type 1
PTS2	PTS type 2
RCDP	Rhizomelic chondrodysplasia punctata
REM	Receptor export module

RING	Really interesting new gene
RRL	Rabbit reticulocyte lysate
S. cerevisiae	*Saccharomyces cerevisiae*
SDS-PAGE	Sodium dodecyl sulfate - polyacrylamide gel electrophoresis
TPRs	Tetratricopeptide repeats
Ub-PEX5	Monoubiquitinated PEX5
UOX	Urate oxidase
VLCFAs	Very long-chain fatty acids
ZS	Zellweger syndrome
ZSD	Zellweger spectrum disorder

I - INTRODUCTION

1. Peroxisomes: structure and function

Peroxisomes are present in almost all eukaryotic cells. They were first observed in 1954 by Johannes Rhodin and named “microbodies”, a cytoplasmic body characterized by a single membrane and a finely granular matrix in electron microscopy (1). The designation “peroxisome” was introduced in 1965 by Christian de Duve to highlight their content in several hydrogen peroxide-producing oxidases and catalase, which dismutates the hydrogen peroxide to water and molecular oxygen (2, 3). In some cells, a remarkable electron-dense paracrystalline structure is easily detected. For example, in mouse/rat liver cells, a core of urate oxidase is frequently observed ((3–5); see Figure 1), and in yeast *Candida boidinii* a core of alcohol oxidase is also common (4). Unlike mitochondria and chloroplasts, peroxisomes are devoid of DNA (4, 6, 7). Usually, these organelles are spherical and range from 0.1-1 µm in diameter. They can, however, also adopt elongated tubular or short rod-shaped forms (4, 8). In fact, peroxisome morphology, size and abundance may vary according to the organism, tissue, cell type and even prevailing environmental conditions (reviewed in (4, 9, 10)).

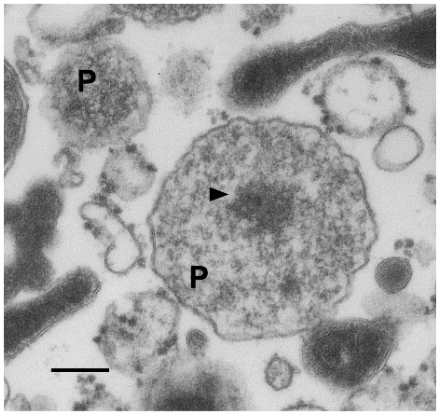

Figure 1. Peroxisomes. Electron micrograph showing peroxisomes (P) from a rat liver post-nuclear supernatant. A crystalline core of urate oxidase is marked (►). Scale bar 0.2 µm. Electron micrograph kindly taken by Prof. Dr. Manuel Teixeira da Silva, IBMC, Porto, Portugal.

Peroxisome functions are extremely diverse. While some functions are transversal and common to all kingdoms, others are very specialized and only found in a few organisms or cell types. Highly conserved functions are the metabolism of hydrogen peroxide (H_2O_2) and the β-oxidation of fatty acids (11, 12). The H_2O_2 is produced as a metabolic by-product of many peroxisomal oxidases. Its decomposition occurs mainly via catalase, the primary peroxisomal antioxidant enzyme and also the classical peroxisomal marker enzyme. Besides catalase, peroxisomes may contain other proteins capable of removing H_2O_2, such as peroxiredoxin V (PMP20) and glutathione peroxidase (13). β-oxidation is the main pathway of fatty acid degradation. In yeast and plants, it seems to be an exclusively peroxisomal

process. In mammals, the β-oxidation of medium and long-chain fatty acids occurs mainly in mitochondria with only a little contribution of the peroxisomal β-oxidation system (11). However, this system is critical for the β-oxidation of very long-chain fatty acids (VLCFAs) (11, 14, 15). In higher eukaryotes, peroxisomes are also important for the α-oxidation of fatty acids, biosynthesis of ether phospholipids (plasmalogens), detoxification of glyoxylate and synthesis of bile acids (11, 12, 14, 15). Some peroxisomes found in specific groups of organisms or tissues are so different and specialized that they were initially classified as distinct organelles and have alternative names. Peroxisomes from trypanosomatids of the genera *Trypanosoma* and *Leishmania* have the particularity of generally lacking catalase and are designated glycosomes since they contain most of the glycolytic enzymes (16, 17). Germinating fatty seedlings from higher plants have glyoxysomes, specialized peroxisomes that contain β-oxidation enzymes but also key enzymes of the glyoxylate cycle. The combined action of these enzymes allows glyoxysomes to convert the seed storage lipids into sugar, needed for seed germination and growth (18).

2. Peroxisome disorders

Peroxisomes are essential for human health and development. Their relevance is highlighted by the existence of a group of genetic diseases, the peroxisomal disorders, in which there is an impairment of peroxisomal function. Peroxisomal disorders are usually classified into two major groups: i) the peroxisomal single enzyme deficiencies, and ii) the peroxisome biogenesis disorders (19).

2.1. Peroxisomal single enzyme deficiencies

Peroxisomal single enzyme deficiencies are subdivided according to which specific peroxisomal function is compromised, namely: i) fatty acid β-oxidation, ii) fatty acid α-oxidation, iii) ether phospholipid (plasmalogen) biosynthesis, iv) glyoxylate detoxification, v) H_2O_2 metabolism, or vi) bile acid synthesis ((15, 19, 20); see Table 1).

The most common of these diseases is X-linked adrenoleukodystrophy (X-ALD), with an estimated incidence of 1:20000 to 1:30000 (21). X-ALD is caused by mutations in the *ABCD1* gene that encodes a peroxisomal transmembrane protein, the adrenoleukodystrophy protein (ALDP), needed for the β-oxidation of VLCFAs. ALDP deficiency results in the accumulation of VLCFAs in all tissues and leads to a progressive disease characterized by chronic myelopathy and peripheral neuropathy (22).

Table 1. The peroxisomal single enzyme deficiencies.

Peroxisomal function impaired	Peroxisomal disorder	Defective protein
Fatty acid β-oxidation	X-linked adrenoleukodystrophy	ALDP/ABCD1
	Acyl-CoA oxidase deficiency	ACOX1
	D-Bifunctional protein deficiency	DBP
	Sterol carrier protein x deficiency	SCPx
	2-Methylacyl-CoA racemase deficiency	AMACR
Fatty acid α-oxidation	Refsum disease	PHYH
Ether phospholipid biosynthesis	Rhizomelic chondrodysplasia punctata type 2	DHAPAT
	Rhizomelic chondrodysplasia punctata type 3	ADHAPS
	Rhizomelic chondrodysplasia punctata type 4	FAR1
Glyoxylate detoxification	Primary hyperoxaluria type 1	AGT
H_2O_2 metabolism	Acatalasemia	Catalase
Bile acid synthesis	Bile acid-CoA: amino acid N-acyltransferase deficiency	BAAT
	Acyl-CoA oxidase 2 deficiency	ACOX2
	ABCD3 (PMP70) deficiency	PMP70/ABCD3

Adapted from (23, 24). Abbreviations used: ALDP, adrenoleukodystrophy protein; ACOX1, acyl-CoA oxidase 1; DBP, D-bifunctional protein; SCPx, sterol carrier protein x; AMACR, 2-methylacyl-CoA racemase; PHYH, phytanoyl-CoA hydroxylase; DHAPAT, dihydroxyacetone phosphate acyltransferase; ADHAPS, alkyl dihydroxyacetone phosphate synthase; FAR1, fatty acyl-CoA reductase 1; AGT, alanine:glyoxylate aminotransferase; BAAT: Bile acid-CoA: amino acid N-acyltransferase; ACOX2, acyl-CoA oxidase 2; PMP70, 70-kDa peroxisomal membrane protein.

2.2. Peroxisome biogenesis disorders

Peroxisome biogenesis disorders (PBDs) are mainly caused by mutations in *PEX* genes, which encode peroxins, proteins involved in the biogenesis and maintenance of peroxisomes (19). Contrary to single enzyme deficiencies, in which one specific peroxisomal function is affected, in PBDs, several or all peroxisomal functions can be affected, and, in some cases, peroxisomes can be completely absent (19, 25).

The PBDs group includes Zellweger syndrome (ZS), neonatal adrenoleukodystrophy (NALD), infantile Refsum disease (IRD), Heimler syndrome (HS) (these four conditions belong to the so-called Zellweger spectrum disorders (ZSDs)), rhizomelic chondrodysplasia punctata (RCDP) type1 and type 5, and peroxisomal fission defects (19, 25, 26).

ZS is the most severe of the PBDs, being a fatal cerebro-hepato-renal syndrome. ZS patients are newborns with severe hypotonia, distinct craniofacial dimorphism, profound neurological abnormalities such as neuronal migration defects, hepatomegaly and renal cysts, and usually die before one year of age (19, 25). ZS is characterized by the absence of functional peroxisomes in cells and subsequent accumulation of peroxisomal substrates such

as VLCFAs, bile acid intermediates and phytanic acid in the plasma (25, 27, 28). NALD and IRD are less severe disorders resulting in a longer life span. NALD patients usually live until late infancy; they have hypotonia, seizures and progressive white matter disease. In patients with IRD, survival until adulthood is possible. IRD patients typically have retinopathy, hearing loss and psychomotor delay but do not show disordered neuronal migration or progressive white matter disease (19, 25). HS is the mildest PBD, with patients presenting hearing loss, abnormalities in teeth and nails, and sometimes retinal pigmentation. HS is characterized by a slight peroxisomal dysfunction (26).

RCDP type 1 is clinically distinguished from Zellweger spectrum disorders by prominent skeletal manifestations. RCDP type 1 patients have symmetrical shortening of the limbs (*i.e.*, rhizomelia), periarticular calcifications, cataracts, severe growth and mental deficiency, and, in the most severe cases, usually do not survive the first decade of life (19, 25). RCDP type 5 was recently described in four patients from two families. The phenotype of RCDP type 5 may include cataracts, postnatal growth delay, microcephaly, severe intellectual disability and chondrodysplasia punctata (29). In RCDP type 1 and type 5 disorders, only the function of a smaller subset of peroxisomal proteins (those containing a peroxisomal targeting signal type 2, see below) is compromised (29–32). RCDP type 1 and type 5 are characterized by the accumulation of phytanic acid, but not VLCFAs, in plasma from patients (29, 33).

Peroxisomal fission defects were reported in a very small number of patients, one of them presenting ZSD-like symptoms but, strikingly, normal biochemical peroxisomal parameters (19) (see below).

Whereas RCDP type 1 and type 5 are caused by mutations in *PEX7* and very specific mutations in *PEX5*, respectively (29–32), Zellweger spectrum disorders are caused by mutations in any of different *PEX* genes, including *PEX 1*, *2*, *3*, *5*, *6*, *10*, *12*, *13*, *14*, *16*, *19* and *26* ((19, 25, 26); see Table 2). Defects in most of them result in peroxisomal vesicles containing peroxisomal membrane proteins but devoid of matrix proteins, the so-called peroxisomal membrane ghosts, reflecting that the encoded peroxins are involved in the import of peroxisomal matrix proteins (34, 35). Defects in *PEX3*, *PEX16* or *PEX19*, however, result in the complete absence of peroxisomal vesicles, implying that the encoded peroxins are essential for the peroxisomal membrane biogenesis (36–40).

Peroxisomal fission defects are associated with mutations in *PEX11β*, *DLP1*, *Mff* or *GDAP1* genes. While a mutation in *PEX11β* results in elongated peroxisomes (41), a mutation in *DLP1*, *Mff* or *GDAP1* results in cells with elongated or tubular peroxisomes and mitochondria (19). Proteins encoded by the three latter genes are required for the division of both peroxisomes and mitochondria, and so, for this reason they are not classified as peroxins.

Table 2. Peroxisome biogenesis disorders – correlation between mutated *PEX* gene, peroxisomal disorders and pathway affected.

***PEX* gene mutated**	**Peroxisomal disorder**	**Pathway affected**
PEX1	ZSDs	Import of matrix proteins
PEX2	ZSDs	Import of matrix proteins
PEX3	ZSDs	Import of membrane proteins
PEX5	ZSDs, RCDP type 5	Import of matrix proteins
PEX6	ZSDs	Import of matrix proteins
PEX7	RCDP type 1	Import of PTS2 matrix proteins
PEX10	ZSDs	Import of matrix proteins
PEX11β	Peroxisomal fission defect	Proliferation of peroxisomes
PEX12	ZSDs	Import of matrix proteins
PEX13	ZSDs	Import of matrix proteins
PEX14	ZSDs	Import of matrix proteins
PEX16	ZSDs	Import of membrane proteins
PEX19	ZSDs	Import of membrane proteins
PEX26	ZSDs	Import of matrix proteins

Adapted from (25). Abbreviations used: ZSDs, Zellweger spectrum disorders; RCDP, rhizomelic chondrodysplasia punctate; PTS2, peroxisomal targeting signal type 2.

3. Peroxisome biogenesis

Peroxisome biogenesis requires the concerted action of many proteins, most of which, but not all, are peroxins. To date, 35 peroxins have been identified among the several studied organisms (42–46). In mammals, however, only sixteen have been reported ((47); see Table 3). This discrepancy might suggest that there are mammalian peroxins with highly divergent sequences that were not identified yet by homology searching in databases. However, this is probably not the case. For instance, in *Saccharomyces cerevisiae*, due to an ancient whole-genome duplication event, several pairs of *PEX* genes performing the same or similar function are present. This is the case of PEX18 and PEX21, and PEX5 and PEX9 (42, 48). This large redundancy is not found in mammals. Furthermore, some orthologue peroxins have received different names for historical reasons because their functional/structural homology was not perceived when they were first identified. For instance, PEX18 and PEX21 from *S. cerevisiae* are actually equivalent to PEX20 from other yeasts and filamentous fungi. Additionally, the function of some peroxins not present in mammals was actually transferred to other peroxins or even to non-peroxin proteins. This is the case of PEX18, PEX21 and PEX20 from lower eukaryotes, the function of which is performed by PEX5 in higher

eukaryotes, or the situation for yeast and plant ubiquitin-conjugating enzyme (E2), PEX4, and its membrane anchor, PEX22, the function of which is carried out by mammalian E2D1/2/3, three multipurpose E2 enzymes involved in a myriad of other biological pathways (see below). Thus, it is likely that all, or almost all, genes encoding components of the mammalian peroxisomal matrix protein import machinery (PIM) were already identified. If so, then we can conclude that evolution led to simpler peroxisome biogenesis machineries (42, 44). Importantly, despite the large species-specific differences, the mechanistic features of peroxisomal biogenesis have been conserved throughout evolution.

Peroxins are usually divided into three groups, according to their roles in peroxisome biogenesis: i) assembly of the peroxisomal membrane, ii) import of matrix proteins into the organelle, and iii) peroxisome proliferation ((47); see Table 3).

Table 3. Localization, properties and functions of mammalian peroxins.

Pathway	Peroxin	Localization	Properties / Functions
Import of membrane proteins	PEX3	Perox	Intrinsic PMP
	PEX16	Perox	Intrinsic PMP
	PEX19	Cyt/Perox	Farnesylation motif; PMP receptor
Import of matrix proteins	PEX1	Perox	Peripheral PMP, AAA ATPase; receptor export
	PEX2	Perox	Intrinsic PMP, RING Zn^{2+}-binding domain; E3
	PEX5	Cyt/Perox	IDD, TPRs; PTS1 and PTS2 receptor
	PEX6	Perox	Peripheral PMP, AAA ATPase; receptor export
	PEX7	Cyt/Perox	WD-repeats; PTS2 adaptor receptor
	PEX10	Perox	Intrinsic PMP, RING Zn^{2+}-binding domain; E3
	PEX12	Perox	Intrinsic PMP, RING Zn^{2+}-binding domain; E3
	PEX13	Perox	Intrinsic PMP, SH3 domain
	PEX14	Perox	Intrinsic PMP, Coiled-coil domain
	PEX26	Perox	Intrinsic PMP, PEX1/PEX6 membrane anchor
Proliferation of peroxisomes	PEX11β	Perox	Intrinsic PMP
	PEX11α	Perox	Intrinsic PMP
	PEX11γ	Perox	Intrinsic PMP

Adapted from (25). Abbreviations used: Perox, peroxisome; PMP, peroxisomal membrane protein; Cyt, cytosol; AAA, ATPases associated with diverse cellular activities; RING, really interesting new gene; E3, ubiquitin ligase; IDD, intrinsically disordered domain; TPRs, tetratricopeptide repeats; PTS1, peroxisomal targeting signal type 1; PTS2, peroxisomal targeting signal type 2; WD, tryptophan-aspartate repeat; SH3, Src homology 3.

Since peroxisomes do not contain DNA or ribosomes, all peroxisomal proteins are encoded by nuclear genes, synthesized in the cytoplasm and post-translationally transported

to the organelle (49–52). Peroxisomal membrane proteins and matrix proteins are sorted to peroxisomes by different and independent machineries, presented in sections I-3.1.1. and I-3.2., respectively.

3.1. Peroxisomal membrane biogenesis

The origin of the peroxisomal membrane has continuously been a subject of debate in the field. Two different models have been proposed: the “growth and division model”, which proposes that mature peroxisomes divide giving rise to smaller new organelles, and the “*de novo* formation model”, which proposes that peroxisomes are a branch of the secretory pathway and, therefore, that their membrane derives from the endoplasmic reticulum (ER) (reviewed in (3, 4, 53–56)). Initial studies, based on electron microscopy, showed peroxisomes surrounded by the ER, and pointed to the idea that peroxisomes are formed by budding from the ER (3). Subsequent data indicating that peroxisomal matrix and membrane proteins are synthesized on free cytosolic ribosomes and post-translationally imported into peroxisomes, introduced the idea that peroxisomes are autonomous organelles capable of proliferating by growth and division of pre-existing ones (4, 49–52). However, the observation that in mutant cells lacking any peroxisomal vesicle (with defects in PEX3, PEX16 or PEX19 peroxins), peroxisomes can form *de novo* upon introduction of the wild-type peroxin, gave again some momentum to the ER-derived model (36–39). This momentum was lost, however, a few years later when it was shown that yeast *pex3* mutant cells do contain some membrane structures (formed independently of PEX3) possessing PEX13 and PEX14 and also some matrix proteins. When the *PEX3* gene is reintroduced in these cells, PEX3 protein sorts directly to the preperoxisomal structures, which then mature into normal peroxisomes (57). Thus, presently, the “growth and division” model seems more appealing to many researchers. But this does not mean that a consensus on this issue has been reached. Far from that, as illustrated, for instance, by a recent study proposing that mammalian peroxisomes form *de novo* through the fusion of mitochondrial- and ER-derived vesicles ((58), see also (56) for a discussion of this finding).

Regardless of the true origin for the peroxisomal membrane, it is obvious that its assembly requires both the incorporation of new lipids and the insertion of membrane proteins into the lipid bilayer. Considering that cells synthesize membrane lipids mostly in the ER, and that contact sites between ER and peroxisomes have been observed (59–61), it is reasonable to assume that peroxisomes receive most of their membrane lipids from the ER.

3.1.1. Import of membrane proteins into the organelle

In mammals, the sorting of peroxisomal membrane proteins (PMPs) to the organelle requires PEX19, PEX3 and PEX16 peroxins (36–40). Newly synthesized PMPs have a

membrane peroxisomal targeting signal (reviewed in (62)) which is recognized by soluble PEX19 (63, 64). PEX19 behaves as a chaperone-like protein; it interacts with the hydrophobic domains of PMPs and prevents their aggregation in the cytosol (64–66). Moreover, PEX19 functions as import receptor and transports the PMPs to the organelle (67, 68). At the peroxisomal membrane, PEX19 interacts with the docking protein PEX3, and in some way, this event results in the insertion of the PMP into the lipid bilayer, without ATP consumption (52, 68–70). One hypothesis is that, after docking, the cytosolic PEX19-interacting domain of PEX3 adopts a different conformation and binds membrane lipids causing the release of PEX19 back to the cytosol and the insertion of PMP into the peroxisomal membrane (71, 72). Regarding PEX16, its function in biogenesis is still unclear. Even though PEX16 is essential for mammalian peroxisomal membrane biogenesis, this peroxin is absent in yeasts with exception of *Yarrowia lipolytica* (73). Although many PMPs are sorted to the organelle through this pathway (74), PEX3 seems to be an exception. Indeed, *in vitro* and *in vivo* studies have shown that PEX3 inserts into the ER, and, therefore, some authors believe that PEX3 reaches peroxisomes via budding vesicles (75, 76).

3.2. Import of matrix proteins into the organelle

In mammals, the PIM includes 10 peroxins organized in three functional/structural units: 1) the shuttling receptors for newly synthesized matrix proteins destined for the organelle, PEX5 and PEX5.PEX7 complex (30, 77, 78); 2) the peroxisomal membrane docking/translocation module (DTM), comprising PEX14, PEX13 and the really interesting new gene (RING) finger proteins PEX2, PEX10 and PEX12 (79–81); and 3) the receptor export module (REM) that comprises the two AAA ATPases PEX1 and PEX6, and their membrane anchor PEX26 (82–84). In addition to these 10 peroxins, the mammalian PIM includes a few other proteins most of which are involved in ubiquitin conjugation and deconjugation (85, 86).

The import of peroxisomal matrix proteins comprises five main events, namely (see Figure 2): 1) recognition of the cytosolic peroxisomal matrix protein (cargo protein) by the shuttling receptor(s); 2) docking of the receptor-cargo complex at the peroxisomal membrane; 3) insertion of the complex into the organelle membrane, resulting in the release of cargo protein into the organelle matrix; 4) monoubiquitination of DTM-embedded PEX5, and; 5) dislocation of monoubiquitinated PEX5 back into the cytosol, followed by its deubiquitination. A detailed description of each of these events is presented below.

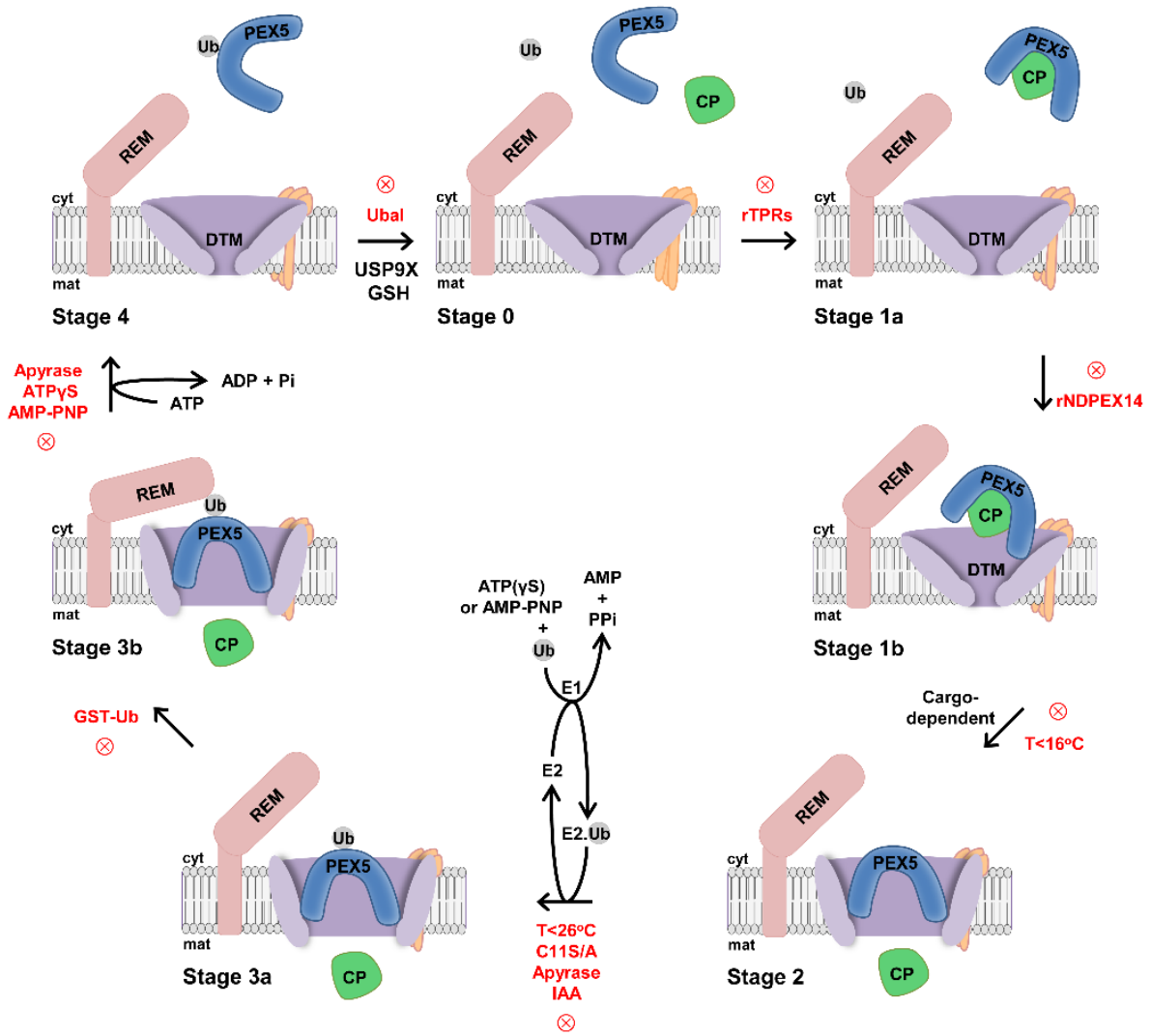

Figure 2. Peroxisomal matrix protein import cycle in mammals. For simplicity, the import pathway is described using a PEX5-centered perspective, so PEX7 is not represented (note that during most of the stages of the PEX5.PEX7-mediated import pathway, PEX7 remains bound to PEX5). Cytosolic PEX5 (stage 0) recognizes newly synthesized peroxisomal matrix proteins – cargo proteins (CP; stage 1a). Then, the receptor-cargo complex docks (stage 1b), and in a cargo- and temperature-dependent event, gets inserted at the docking/translocation module (DTM; stage 2). The insertion of PEX5 results in the release of the cargo protein into the organelle matrix. DTM-embedded PEX5 is monoubiquitinated (stage 3a), recognized by the receptor export module (REM; stage 3b), and dislocated back into the cytosol in an ATP-dependent process. Cytosolic monoubiquitinated PEX5 (stage 4) is deubiquitinated, most likely by a combination of enzymatic (USP9X) and non-enzymatic (*e.g.*, GSH) mechanisms, yielding cytosolic free PEX5 (stage 0). Diverse strategies/tools to block this pathway at different and specific steps (shown by red ⊗ symbol) are indicated. Abbreviations used: cyt, cytosol; mat, peroxisomal matrix; CP, cargo protein; DTM, docking/translocation module; Ub, ubiquitin; E1, ubiquitin-activating enzyme; E2, ubiquitin-conjugating enzyme; ATPγS, adenosine 5'[γ-thio]triphosphate; PPi, pyrophosphate; REM, receptor export module; Pi, inorganic phosphate; USP9X, ubiquitin-specific protease 9X; GSH, glutathione; TPRs, recombinant protein comprising only the PEX5 tetratricopeptide repeats domain; NDPEX14, recombinant protein comprising the soluble N-terminal domain of PEX14; T, temperature; C11S/A, PEX5 protein-mutated version with the conserved cysteine 11 replaced by a serine or an alanine residue, respectively; IAA, iodoacetamide; GST-Ub, glutathione S-transferase ubiquitin fusion protein; Ubal, ubiquitin aldehyde. Adapted from (87).

3.2.1. Cargo recognition by shuttling receptors

A newly synthesized peroxisomal matrix protein must have a peroxisomal targeting signal (PTS) in order to be correctly targeted to the organelle. The vast majority of matrix proteins have a PTS type 1 (PTS1), a C-terminal tripeptide, with the sequence serine-lysine-leucine (S-K-L) or conservative variants ((S/A/C)-(K/R/H)-(L)) (88–90). In some cases, the residues upstream of the tripeptide are also important for import (90–93). A small number of matrix proteins lack a PTS1 and have instead a PTS type 2 (PTS2). This is a degenerated nonapeptide with the consensus sequence R-(L/V/I/Q)-X-X-(L/V/I/H)-(L/S/G/A)-X-(H/Q)-(L/A), present at the N-terminus of the protein (94–96). The PTS2 is generally cleaved in the peroxisomal matrix of higher eukaryotes by a specific protease (Tysnd1 in mammals; (97)) (98), contrary to the PTS1, which is not processed upon import.

In the cytosol, PTS1-containing proteins are recognized by the shuttling receptor PEX5, which specifically targets them to the peroxisome (77, 78, 99, 100). PEX5 is a monomeric protein with a natively unfolded N-terminal half followed by a globular C-terminal domain comprising seven tetratricopeptide repeats (TPRs) (see section I-3.2.3.). The TPR domain interacts directly with the PTS1, and this is the most important binding interface between PEX5 and PTS1-containing proteins (99, 101–103), although the N-terminal domain of PEX5 also contributes for the interaction with these cargo proteins (104–107).

The recognition of PTS2-containing proteins is quite different and requires a protein complex comprising PEX5 and PEX7. PEX7 is a WD-repeat protein that interacts with the PTS2 (30, 108–110) and acts as an adaptor factor of PEX5 in the interaction with the PTS2-containing proteins (111–113). PEX5 binds PEX7 and, taking into account a recent structure of a trimeric complex between yeast PEX7, a PTS2 protein and PEX21 (the yeast orthologue of mammalian/plant PEX5 in the PTS2-mediated protein import pathway) (114), as well as biochemical data (115, 116), it is likely that PEX5 also interacts directly with the PTS2.

In lower eukaryotes, PEX5 is only involved in the PTS1-mediated protein import pathway and PTS2 proteins are transported to the organelle by a complex comprising PEX7 and a species-specific PEX5-like protein (117, 118). These PEX5-like proteins (*i.e.*, PEX18, PEX21 and PEX20), not only display similar functions but also share structure similarities with the N-terminal domain of mammalian PEX5 (119, 120).

A small number of peroxisomal matrix proteins lack either PTS1 or PTS2 within their polypeptide chain, but, are still targeted to the peroxisomes in a PEX5-dependent manner. In some cases, it is possible that there are internal signals in the proteins that interact with the N-terminal domain of PEX5 (104). The other possibility is that these proteins are imported "piggy-backed" with other proteins that do have a PTS (121–123).

The PTS receptors, PEX5 and PEX7, show a dual subcellular localization, both are predominantly cytosolic with a small population found associated with the peroxisome (77,

100, 108, 124, 125). This dual distribution is at the basis of the so-called shuttling receptor model. According to this concept, PEX5 and PEX7 cycle between the cytosol and the peroxisome, thus, delivering newly synthesized (cytosolic) cargo proteins to the organelle (100, 108).

3.2.2. PEX5 as a holdase-like protein

An interesting property of peroxisomes is their ability to import already oligomerized proteins (reviewed in (126, 127)). Even though studies supporting the import of oligomerized proteins are plentiful, this route may not be that frequent. Actually, many peroxisomal matrix proteins that are oligomeric in their native state seem to arrive at the organelle matrix still as monomers. The earlier experimental evidences supporting this idea come from pulse-chase analysis (128). It was demonstrated that rat liver catalase – a tetrameric protein in its native state – is synthesized in the cytosol and subsequently transferred to peroxisomes (with a half-time of import of 14 min), where it appears as a monomeric protein. The oligomerization of catalase occurred within the peroxisomes (128). Similar experiments revealed that alcohol oxidase from *Candida boidinii* – an octameric protein – remains in a monomeric state in the cytosol and oligomerizes only after import into peroxisomes (129, 130). Other experimental evidences come from *in vitro* import assays, where the import efficiencies of monomeric and oligomeric versions of the same protein were compared. The monomeric form of isocitrate lyase from *Cucurbita pepo* – a tetrameric protein – was found to be a better peroxisomal import substrate than the corresponding oligomeric form (131). For mouse acyl-CoA oxidase 1 (ACOX1) – a dimeric protein – and urate oxidase (UOX) – a tetrameric protein – the same preference was observed. In fact, specific peroxisomal import of the oligomeric proteins was not detected (132). Some additional observations support the idea that peroxisomal matrix proteins arrive at the organelle matrix as monomers. For example, there are peroxisomal matrix proteins that no longer interact with the receptor PEX5 upon oligomerization because their PTS1 is no longer exposed; apparently, these proteins have to stay monomeric to bind PEX5 and thus be transported to peroxisomes (133–135). Also, at least in rat hepatocytes, there is enough cytosolic PEX5 to interact with all newly synthesized peroxisomal proteins that are *en route* to the organelle (107). Additionally, PEX5 binds monomeric human catalase and mouse ACOX1 and UOX, strongly inhibiting their oligomerization (107, 132). The latter two observations led to the proposal that PEX5 is a holdase-like protein that binds newly synthesized monomeric peroxisomal matrix proteins and prevents premature or incorrect interactions in the cytosol (107, 132).

There are, however, three examples where peroxisomes seem to import oligomeric proteins. These are rat liver Cu/Zn superoxide dismutase 1 (121), the two isoforms of human lactate dehydrogenase (122) and the yeast nicotinamidase Pnc1p (123). All these proteins

lack either a PTS1 or a PTS2 within their polypeptide chain, and seem to reach the peroxisomal matrix “piggy-backed” with specific partners that do have a PTS. Importantly, import of these oligomers seems to be a rather low efficiency process because a large fraction of them is actually found in the cytosol under steady-state conditions.

3.2.3. PEX5 – structural and functional relationships

PEX5 is present in all organisms containing peroxisomes. In mammals, the *PEX5* transcript undergoes alternative splicing to produce two main PEX5 isoforms, a larger (PEX5L) and a smaller (PEX5S) one. These two proteins differ by 37 amino acids, which actually form the PEX7-binding domain. This means that only PEX5L has the ability to interact with PEX7 and, thus, to target PTS2-containing proteins to the peroxisomal matrix (111, 112, 119). In lower eukaryotes, PEX5 lacks the PEX7-binding domain and is, therefore, only involved in the PTS1-mediated protein import pathway (136, 137).

PEX5 is a 70-kDa monomeric protein (138), structural and functionally divided into two domains, the N-terminal and C-terminal halves, respectively (see Figure 3).

As mentioned above, the C-terminal half of PEX5 is a globular domain and comprises seven tetratricopeptide repeats (TPRs) involved in recognition of PTS1-containing proteins. TPRs 1-3 and TPRs 5-7 form two clusters separated by TPR4, a α-helix of 21 residues, that corresponds to a “hinge” region. The crystal structures of the C-terminal half of PEX5 in complex with a PTS1-containing peptide or with a functional PTS1 protein show that the two clusters of TPRs create a groove that is the binding site for PTS1. When the cargo protein is not bound to TPRs, structural changes occur with TPRs which then presents an open “snail-like” conformation (99, 101, 102, 139).

The N-terminal domain of PEX5 is natively unfolded (140); it includes regions of interaction with three other peroxins of the PIM. These are PEX7 (in mammals and plants; (111, 112, 119, 141)), PEX14 and PEX13. The interaction of mammalian PEX5 with PEX14 involves multiple sites present at the N-terminal half of PEX5. There are such eight sites, seven of which are the so-called di-aromatic pentapeptide repeats – the WXXXF/Y motifs – and another which presents the sequence LVXEF (142–146). All these motifs bind individually to PEX14 with high affinity (dissociation constants in the low nanomolar range) (142, 146). PEX5 binds mainly to the conserved N-terminal domain of PEX14 (143). The interaction of mammalian PEX5 with PEX13 also involves the WXXXF/Y motifs. Specifically, motifs 2 to 4 were implicated in PEX5 binding to the N-terminal domain of PEX13 (145). Additionally, PEX5 also interacts with the Src homology 3 (SH3) domain present at the C-terminal region of PEX13 (138). In addition to these pentapeptide repeats, the N-terminal domain of PEX5 contains a strictly conserved cysteine residue near its N-terminus (Cys11 in

humans). As described later (see section I-3.2.5.), this cysteine residue is transiently monoubiquitinated during import of peroxisomal matrix proteins (147, 148).

While the C-terminal half of PEX5 is highly conserved among species, the N-terminal half is poorly conserved, with the exception of di-aromatic pentapeptide repeats and cysteine residue referred to above (101, 112, 143, 149).

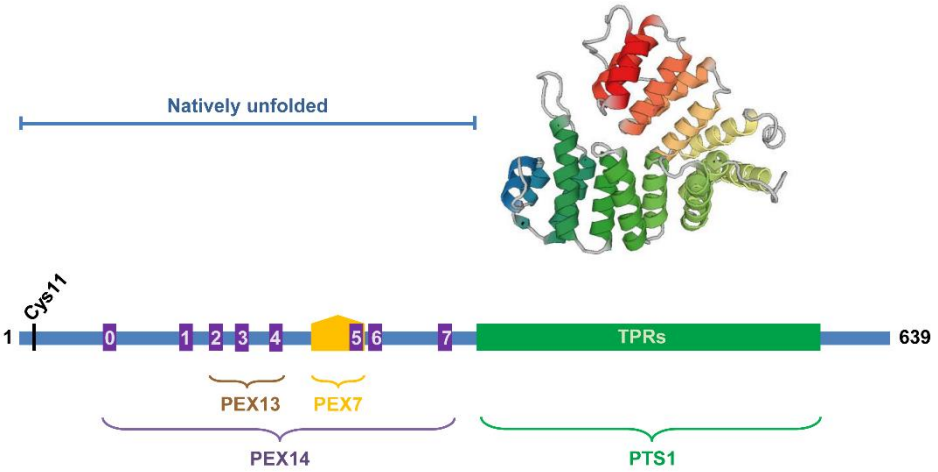

Figure 3. Structure and functional components of mammalian PEX5. The large isoform of mammalian PEX5 is schematically represented. The conserved cysteine residue at position 11 (Cys11) is marked; purple bars indicate the pentapeptides motifs (LVXEF (0) and WXXXF/Y (1-7)) responsible for the interaction with PEX14 and PEX13; the yellow box indicates the PEX7-binding domain, only present in PEX5L (absent in PEX5S); the green box represents the seven tetratricopeptide repeats (TPRs), the PTS1-binding domain. A crystal structure of the TPRs is shown above (PDB ID: 1FCH), the colors range from red to green, corresponding to TPRs 1 to 7.

3.2.4. Docking and insertion of the receptor-cargo complex into the DTM and cargo release

After cargo recognition in the cytosol, PEX5 interacts with the docking/translocation module (150–152). As previously mentioned, the DTM comprises PEX14, PEX13 and the RING finger proteins PEX2, PEX10 and PEX12, all peroxisomal transmembrane proteins (79, 81). The overall architecture of this protein complex remains unknown. From all these components, at least PEX14 and PEX13 have the ability to form homo-oligomers (81, 144, 153–155) and to interact with the N-terminal domain of PEX5 (see section I-3.2.3.). Thus, these two proteins are most likely the main components of the peroxisomal protein translocon (reviewed in (156, 157)).

The interaction between the receptor-cargo complex and the DTM happens in two distinct steps: docking followed by insertion. Docking of the PEX5-cargo protein complex at the organelle surface is a reversible step that can occur even at low temperatures (0 ºC) (152). On the contrary, its insertion is only observed at higher temperatures (> 16 ºC) and is an irreversible event in the absence of ATP (152, 158). Importantly, this insertion step is

cargo-dependent, meaning that it only occurs when PEX5 is in complex with a cargo protein (150). Strikingly, truncated versions of PEX5 lacking the TPRs, as well as a PEX5 protein with the N526K mutation that abrogates its PTS1-binding activity, are capable of inserting into the DTM (102, 150, 159). These and other observations led to the proposal that the insertion of PEX5 into the peroxisomal membrane is a process regulated by PEX5 itself (150, 159). According to this model, the C-terminal half of PEX5 is a cis-acting repressor of the N-terminal DTM-interacting domain of PEX5. Repression is abolished when PEX5 binds a cargo protein (see (160)).

When PEX5 becomes inserted into the DTM, it acquires a transmembrane topology, exposing most of its polypeptide chain into the organelle matrix, and only a small 2-kDa fragment of its N-terminus into the cytosol. This finding suggests that cargo proteins are translocated across the peroxisomal membrane by their own receptor (151, 161). The insertion/cargo-translocation step is ATP-independent, since ATP-depleted conditions (such as the presence of non-hydrolysable ATP analogs or treatment with ATP-diphosphohydrolases) do not compromise insertion of PEX5 into the peroxisomal membrane (162) nor the translocation of PTS1- and PTS2-containing proteins into the organelle matrix (152, 163). This observation, together with data showing that ionophores have no effect on protein import into peroxisomes (163–165), suggest that the protein-protein interactions established between PEX5 and the components of the DTM are the driving force for cargo protein translocation across the peroxisomal membrane (162, 166).

Interestingly, cargo release from DTM-bound receptor into the organelle matrix is also ATP-independent. Possibly, PEX5(.PEX7) suffer(s) DTM-induced conformational alterations that decrease their cargo-binding affinity and thus enable the release of cargo into organelle matrix (107, 116, 167).

Once the cargo protein is in its final destination, the receptor PEX5 has to be extracted from the peroxisomal membrane in order to participate in a new protein transport cycle. The extraction of PEX5 comprises two distinct events: 1) monoubiquitination of PEX5, and 2) its dislocation back into the cytosol.

3.2.5. Monoubiquitination of PEX5

PEX5 is monoubiquitinated during its transient passage through the peroxisomal membrane (147, 148). As previously mentioned, DTM-embedded PEX5 exposes into the cytosol a 2-kDa N-terminal domain (151). This small domain includes the highly conserved cysteine residue (Cys11 in human PEX5) that is the acceptor of ubiquitin (147, 148). Monoubiquitination of PEX5 depends on the ubiquitin-conjugating cascade, which comprises: an ubiquitin-activating enzyme (E1), an ubiquitin-conjugating enzyme (E2) and an ubiquitin ligase (E3) (168). In mammals, the E2 activity is provided by cytosolic E2D1/2/3 (UbcH5a/b/c

in humans) (85). These are three multipurpose E2s involved in many other biological pathways (169, 170). Yeast, other fungi and plants, contrary to mammals, have a peroxisomal E2. This is PEX4, which is anchored by PEX22 to the peroxisomal membrane (148, 171–174). The E3 activity is attributed to the DTM RING finger peroxins PEX2, PEX10 and PEX12 (175–178), which contain RING Zn^{2+}-binding domains that define the largest class of E3 ligases (179). However, the exact role of each one of these peroxins in this event remains unknown.

Generally, ubiquitin is attached to a lysine residue of a substrate protein via an isopeptidic bond involving the carboxyl-terminus of ubiquitin and the ε-amine group of that lysine (168). As stated above, monoubiquitination of PEX5 occurs at a cysteine residue, via a thioester bond (147). The reason why PEX5 is ubiquitinated at a cysteine is still not well understood. An engineered PEX5 having a lysine at position 11 (instead of the cysteine) is able to insert into the DTM, acquire an ubiquitin and be dislocated to the cytosol as efficiently as wild-type PEX5 (180). Therefore, some hypotheses have been formulated suggesting an additional function/regulatory role for the conserved cysteine. Experimental evidence has been provided showing that Cys11 in human PEX5 functions as a redox switch, regulating PEX5 activity (and, thus, the cytosolic/peroxisomal localization of peroxisomal proteins) in response to intracellular oxidative stress (181, 182). It is possible that compromising the import of newly synthesized peroxisomal matrix proteins (such as catalase), is advantageous to the cell under oxidative stress conditions in the cytosol (10, 180, 181). Another possible explanation for the ubiquitination at a cysteine residue is that it might prevent the degradation of cytosolic ubiquitinated PEX5 by the ubiquitin-proteasome pathway (180, 183). Indeed, the extreme lability of the thioester bond linking ubiquitin to PEX5 under physiological conditions may decrease the probability of monoubiquitinated PEX5 being polyubiquitinated and targeted to the proteasome.

Monoubiquitination of PEX5 is absolutely mandatory for the next step of the pathway – the dislocation of PEX5 back into the cytosol (147, 184). Indeed, N-terminal truncated version of PEX5 without the first 17 amino acid residues (lacking the conserved Cys11) (158), as well as PEX5 with the Cys11 replaced by an alanine (a non-ubiquitinatable residue), are both unable to return to the cytosol (159).

3.2.6. PEX5 dislocation to the cytosol

Dislocation of monoubiquitinated PEX5 (Ub-PEX5) is an ATP-hydrolysis dependent event (162) and is mediated by the receptor export module, which comprises the two AAA ATPases PEX1 and PEX6, and their membrane anchor PEX26 (82–84). Some data suggesting that AWP1, an ubiquitin-binding protein, is also a component of the REM are also available (185). This step is very fast in the presence of ATP (158, 186). However, the

mechanistic details of how Ub-PEX5 is recognized by the REM and how its mechanoenzymes dislocate Ub-PEX5 back into the cytosol are not yet understood. It is possible that the ubiquitin in the DTM-embedded Ub-PEX5 activates the REM by providing a context-specific protein interface. In fact, monoubiquitination of PEX5 with a GST-Ub fusion protein, a bulky ubiquitin analog, blocks completely the export of PEX5 (147). This might suggest that the Ub-PEX5 recognition by the REM includes a direct interaction between ubiquitin and the REM. Nevertheless, other interactions with the REM may occur. Indeed, it was recently proposed that PEX14 and PEX5 can also interact directly with REM (187).

Recently, the structure of yeast PEX1/PEX6 complex has been determined (188–190). The two AAA ATPases form a heterohexamer composed by a trimer of PEX1/PEX6 dimers (188–191). However, the available data are not enough to reveal how this complex works (reviewed in (191)). Nevertheless, by analogy with other AAA ATPases it was suggested that the substrate of the REM is moved through the central pore of the PEX1/PEX6 complex (191). In agreement with that hypothesis, a recent study showed that PEX5 fused to a tightly folded, bulky, C-terminal tag (EGFP), is monoubiquitinated in the DTM and is a substrate for the REM. However, PEX5-EGFP is only partially extracted from the peroxisomal membrane. Indeed, it was shown that the Ub-PEX5 portion of Ub-PEX5-EGFP is exposed into the cytosol whereas the EGFP moiety and some PEX5 C-terminal residues remained associated with the organelle, probably blocked at the REM. Thus, the presence of the tightly folded tag at the C-terminus of PEX5 compromises its export, presumably because the REM cannot thread tightly folded domains (192).

Extraction of PEX5 from the DTM is the only process of the peroxisomal matrix protein import pathway that needs ATP hydrolysis (162). Thus, unlike other protein import machineries that use the energy input from ATP/GTP hydrolysis for the vectorial transport proteins through a membrane (193, 194), the PIM consumes energy not for the protein translocation process, but rather to reset the protein transport pathway.

3.2.7. Deubiquitination of PEX5

Once in the cytosol, Ub-PEX5 is deubiquitinated, most likely by a combination of enzymatic and non-enzymatic mechanisms (180). The first, is probably carried out by ubiquitin-specific protease 9X (USP9X), the most active mammalian deubiquitinase acting on soluble Ub-PEX5 (86). The second may involve nucleophiles, such as glutathione. Indeed, it was shown that the thioester bond linking ubiquitin to PEX5 is easily disrupted by physiological concentrations of glutathione (180). Since Ub-PEX5 was never detected in cytosolic fractions obtained from rat liver or yeast cells, its deubiquitination is possibly very fast *in vivo* (148, 180).

Deubiquitination of PEX5 is the last step of the import of peroxisomal matrix proteins. Now, free soluble PEX5 can participate in a new protein transport cycle.

4. Peroxisome homeostasis

As previously mentioned, peroxisomes are crucial for numerous metabolic pathways, including the metabolism of hydrogen peroxide and the β-oxidation of fatty acids (11, 12). As a result, cells have to ensure the homeostasis of peroxisomes, by controlling their abundance and quality, in order to maintain a healthy intracellular environment. This requires, on one side, the biogenesis of new organelles, and, on the other, the degradation of excessive or dysfunctional ones (195, 196). As stated above, it is commonly accepted that peroxisomes multiply by growth and division of mature peroxisomes. The turnover of unnecessary or dysfunctional peroxisomes mainly occurs by pexophagy, *i.e.*, the specific autophagic degradation of the peroxisome.

4.1. Proliferation of peroxisomes by "growth and division" of mature peroxisomes

Peroxisome proliferation encompasses membrane elongation (growth), constriction and scission (division). This is a multi-step process mediated by PEX11 peroxin, as well as the mitochondrial fission factor (Mff), fission factor 1 (Fis1), dynamin-like protein 1 (DLP1), and ganglioside induced differentiation associated protein 1 (GDAP1) (reviewed in (197)). In mammals, three isoforms of PEX11 exist, PEX11α, PEX11β and PEX11γ. All of them are integral membrane proteins exposing both the N- and C-termini into the cytosol (198–201). While PEX11β is constitutively expressed, PEX11α and PEX11γ are expressed in a tissue-specific manner (198, 200). Mff, Fis1, DLP1 and GDAP1 proteins are shared with mitochondria. During peroxisome proliferation, PEX11β is responsible for the peroxisomal membrane remodeling and elongation, and perhaps for the following assembling of Mff and Fis1 proteins. These proteins can recruit cytosolic DLP1, which is required for membrane scission. The exact function of Mff, Fis1 and GDAP1 proteins is unclear (reviewed in (197)). In yeasts, besides PEX11, other additional and related peroxins have been associated with peroxisome proliferation (202).

4.2. Degradation of peroxisomes by pexophagy

Autophagy is the intracellular process by which cytoplasmic components, including proteins and organelles, are delivered to the lysosome in order to be degraded. There are three types of autophagy – macroautophagy, microautophagy, and chaperone-mediated autophagy (reviewed in (203)) – but for the present discussion only the first type is relevant.

During macroautophagy, an isolation membrane, also named phagophore, encloses cytoplasmic components to form an intermediate organelle called autophagosome. This autophagosome fuses with the lysosome to become an autolysosome, where the internal components are degraded. Macroautophagy can occur both non-selectively or selectively. The selective pathway involves specific receptors that recognize specific substrates targeted for degradation and interact with other components of the macroautophagy machinery (203). Pexophagy is a selective form of macroautophagy.

p62 and NBR1 were identified as pexophagy receptors in mammalian cells (204, 205). They both contain 1) an ubiquitin-associated (UBA) domain, that recognizes ubiquitinated substrates, and 2) an LC3-interacting region, that interacts with the LC3 protein present at the autophagosomal membranes (206). Overexpression of peroxisomal membrane proteins (PMP34 and PEX3) attached to an ubiquitin moiety facing the cytosol, resulted in loss of peroxisomes within cells in a p62-dependent manner (204). On the other hand, overexpression of NBR1 also triggers pexophagy, being the NBR1 UBA and J (a membrane-interacting, amphipathic α-helix region) domains necessary for degradation of peroxisomes (205). Overexpression of PEX3 also induces pexophagy in an ubiquitin-dependent mode (207). Thus, these studies suggest that the presentation of ubiquitin at the surface of the organelle is important for peroxisome recognition during pexophagy in mammalian cells.

Evidence for a quality control mechanism to eliminate dysfunctional peroxisomes in mammalian cells was recently provided (192). The expression of a PEX5 protein that is monoubiquitinated at Cys11 but export-incompetent due to a bulky C-terminal tag, results in the accumulation of ubiquitinated PEX5 at the peroxisomal membrane, and triggers pexophagy in SV40 large T antigen-transformed mouse embryonic fibroblasts. This study showed that alterations in PEX5 and ubiquitin dynamics at the peroxisome membrane can regulate the mammalian pexophagy (192). Accordingly, the depletion of REM function causes the loss of peroxisomes by pexophagy in yeast and mammalian cells (208, 209). However, while in *S. cerevisiae*, the accumulation of import receptors at the peroxisomal membrane is not required for pexophagy (208), in mammalian cells, the accumulation of ubiquitinated PEX5 signaled peroxisomes for pexophagy (209). The latter study suggests that the REM prevents mammalian pexophagy by extracting ubiquitinated proteins from peroxisomes (209).

5. Unsolved questions regarding the import of matrix proteins into peroxisomes

Although, in the last years, our knowledge on the peroxisomal matrix protein import machinery has increased extraordinarily, many of its “details” are still unknown. For instance,

we still have no idea of why there are three RING peroxins in the DTM, or how the REM recognizes and extracts ubiquitinated receptors. However, perhaps the most intriguing property of the PIM regards its ability to import already folded and even oligomerized proteins (reviewed in (126, 127, 210)). This leads us to one of the most important questions about the PIM: how can the PIM accept already folded proteins as substrates while at the same time ensuring that matrix proteins are retained in the organelle. Two main models have been proposed (see below), but, the data supporting each these perspectives are indirect and still scarce.

Our group proposed the model presented in the previous sections, where newly synthesized folded matrix proteins are translocated across the peroxisomal membrane by PEX5 itself, when the receptor becomes inserted into the DTM (151, 161, 166, 211). This model proposes that the soluble receptor-cargo complex is recruited into a proteinaceous pore/channel formed by the DTM components, and takes into account: 1) the transmembrane topology of DTM-embedded PEX5 (151, 211), 2) the absence of any obvious phylogenetically conserved hydrophobic or amphipathic domain in PEX5 (PEX5 is a particularly hydrophilic protein), and 3) the fact that the region that contains the DTM-interacting domains of PEX5, its natively unfolded N-terminal half, remains in solution even upon boiling (140).

The second model, the so-called “transient pore model” (212), proposes that PEX5 is a pore-forming toxin-like protein. In essence that model is similar to the one described above, *i.e.*, it also proposes that cargo proteins are pushed across the organelle membrane by PEX5 itself, when the receptor interacts with the DTM. However, it introduces the novelty that the pore is formed by a combination of PEX5 molecules and DTM components, all of them interacting directly with the lipid bilayer of the peroxisomal membrane, and all together creating the hydrophilic pore that allows the translocation of cargo proteins across the membrane (212, 213). The data that supports this model, excluding at the same time the model from our group, can be reduced to a single experimental fact: peroxisome-associated PEX5 is resistant to alkaline extraction, a property generally attributed to intrinsic membrane proteins.

Clearly, all these issues have to be clarified if we are to understand how this remarkable protein sorting machinery works.

II - AIMS

The study here presented focused on two aspects of the peroxisomal matrix protein import machinery.

The first aim of this study was to explore the role of PEX5 as a holdase-like protein. Recently, our laboratory proposed that PEX5, in addition to its role as a shuttling receptor that recognizes newly synthesized peroxisomal matrix proteins in the cytosol and targets them to the organelle, is also a holdase-like protein that avoids premature or unspecific interactions of its cargo proteins in the cytosol (107, 132). In this study, several approaches commonly used to assess the holdase activity of a given protein were applied to PEX5.

The second aim of this study was to probe the architecture of the peroxisomal matrix protein translocon. Initially, the intriguing biochemical behavior of peroxisomal PEX5, *i.e.*, its resistance to alkaline extraction (211), that has been interpreted in different ways resulting in quite different models concerning the mechanism of the PIM (161, 212), was revisited. Then, an established cell-free organelle-based *in vitro* system (87) and several truncated versions of PEX5 were used to probe the DTM architecture.

III - EXPERIMENTAL PROCEDURES

1. DNA constructs

pET-28-PEX5 – The cDNA encoding the large isoform of human PEX5 ((78); hereafter referred to as PEX5) was obtained by PCR amplification of the plasmid pQE-30-PEX5 (138) using the primers 5'.GCGAACTGCATATGGCAATGCGGGAGCTGG.3' and 5'.GCGTAATTAAGCTTGGCTGCAGGTC.3'. The amplified DNA fragment was digested with *Nde*I and *Sal*I and cloned into the *Nde*I/*Sal*I restriction sites of pET-28c (Novagen).

pET-28-PEX5(C11A) – To obtain the plasmid encoding PEX5 possessing an alanine instead of a cysteine at position 11 (PEX5(C11A)), plasmids pET-28-PEX5 and pET-28-PEX5(1-324;C11A) (186) were digested with *Nco*I and *Sda*I. The 0.3 kb *Nco*I/*Sda*I fragment of pET-28-PEX5(1-324;C11A) was inserted into the *Nco*I/*Sda*I-digested vector pET-28-PEX5.

pET-28-PEX5(1-197;C11A) – The cDNA encoding the first 197 amino acid residues of PEX5 possessing an alanine at position 11 (PEX5(1-197;C11A)) was obtained by PCR amplification of the plasmid pET-28-PEX5(1-324;C11A) using the primers 5'.CTCGATCCCGCGAAATTAATACGACTC.3´ and 5'.CGCCAAGCTTTTACGTGTGCTGCAGATCCTCCTC.3'. The amplified DNA fragment was digested with *Xba*I and *Hin*dIII and cloned into the *Xba*I/*Hin*dIII restriction sites of pET-28a (Novagen).

pET-28-PEX5(1-125;C11A) – The cDNA encoding the first 125 amino acid residues of PEX5 possessing an alanine at position 11 (PEX5(1-125;C11A)) was obtained by PCR amplification of the plasmid pET-28-PEX5(1-324;C11A) using the primers 5'.GATGCGTCATATGGCAATGCGGGAGCTGGT.3' and 5'.GATCGCAAGCTTTCAAGCTGCAAGAAACTCCTG.3'. The amplified DNA fragment was digested with *Nde*I and *Hin*dIII and cloned into the *Nde*I/*Hin*dIII restriction sites of pET-28a (Novagen).

pET-28-PEX5(1-324;C11K) – The plasmid encoding the first 324 amino acid residues of PEX5 possessing a lysine instead of a cysteine at position 11 (PEX5(1-324;C11K)) was obtained with the QuikChange® site-directed mutagenesis kit (Agilent Technologies), using pET-28-PEX5(1-324) (85) as template and the primers described elsewhere (180).

pET-28-PEX5(1-197;C11K) – To obtain the plasmid encoding the first 197 amino acid residues of PEX5 possessing a lysine at position 11 (PEX5(1-197;C11K)), plasmids pET-28-PEX5(1-324;C11K) and pET-28-PEX5(1-197;C11A) were digested with *Eco*RV and *Sda*I.

The 1.5 kb *Eco*RV-*Sda*I fragment of pET-28-PEX5(1-324;C11K) was inserted into the *Eco*RV-*Sda*I-digested vector pET-28-PEX5(1-197;C11A).

pET-28-PEX5(1-125;C11K) – To obtain the plasmid encoding the first 125 amino acid residues of PEX5 possessing a lysine at position 11 (PEX5(1-125;C11K)), plasmids pET-28-PEX5(1-324;C11K) and pET-28-PEX5(1-125;C11A) were digested with *Eco*RV and *Sda*I. The 1.5 kb *Eco*RV-*Sda*I fragment of pET-28-PEX5(1-324;C11K) was inserted into the *Eco*RV-*Sda*I-digested vector pET-28-PEX5(1-125;C11A).

pET-28-PEX5(1-125;C11K)-clv – This plasmid encodes PEX5(1-125;C11K) protein fused to amino acid residues 1 to 30 of human pre-thiolase harboring the L4R mutation, which abolishes its PTS2 function (214), followed by the first 19 residues of the human sterol carrier protein-2 (SCP2) precursor (PEX5(1-125;C11K)-clv). The synthetic gene encoding PEX5(1-125;C11K) possessing at its C-terminus the polypeptide MQRRQVVLGHLRGPADSGWMPQAAPC*LSGA*GFPEAASSFRTHQVSAAPT* was codon optimized for expression in rabbit reticulocyte lysate, synthesized and cloned into the *Nde*I/*Bam*HI sites of pET-28a (Novagen) by Genscript. The cleavage site for the peroxisomal matrix protease Tysnd1 is marked with an asterisk (94, 97) and the 19 residues of the SCP2 precursor are in *italic*.

pET-28-PEX5(1-125;C11K)-nclv – This plasmid is nearly identical to pET-28-PEX5(1-125;C11K)-clv but encoding a fusion protein lacking the -2 and -1 residues of the Tysnd1 cleavage site (Pro25 and Cys26, numbering of full-length human pre-thiolase, underlined in sequence above); constructed in the exact same way by Genscript.

cDNA PEX5(1-197;C11A) – The cDNA encoding amino acid residues 1 to 197 of PEX5 possessing an alanine at position 11 (PEX5(1-197;C11A)), without the N-terminal histidine tag and preceded by a T7 RNA polymerase promoter, was obtained by PCR amplification of the plasmid pGEM4-PEX5(C11A) (180) using the primers 5'.GCCCAATACGCAAACCGCCTCTCC.3' and 5'.GATAATCACGTGTGCTGCAGATCCTCCTCAGG.3'.

2. Expression and purification of recombinant proteins

Recombinant histidine-tagged PEX5, PEX5(C11A), PEX5 containing the missense mutation N526K (PEX5(N526K); (159)), a protein comprising amino acid residues 138 to 639 of PEX5 (PEX5(ΔN137); (215)) (138), a protein comprising amino acid residues 315 to 639 of PEX5 (TPRs) (102, 140), a protein comprising amino acid residues 1 to 324 of PEX5

(PEX5(1-324)), a protein comprising amino acid residues 1 to 197 of PEX5 (PEX5(1-197;C11A)) (87), a protein comprising the first 80 amino acid residues of human PEX14 (NDPEX14) (140), and human PEX19 (68), were produced as described before. The N-terminal histidine tag of PEX5(ΔN137) was removed using histidine-tagged TEV (Tobacco Etch Virus) protease in 50 mM Tris-HCl, pH 8.0, 150 mM NaCl, 1 mM EDTA-NaOH, pH 8.0, 1 mM DTT, overnight at 4 ºC. The protein solution was then incubated with HIS-Select Nickel Affinity Gel beads (Sigma) for 2 hours at 4 ºC, and PEX5(ΔN137) was recovered in the non-bound fraction. The protein was concentrated by repeated centrifugation and dilution using Vivaspin® 2 sample concentrators, as described before (87).

3. Thermal-induced aggregation of malate dehydrogenase

The holdase-like activity of PEX5 was studied using commercially available malate dehydrogenase (MDH) from porcine heart (Sigma, cat. no. M1567) as substrate protein, as described in (216). MDH (2 µM final concentration) was incubated in 250 µL of 50 mM Tris-HCl, pH 8.0 buffer, in the absence or presence of PEX5(1-324) (10 µM final concentration) or BSA (10 µM final concentration), at 43 ºC for 90 min. The aggregation of MDH was followed by measuring light scattering at 340 nm in a temperature controlled spectrophotometer (Shimadzu UV-2401PC). Three independent experiments for each condition were performed.

4. Thermal-induced inactivation of citrate synthase

The holdase-like activity of PEX5 was studied using commercially available citrate synthase (CS) from porcine heart (Sigma, cat. no. C3260) as substrate protein, as described in (217). Samples of CS (final concentration of 0.15 µM for monomer) in the absence or presence of PEX5(1-324) (final concentration of 250 µM) or BSA (final concentration of 250 µM) were prepared in a 50-µL final volume of 50 mM Tris-HCl, pH 8.0, 2 mM EDTA-NaOH, and kept on ice. A 5 µL-aliquot was taken to measure the activity of CS at zero time, which was set to 100%. The inactivation of CS was then started by sample incubation at 44 ºC, with stirring. 5 µL-aliquots were taken at indicated time points (2, 5, 10, 20 and 30 min) to determine the remaining activity of CS. For each enzyme activity assay, the 5 µL-aliquot was mixed with 245 µL of 50 mM Tris-HCl, pH 8.0, 2 mM EDTA-NaOH, 10 µM oxaloacetic acid, 15 µM acetyl-CoA, 10 µM Ellman's Reagent, previously incubated at 25 ºC, and the absorbance at 412 nm was recorded for 4 min at room temperature. The values obtained were used to determine the percentage of CS activity. Four independent experiments for each condition were performed.

5. *In vitro* synthesis and folding of luciferase

This assay was adapted from (218). Luciferase was synthesized *in vitro* using the TnT® T7 Quick Coupled Transcription/ Translation System (Promega), the plasmid DNA provided by the kit, and EasyTag L-^{35}S-methionine (specific activity >1000 Ci (37.0 TBq)/mmol; PerkinElmer Life Sciences). Different transcription/translation reactions were prepared in the presence of 0.1 mM luciferin and in the presence of either 0.5 µM recombinant PEX5, 0.5 µM PEX5(N526K), 0.5 µM PEX5 plus 50 µM of a PTS1-containing peptide (CRYHLKPLQSKL), or 0.5 µM PEX5 plus 50 µM of a negative control peptide (CRYHLKPLQLKS). The transcription/translation reactions were incubated into a luminometer at 25 ºC, and the light emission during synthesis was recorded during 1 hour.

6. Size-exclusion chromatography at pH 11.5

Recombinant proteins PEX5 (180 µg), PEX5(1-324) (125 µg), and NDPEX14 (300 µg), as well as mixtures containing either PEX5 and NDPEX14 or PEX5(1-324) and NDPEX14, were incubated in 50 mM Tris-HCl, pH 8.0, 150 mM NaCl, 1 mM EDTA-NaOH, pH 8.0, 1 mM DTT (final volume of 50 µL) for 15 min at 23 ºC. Samples were then diluted with 200 µL of 0.15 M sodium carbonate (pH after dilution = 10.9), incubated for 30 min on ice, and a 200 µL-aliquot was injected into a Superose^{TM} 12 10/300 GL column running with 0.12 M Na_2CO_3, 0.5 mM DTT (pH 11.6), at 4 ºC, and at a flow rate of 0.5 mL/min. Fractions of 0.5 mL were collected and 30-µL aliquots were analyzed by SDS-PAGE/Coomassie blue staining.

7. Preparation of rat liver post-nuclear supernatant

Liver post-nuclear supernatant (PNS) was prepared from overnight-fasted Wistar Han male rats with 6 to 10 weeks of age, exactly as described in (87). Briefly, the liver was collected, washed and quickly homogenized in ice-cold SEM buffer (0.25 M sucrose, 20 mM MOPS-KOH, pH 7.2, 1 mM EDTA-NaOH, pH 8.0) supplemented with 2 µg/mL of N-(trans-epoxysuccinyl)-l-leucine 4-guanidinobutylamide (E-64). The homogenate was centrifuged twice at 600 *g* for 10 min at 4 ^{o}C (SS-34 rotor in a RC5B Sorvall® centrifuge). Single-use aliquots of the final supernatant were frozen in liquid nitrogen and stored at -80 ^{o}C. Protein concentration of the PNS was determined by the Bradford method.

8. *In vitro* synthesis of radiolabeled proteins in rabbit reticulocyte lysate

^{35}S-methionine-labeled proteins were synthesized *in vitro* using the TnT® T7 Quick Coupled Transcription/Translation System (Promega), according to manufacturer's instructions. Briefly, the TnT® Quick Master Mix was mixed with EasyTag L-^{35}S-methionine (specific activity >1000 Ci (37.0 TBq)/mmol; PerkinElmer Life Sciences) and the plasmid

DNA or cDNA template, and the reaction was incubated for 90 min at 30 ^{o}C. An aliquot of the rabbit reticulocyte lysate (RRL) containing the radiolabeled protein was analyzed by SDS-PAGE/autoradiography to verify yields and quality of the radiolabeled protein.

Unless otherwise specified, ^{35}S-labeled proteins were synthesized *in vitro* as N-terminally histidine-tagged fusion proteins from pET-28-derived plasmids. Syntheses yields from these plasmids were significantly larger than those obtained with pGEM-4-derived plasmids, used in previous works (*e.g.*, (180)). For radiolabeled PEX5(C11A), a semi-quantitative western-blot analysis using the recombinant protein as a standard and a Tetra-his antibody (see section III-17) revealed yields of about 20 ng/µL of RRL. Yields were 2-3 fold larger for PEX5(1-197;C11A/K) and PEX5(1-324;C11A/K), as assessed by quantitative autoradiography using radiolabeled PEX5(C11A) as a standard, and taking into account the methionine content of each protein.

9. Cell-free PNS-based *in vitro* assays

PNS-based *in vitro* reactions were performed as recently described (87), with 600 µg of total PNS protein and 0.1 to 16 µL of RRL containing the indicated ^{35}S-labeled protein, *per* 100 µL of reaction, in import buffer (0.25 M sucrose, 20 mM MOPS-KOH, pH 7.2, 50 mM KCl, 3 mM $MgCl_2$, 2 µg/mL E-64, 96 µg/mL methionine) supplemented with 2 mM reduced L-glutathione, pH ~7.0 with NaOH, 10 µM bovine ubiquitin, and 5 mM ATP or 5 mM AMP-PNP. In the latter case, the PNS was previously primed for import by incubating it for 5 min at 37 ^{o}C in the presence of 0.3 mM ATP. The priming of PNS allows endogenous DTM-embedded PEX5 to be exported back into the soluble fraction, thus increasing the number of free DTMs available. Where indicated, ubiquitin aldehyde, a potent and highly specific inhibitor of deubiquitinases (219), was used at 1 µM final concentration. Where indicated, the reactions were additionally supplemented with recombinant NDPEX14, PEX5(1-197;C11A), PEX5(C11A), TPRs, PEX5(1-324), PEX19 or PEX5(ΔN137) (as specified in the respective figure legends). PNS-based *in vitro* reactions were incubated for 45 min at 37 ^{o}C (unless otherwise specified), and treated with 400 µg/mL (final concentration) of proteinase K (PK) for 40 min on ice, to degrade protein that had not associated with peroxisomes, followed by PK inactivation with 500 µg/mL (final concentration) of phenylmethanesulfonyl fluoride. *In vitro* reactions were then diluted to 1 mL with SEMK buffer (SEM buffer supplemented with 80 mM KCl) and the organelles were isolated by centrifugation at 11300 *g* for 15 min at 4 ^{o}C. Proteins were precipitated with 10% (w/v) trichloroacetic acid (TCA) for 30 min on ice, and recovered by centrifugation at 11300 *g* for 15 min at 4 ^{o}C. Protein pellets were washed with 1 mL acetone, centrifuged again at 11300 *g* for 15 min at 4 ^{o}C, dried at 37 ^{o}C, and analyzed by SDS-PAGE/autoradiography. In the two-step *in vitro* import/export assays, ^{35}S-labeled proteins were first incubated with the primed PNS for 30 min at 37 ^{o}C in the presence of

AMP-PNP. The reactions were then diluted to 1 mL with SEMK buffer and the organelles isolated by centrifugation at 11300 *g* for 15 min at 4 ^{o}C. The organelles were resuspended in import buffer and incubated in the presence of either 5 mM ATP or 5 mM AMP-PNP for 15 min at 37 ^{o}C. The organelle suspensions were then diluted to 1 mL with SEMK buffer and centrifuged at 11300 *g* for 15 min at 4 ^{o}C. Proteins of both organelle and soluble fractions were precipitated with 10% (w/v) TCA, processed as described above, and analyzed by SDS-PAGE/autoradiography.

10. Digestion with Genenase I

Organelles from a PK-treated PNS-based *in vitro* reaction programmed with ^{35}S-PEX5(1-197;C11A), or 0.25 µL of RRL containing ^{35}S-PEX5(1-197;C11A), were digested with 2 µg of Genenase I (New England BioLabs; (220)) in a buffer containing 0.25 M sucrose, 20 mM Tris-HCl, pH 8.0, 100 mM NaCl, 1% (w/v) Triton X-100, 1 mM EDTA-NaOH, pH 8.0, 1 mM DTT, 50 µg/mL phenylmethanesulfonyl fluoride, and 1:300 (v/v) mammalian protease inhibitor mixture (Sigma), for 30 min at 23 ºC. Digestions were stopped with 10% (w/v) TCA, processed as described above, and analyzed by SDS-PAGE/autoradiography.

Recombinant PEX5(1-197;C11A) (1 µg) was incubated in 50 mM Tris-HCl, pH 8.0, 150 mM NaCl, 1 mM EDTA-NaOH, pH 8.0, 1 mM DTT (final volume of 10 µL) for 3 h 30 m at 23 ºC, in the absence or presence of 0.25 µg of Genenase I. Samples were analyzed by SDS-PAGE/Coomassie blue staining and by mass spectrometry.

11. Mass spectrometry analyses

Mass spectra were acquired in a MALDI mass spectrometer (4800 Plus MALDI TOF/TOD Analyzer, SCIEX) using the 4000 Series Explorer v3.7.0 (build 1) SCIEX software, at i3S Proteomics Core Facility (Portugal) by Doctor Hugo Osório. For peptide molecular mass determination, samples were diluted 10-fold in 10 mg/mL of α-Cyano-4-hydroxycinnamic acid (50% ACN, 0.1% TFA) and 1 µL was spotted in a MALDI sample plate and allowed to dry. Spectra were acquired in reflector positive mode for the mass range m/z 1000 - m/z 3000 with and without internal standards (Angiotensin I, DRVYIHPFHL, m/z 1296.68, ACTH 1-17, SYSMEHFRWGKPVGKKR, m/z 2093.09, and ACTH 18–39, RPVKVYPNGAEDESAEAFPLEF, m/z 2465.20). For protein molecular mass determination, samples were diluted 10-fold in 10 mg/mL of sinapic acid matrix (50% ACN, 0.1% TFA), and 1 µL was spotted in the MALDI sample plate and allowed to dry. Mass spectra were acquired in linear positive mode for the mass window m/z 15000 - m/z 35000. Mass spectra were internally calibrated with horse apomyoglobin, m/z 16952. For determination of protein cleavage location, data analysis was performed with the Findpept software ((221);

http://web.expasy.org/findpept/). The maximum allowed error was 10 ppm for peptide masses.

12. Density gradient centrifugation

A PK-treated PNS-based *in vitro* reaction (4.8 mg of total PNS protein) was diluted to 1.6 mL with SEM buffer, and loaded onto the top of a Histodenz™ step gradient comprising 1.5 mL of 45% (w/v), 5.5 mL of 28% (w/v), and 1 mL of 20% (w/v) Histodenz™ in 5 mM MOPS-KOH, pH 7.2, 1 mM EDTA-NaOH, pH 8.0. The gradient was centrifuged at 82500 *g* for 3 h at 4 ºC (70.1 Ti rotor in an Optima™ L-80 XP Beckman Coulter ultracentrifuge), and 12 fractions were collected from the bottom of the gradient. After protein precipitation with 10% (w/v) TCA, ¼ of each fraction was analyzed by SDS-PAGE/western-blotting/ autoradiography. After exposing to an x-ray film, the nitrocellulose membrane was probed with several antibodies, as indicated.

13. Extraction of peroxisomal proteins by sonication

Organelles from a PK-treated PNS-based *in vitro* reaction were resuspended in SEM buffer supplemented with 2 mM DTT, 0.1 mg/mL phenylmethanesulfonyl fluoride, and 1:500 (v/v) mammalian protease inhibitor mixture (Sigma), and disrupted by sonication as described before (186). Membrane and matrix components were separated by centrifugation at 100000 *g* for 60 min at 4 ºC (70.1 Ti rotor in an Optima™ L-80 XP Beckman Coulter ultracentrifuge). After protein precipitation with 10% (w/v) TCA, samples were analyzed by SDS-PAGE/western-blotting/autoradiography. After exposing to an x-ray film, the nitrocellulose membrane was probed with several antibodies, as indicated.

14. SDS-PAGE/autoradiography

Protein samples were solubilized in Laemmli sample buffer (50 mM Tris-HCl, pH 8.8, 2% (w/v) SDS, 0.017% (w/v) bromophenol blue, 10% (v/v) glycerol, 2 mM EDTA-NaOH, pH 8.0, 100 mM DTT) by incubation for 10 min at 65 ºC followed by 5 min at 95 ºC, and loaded onto SDS polyacrylamide gels (16.5 cm x 14.5 cm x 0.75 mm). Typically, gels were blotted onto a nitrocellulose membrane for autoradiography. For quantitative autoradiography, the gels were instead stained with 0.2% (w/v) Coomassie, 50% (v/v) methanol, and 10% (v/v) glacial acetic acid, dried for 2 hours at 80 ^{o}C, and exposed to a storage phosphor screen.

15. PAGE at pH 11.5

Recombinant proteins PEX5 (2 µg), PEX5(1-324) (2 µg), and NDPEX14 (5 µg), as well as mixtures containing either PEX5 and NDPEX14 or PEX5(1-324) and NDPEX14, were incubated in 50 mM Tris-HCl, pH 8.0, 150 mM NaCl, 1 mM EDTA-NaOH, pH 8.0, 1 mM DTT

(final volume of 2 µL) for 15 min at 23 ºC. Samples were diluted with 8 µL of 25 mM phosphate buffer, pH 11.5, 2.5 mM DTT, 18% (w/v) glycerol, 0.05% (w/v) bromophenol blue, and loaded onto a 9% polyacrylamide gel (16.5 cm x 14.5 cm x 0.75 mm) made in 50 mM Na_2HPO_4, pH 11.5 with 5 M KOH. The gel was run in the same pH 11.5 buffer at 4 ºC for 5 h 30 m, with power limited to 3W. Proteins were transferred onto a nitrocellulose membrane, stained with Ponceau S, and protein bands were excised from the wet membrane and distained in water. Proteins were eluted from the membrane slices by incubation in Laemmli sample buffer (50 mM Tris-HCl, pH 8.8, 2% (w/v) SDS, 0.017% (w/v) bromophenol blue, 10% (v/v) glycerol, 2 mM EDTA-NaOH, pH 8.0, 100 mM DTT) for 30 min at 37 ºC followed by incubation at 65 ºC for 30 min, and analyzed by SDS-PAGE/Coomassie blue staining, as described before (71).

16. Blot-overlay assay

Endogenous rat liver PEX5 was detected in western-blots by blot-overlay using ^{35}S-PEX14 as described before (153). The nitrocellulose membrane was incubated in renaturing buffer (50 mM Tris-HCl, pH 7.5, 150 mM NaCl, 100 mM potassium acetate, 5 mM $MgCl_2$, 100 µM $ZnCl_2$, 1 mM DTT, 1 mM EDTA, 0.3% (w/v) Tween-20, 100 mM methionine, 5% (w/v) nonfat dry milk) for 2 h at 4 ºC, and probed with ^{35}S-PEX14 (25 µL of RRL in 25 mL of renaturing buffer). Following incubation overnight at 4 ^{o}C, the membrane was washed twice with renaturing buffer, dried and exposed to an x-ray film.

17. Antibodies

Antibodies directed to catalase (RDI-CATALASEabr, Research Diagnostics, Inc.), KDEL (ab12223, Abcam), cytochrome *c* (556433, BD Pharmingen™), SCPx (19182-1-AP, ProteinTech™), and Tetra-his (34670, Qiagen) were purchased. The antibody directed to PEX14 was described before (81). The antibody directed to PEX13 was prepared by Doctor Tânia Francisco. Antibodies were detected using goat alkaline phosphatase-conjugated anti-rabbit or anti-mouse antibodies (A9919 and A2429, respectively, Sigma).

18. Determination of molar ratios of DTM-bound PEX5 molecules

For reasons that will become apparent below (see section IV-2.2.), the distribution of methionine residues at the N-terminus of PEX5 (see Figure 4A) had to be considered for the determination of molar ratios of radiolabeled DTM-bound PEX5 molecules. Also, since these experiments demanded quantitative autoradiography data, a storage phosphor screen and a Storm 860 Phosphorimager instrument (GE Healthcare) were used. According to the manufacturer, the captured information is proportional to the radioactivity in the sample. Thus, both weak and strong signals can be visualized and quantitated in a single exposure.

The densitometric analysis of radiolabeled protein bands in the phosphor images was performed with the ImageQuant® version 5.0 software (GE Healthcare). Bands were surrounded by rectangles (see Figure 4B), and for each selected rectangle, a single volume value (the volume under the surface created by a 3D plot of the pixel locations and pixel intensities) was determined. Volume quantitation was performed with the local median background correction (the middle value of all the pixel values in the rectangle outline was used for the background). Volume values for PEX5(C11A) were multiplied by three, as only one third of the *in vitro* reactions were loaded onto the gels. For both PEX5(1-197;C11A) and PEX5(1-324;C11A), the contribution of each individual band was determined. Intersecting lines were drawn (see Figure 4C), and the respective intensity profiles were plotted (see Figure 4D). The intensity profiles were then deconvoluted with the Fityk – curve fitting and data analysis software ((222); see Figure 4E). Then, the signal intensities of the PEX5 species were normalized for the number of methionines (proteins were synthesized *in vitro* using ^{35}S-methionine). To estimate ratios of binding sites at saturation for PEX5(1-324;C11A):PEX5(C11A) and PEX5(1-197;C11A):PEX5(C11A), data from four technical replicates were fitted to a dose response one-site specific binding curve equation, y = Bmax * x / (EC50 + x), using Prism® version 7.03 software (GraphPad software). In this equation y is the methionine- and PNS protein-normalized autoradiography signal of PK-resistant protein bands, x is the volume of RRL containing the radiolabeled protein, Bmax is the maximal response at infinite volume of RRL, and EC50 is the volume of RRL yielding a half-maximal response. Note that since the actual concentrations of radiolabeled proteins in the RRL are not known, the absolute EC50 and Bmax values have no meaning per se. However, Bmax ratios provide the relative binding stoichiometries of the different PEX5 species.

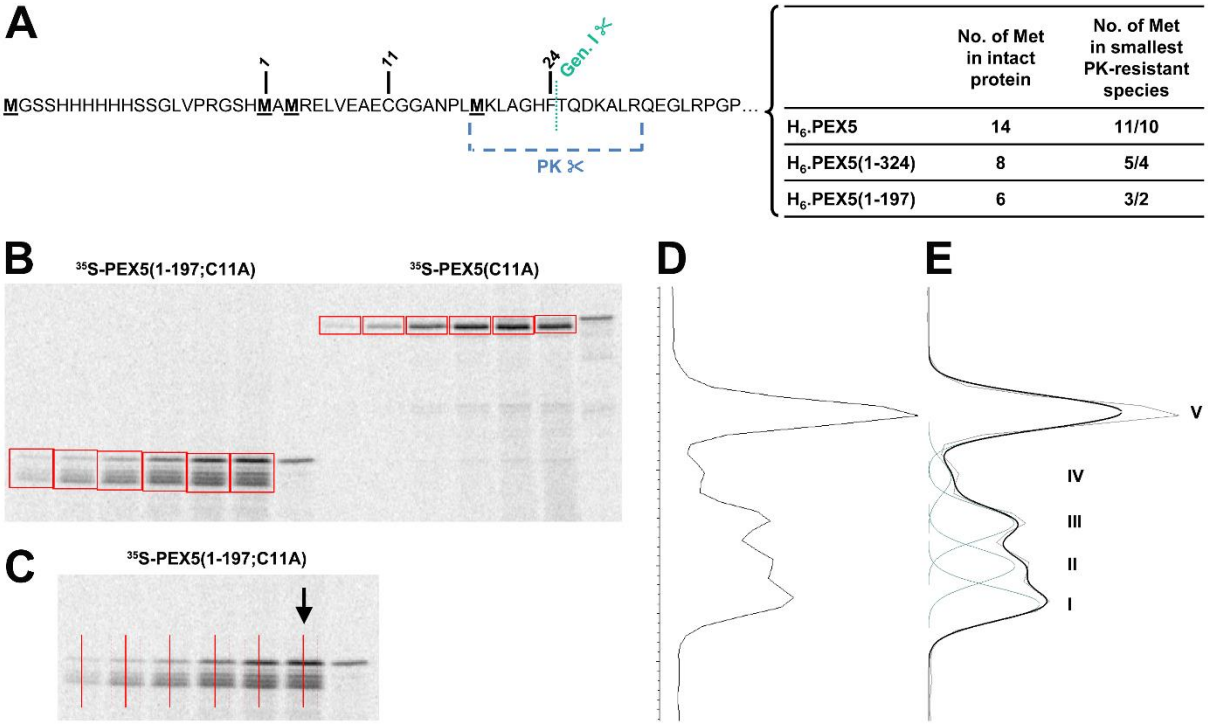

	No. of Met in intact protein	No. of Met in smallest PK-resistant species
H_6.PEX5	14	11/10
H_6.PEX5(1-324)	8	5/4
H_6.PEX5(1-197)	6	3/2

Figure 4. Determination of molar ratios of DTM-bound PEX5 molecules. A, N-terminal sequence of the histidine-tagged PEX5 molecules used in this study. The conserved cysteine at position 11 is marked, as are all methionine residues (bold, underlined). The cleavage site of Genenase I (Gen. I ✂) and the approximate cleavage site of PK (PK ✂) that yields the smallest PK-resistant stage 2 PEX5 species are also shown. Note that there is some uncertainty in defining the latter cleavage site. Thus, two possibilities were considered: PK cleaves after methionine 18 or PK cleaves before methionine 18. The number of methionine residues in both intact protein and smallest PK-resistant PEX5 species are presented in the table on the right side. **B-E,** quantitative analysis of the phosphor images. For the densitometric analysis of radiolabeled protein bands (**B**), for each selected rectangle, a single volume value was determined, with a local median background correction. Volume values for PEX5(C11A) were multiplied by three, as only one third of the *in vitro* reactions were loaded onto the gels. To determine the contribution of each individual band, for both PEX5(1-197;C11A) and PEX5(1-324;C11A), intersecting lines were drawn (**C**), and the respective intensity profiles were plotted (**D**). The intensity profiles were then deconvoluted (**E**); the thin grey line represents the raw data obtained for the intensity profile; the black line represents the assisted fitting of each peak (peaks I to V); the blue lines represent the deconvoluted peaks. D and E, exemplified for the lane marked with an arrow in panel C.

IV - RESULTS

1. PEX5 as a holdase-like protein

Recently, our group proposed that PEX5 functions as a holdase-like protein. The data behind this concept comes from the finding that PEX5 binds monomers of human catalase (a tetrameric protein in its native state) and monomers of mouse ACOX and UOX (dimeric and tetrameric proteins, respectively), strongly inhibiting their oligomerization (107, 132). Additional characterization of the interaction established between PEX5 and catalase showed that this inhibitory effect requires more than the interaction between the PTS1 and the TPRs of PEX5. Indeed, the N-terminal domain of PEX5 alone presents the ability to inhibit catalase tetramerization, although to a lesser extent than the full-length protein (107). Furthermore, evidence that the N-terminal half of PEX5 contributes to the interaction between PEX5 and some PTS1-containing and PTS-less cargo proteins was already available (104–106). Thus, it seems that the natively unfolded N-terminal domain of PEX5 embraces the newly synthesized cargo proteins in the cytosol, possibly keeping them in a molten-globule state (in contrast to their oligomeric forms, monomeric catalase, ACOX and UOX are all extremely susceptible to proteases), avoiding premature specific interactions, such as oligomerization prior to peroxisomal import, or unspecific interactions like unwanted adsorption to membrane structures (107, 132).

To better characterize the role of PEX5 as a holdase-like protein, several strategies were used in this study. In one of the more classical approaches, the capacity of the N-terminal domain of PEX5 to prevent the thermal-induced *in vitro* aggregation of malate dehydrogenase (MDH) and citrate synthase (CS) was analyzed. These two proteins are frequently used as model substrates for molecular chaperones since at T ≥ 43 ºC, both MDH and CS become unfolded and have a tendency to aggregate (216, 217). When a protein becomes unfolded, unspecific hydrophobic interactions occur resulting in protein aggregation. This aggregation is accompanied by an increase in absorbance due to light scattering. Molecular chaperones can bind unfolded proteins and avoid the aggregation process (223). It is of note that the N-terminal domain of PEX5 (specifically, a histidine-tagged recombinant protein comprising the first 324 amino acid residues of PEX5 (PEX5(1-324)) can be used in these assays because it remains in solution even at much higher temperatures, a property derived from its natively unfolded nature (140).

1.1. Thermal-induced aggregation of malate dehydrogenase

For the thermal-induced aggregation assays, MDH was incubated at 43 ºC and its aggregation was monitored by measuring the increase in absorbance at 340 nm (see Figure 5, solid line). When MDH was incubated in the presence of recombinant PEX5(1-324), its thermal-induced aggregation was considerably decelerated (see Figure 5, dash line). On the contrary, BSA, used here as a negative control, had no or almost no effect in the aggregation

of MDH (see Figure 5, dash dot line). Thus, the N-terminal domain of PEX5 has the ability to prevent the thermal-induced aggregation of MDH.

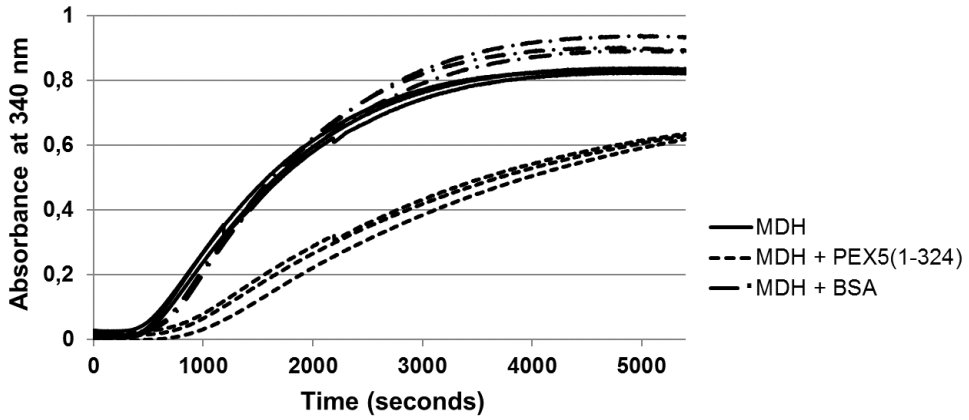

Figure 5. Effect of PEX5(1-324) on the thermal-induced aggregation of malate dehydrogenase. MDH was incubated at 43 ºC in the absence (solid line) or presence of either PEX5(1-324) (dash line) or BSA (dash dot line). Protein aggregation was followed by measuring the absorbance at 340 nm during 5400 seconds (90 min). Three independent experiments are shown for each condition.

1.2. Thermal-induced inactivation of citrate synthase

CS is a mitochondrial dimeric protein that catalyzes the condensation of oxaloacetic acid and acetyl-CoA to yield citrate and coenzyme A. CS is inactivated when incubated at high temperatures, and its inactivation can be easily observed by measuring the remaining activity of the enzyme. The reaction catalyzed by CS can be easily followed using the Ellman's Reagent, which reacts with -SH groups (present in the coenzyme A that is produced) and gives an intense yellow color that can be measured at 412 nm (217).

The results in Figure 6 show that the CS activity rapidly decreased when the protein was incubated at 44 ºC (circles). Indeed, a more than 60% decrease in activity was achieved after only 5 min of incubation. In the presence of recombinant PEX5(1-324), the thermal-induced inactivation of CS was significantly delayed (see Figure 6, triangles), and after 5 and 10 min of incubation at 44 ºC, CS retained around 70% and 50% of its initial activity, respectively. Incubation in the presence of BSA did have a little protective effect on the inactivation of CS (see Figure 6, squares), but to a considerable lesser extent than the one observed for PEX5(1-324). The results obtained demonstrate that the N-terminal half of PEX5 has the capacity to prevent the thermal-induced inactivation of CS, suggesting that PEX5(1-324) can interact transiently with CS or unfolding intermediates of CS.

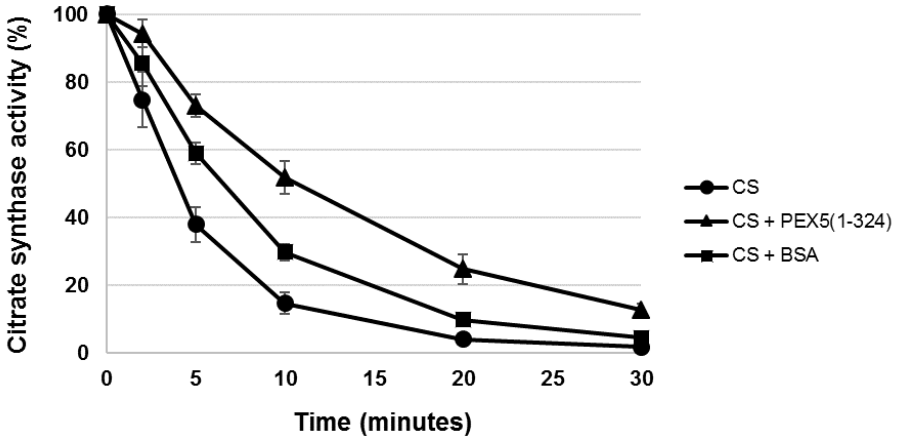

Figure 6. Effect of PEX5(1-324) on the thermal-induced inactivation of citrate synthase. CS was incubated at 44 ºC in the absence (circles) or presence of either PEX5(1-324) (triangles) or BSA (squares). Enzyme activity was measured at several time points, and is given as percentage of the zero-time value. Data points represent the average and standard deviation of the values obtained in four independent experiments.

1.3. The effect of PEX5 on the structure of a *de novo* synthesized peroxisomal matrix protein

The monomeric forms of catalase, ACOX and UOX are all soluble proteins displaying hydrodynamic properties compatible with a globular conformation (107, 132). Yet, all three monomers are extremely sensitive to proteolysis suggesting that they are molten-globules. Interestingly, their sensitivity to proteases is not altered upon binding PEX5 ((107, 132, 224), unpublished results), a finding that could suggest that PEX5 interacts with proteins in the molten-globule state. We wondered whether this might also be true for natively monomeric PTS1-containing proteins. A positive answer for this question would have great mechanistic implications because it would suggest that the best substrates for the PIM are (flexible) molten-globule proteins. We used luciferase as a test substrate, an enzyme that catalyzes a bioluminescent reaction and a protein that is actually a monomeric PTS1-containing peroxisomal matrix protein (88). The PEX5 capacity to bind luciferase nascent polypeptide chains and slow down the acquisition of their native structure, keeping them in a molten-globule state, was tested. Briefly, using a cell-free transcription/translation system, luciferase was synthesized *de novo* and the acquisition of tertiary structure by luciferase, resulting into an enzymatically active conformation, was continuously monitored through the measurement of the light produced during the oxidation of luciferin. *In vitro* synthesis was performed in the presence of recombinant human PEX5, PEX5(N526K) (a PEX5 protein with the mutation N526K that greatly abrogates its PTS1-binding activity), PEX5 plus a PTS1-containing peptide (“SKL”), or PEX5 plus a negative control peptide (“LKS”). As shown in Figure 7, irrespective of whether or not PEX5 was capable or available to bind newly synthesized

luciferase, no differences were observed in the initial time of its activity. Thus, PEX5 did not show the ability to keep luciferase in a molten-globule/enzymatically inactive state.

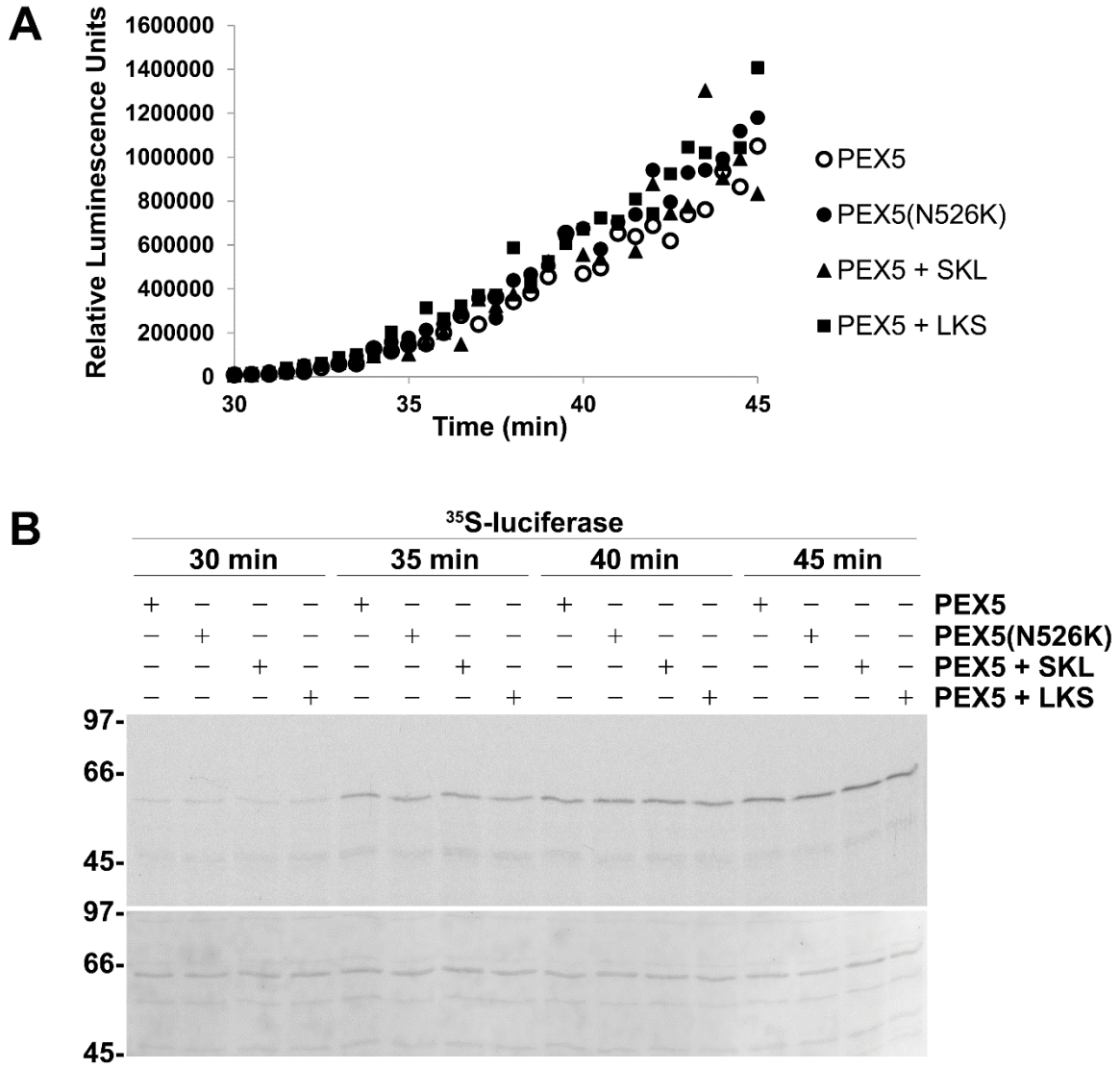

Figure 7. Effect of PEX5 on newly synthesized luciferase activity. A, luciferase was synthesized *in vitro*, at 25 ºC, in the presence of PEX5, PEX5(N526K), PEX5 and a PTS1-containing peptide ("SKL"), or PEX5 and a control peptide ("LKS"), as indicated. The accumulation of active luciferase during synthesis was followed by measuring the light produced by luciferin oxidation. **B,** the same transcription/translation reactions were incubated at 25 ºC in a thermomixer and, during synthesis, at the indicated time points, aliquots were withdrawn and analyzed by SDS-PAGE/autoradiography. The autoradiograph (upper panel) and the corresponding Ponceau S-stained membrane (lower panel) are shown. Numbers to the left indicate the molecular weight (kDa) of protein standards.

2. Probing the architecture of the peroxisomal matrix protein translocon using truncated PEX5 molecules

2.1. The PEX5-PEX14 interaction is resistant to alkaline pH

When PEX5 becomes inserted into the DTM, it acquires a transmembrane topology (211). Strikingly, this peroxisome-associated PEX5 population cannot be extracted from the membrane by alkaline pH solutions (78, 99, 211, 225), a property commonly attributed to integral membrane proteins that directly interact with the lipid bilayer. This biochemical behavior of peroxisomal PEX5 is intriguing. Although the N-terminal domain of PEX5 is essential and sufficient for its insertion into the peroxisomal membrane (it contains the DTM-binding domains; (119, 150)), it does not contain any obvious phylogenetically conserved hydrophobic or amphipathic region that might sustain a direct interaction of PEX5 with the lipid bilayer of the peroxisomal membrane. In fact, the recombinant protein comprising only the natively unfolded N-terminal half of PEX5 is completely soluble and, even after boiling, displays no tendency to aggregate or precipitate (140). Even with this contradiction, the striking alkaline pH resistance of peroxisome-associated PEX5 has been interpreted by some authors as meaning that the protein directly interacts with the lipid bilayer of the organelle membrane and acts as a pore-forming protein (212, 226). A simpler explanation for the peculiar biochemical behavior of peroxisomal PEX5 is that the protein-protein interactions established between PEX5 on one side and the DTM components on the other may be resistant to alkaline pH.

The N-terminal domain of PEX5 interacts with two DTM components, PEX13 (138, 145, 227) and PEX14 (142–146), respectively. While the PEX5-PEX13 interaction is relatively weak and difficult to capture in *in vitro* binding assays (138, 145, 228, 229), PEX5 interacts very strongly with PEX14 (79, 81, 142, 143, 211). Indeed, each of the eight pentapeptide motifs present in the N-terminal half of PEX5 bind to the first 80 amino acid residues of PEX14 (142, 143, 146), a conserved domain that is probably embedded in the peroxisomal membrane or even exposed into the organelle matrix (153, 230). Thus, we focused on the PEX5-PEX14 interaction.

Two different approaches were used to determine whether or not the PEX5-PEX14 interaction is resistant to alkaline pH. In the first, recombinant PEX5, a protein containing the first 80 amino acid residues of PEX14 (hereafter mentioned to as NDPEX14), as well as a mixture of both proteins, were subjected to pH 11.5 polyacrylamide gel electrophoresis (PAGE). As shown in Figure 8A and B (left panel), for the mixture of both PEX5 and NDPEX14 proteins (see Figure 8A, lane 2), a partial disappearance of the bands corresponding to the individual proteins and the presence of a new band, displaying a slower electrophoretic mobility, corresponding to the PEX5-NDPEX14 complex (see Figure 8B (left

panel), lane b) can be observed. Exactly the same results were obtained when PEX5 was replaced in this experiment by a protein comprising only its N-terminal half, PEX5(1-324) (see Figure 8A and B (right panel)).

In the second approach, the same recombinant proteins were subjected to size-exclusion chromatography performed in the presence of 0.1 M sodium carbonate, the solution generally used to extract soluble and peripheral membrane proteins from biological membranes (231). As shown in Figure 8C, protein complexes between PEX5 and NDPEX14 were easily detected in the presence of 0.1 M sodium carbonate (compare panel 2 with panels 1 and 5). Again, the same results were obtained when PEX5 was replaced by PEX5(1-324) (compare panel 4 with panels 3 and 5). Clearly, the PEX5-PEX14 protein is stable at alkaline pH.

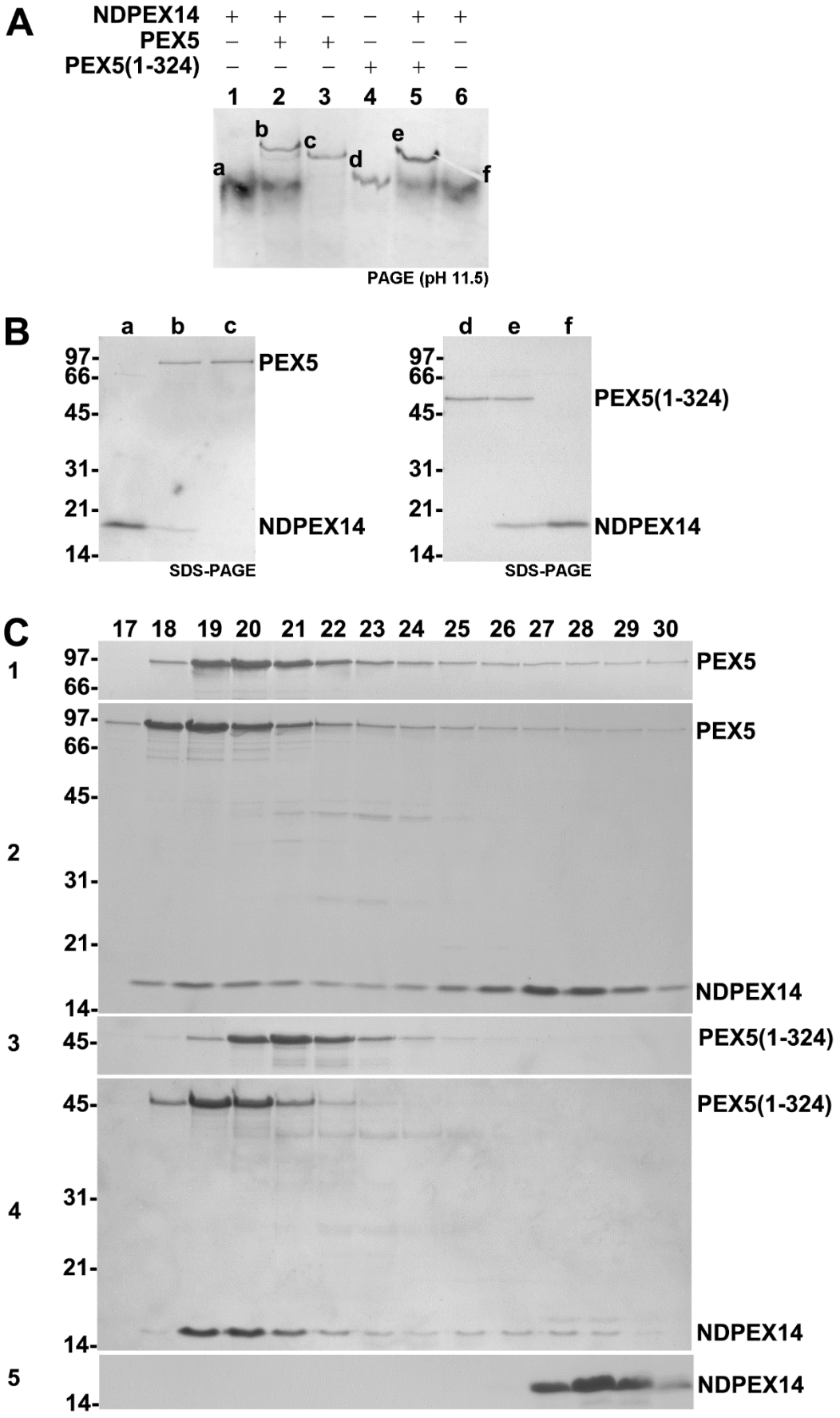

Figure 8. For figure legend, see next page.

Figure 8. The PEX5-PEX14 interaction is resistant to alkaline pH. A, recombinant NDPEX14 (lanes 1 and 6), PEX5 (lane 3), PEX5(1-324) (lane 4), a mixture of NDPEX14 and PEX5 (lane 2) or PEX5(1-324) (lane 5), were subjected to PAGE under alkaline conditions (50 mM phosphate buffer, pH 11.5), blotted onto a nitrocellulose membrane and stained with Ponceau S. **B,** bands marked (in A) from "a" to "c", and from "d" to "f", were excised from the membrane, the proteins were eluted with Laemmli sample buffer and analyzed by SDS-PAGE/Coomassie blue staining (left and right panel, respectively). **C,** recombinant PEX5 (panel 1), PEX5(1-324) (panel 3), NDPEX14 (panel 5), and a mixture of NDPEX14 and PEX5 (panel 2) or PEX5(1-324) (panel 4), were subjected to size-exclusion chromatography under alkaline conditions (0.1 M sodium carbonate). The void volume of the column was in fraction 14. Fractions were collected and analyzed by SDS-PAGE/Coomassie blue staining. In B and C, numbers to the left indicate the molecular weight (kDa) of protein standards.

Thus, there is no need to assume that the resistance of peroxisome-associated PEX5 to alkaline extraction reflects an interaction of the protein with the lipid bilayer of the organelle. The striking biochemical behavior of DTM-embedded PEX5 can now be fully explained by the properties of the PEX5-PEX14 interaction.

2.2. The DTM can accommodate more molecules of a truncated PEX5 species than full-length PEX5

According to our model, the soluble receptor-cargo complex is recruited into a proteinaceous pore/channel formed by DTM components. However, our knowledge on the mechanistic principles of the PIM, *i.e.*, on how the PIM accepts their substrates, is still very incomplete. The fact that PEX5 and DTM components are very low abundant proteins, even in peroxisome-rich cells, together with the lability of detergent-solubilized PEX5-DTM complex during typical biochemical procedures have complicated the structural characterization of the peroxisomal matrix protein translocon (79, 81). Nevertheless, indirect approaches such as *in vitro* binding analyses can still provide valuable data on the architecture/mechanism of protein complexes (232). In this work, we started to apply such a strategy to study the PEX5-DTM complex.

The peroxisomal matrix protein import pathway has been studied in our laboratory using a cell-free organelle-based *in vitro* system (see (87)). Concisely, a ^{35}S-labeled reporter protein is incubated with a rat liver post-nuclear supernatant (PNS), used as a source of peroxisomes and cytosolic components. Then, the organelle suspension is treated with a large amount of an aggressive and non-specific protease. While the radiolabeled reporter protein that became associated with peroxisomes is preserved, because is not accessible to protease, the protein that is not associated with the organelles is degraded by the protease. Since this is an open experimental system, different components can be added or removed and different strategies can be used to block the peroxisomal matrix protein import pathway at different and specific steps (see Figure 2).

In this study, cell-free PNS-based *in vitro* assays programmed with several ^{35}S-labeled PEX5 proteins were used to characterize the architecture of the peroxisomal matrix protein translocon. Proteinase K (PK) was used to evaluate insertion of ^{35}S-labeled PEX5 proteins into the peroxisomal membrane (see Figure 9). As previously mentioned, peroxisome-associated PEX5 displays a transmembrane topology, exposing most of its polypeptide chain into the organelle matrix, and only a small 2-kDa fragment of its N-terminus into the cytosol. This population of PEX5, the so-called stage 2, is mainly inaccessible to protease, and after digestion with PK only the 2-kDa fragment is degraded (151). During its transient passage through the peroxisomal membrane, PEX5 is monoubiquitinated at a conserved cysteine residue (Cys11 in humans). This population of PEX5, the so-called stage 3, is also protease-protected, but, in contrast to stage 2 PEX5, it is completely resistant to digestion with PK, probably because the ubiquitin moiety or even the REM protects Ub-PEX5 from PK (147, 151).

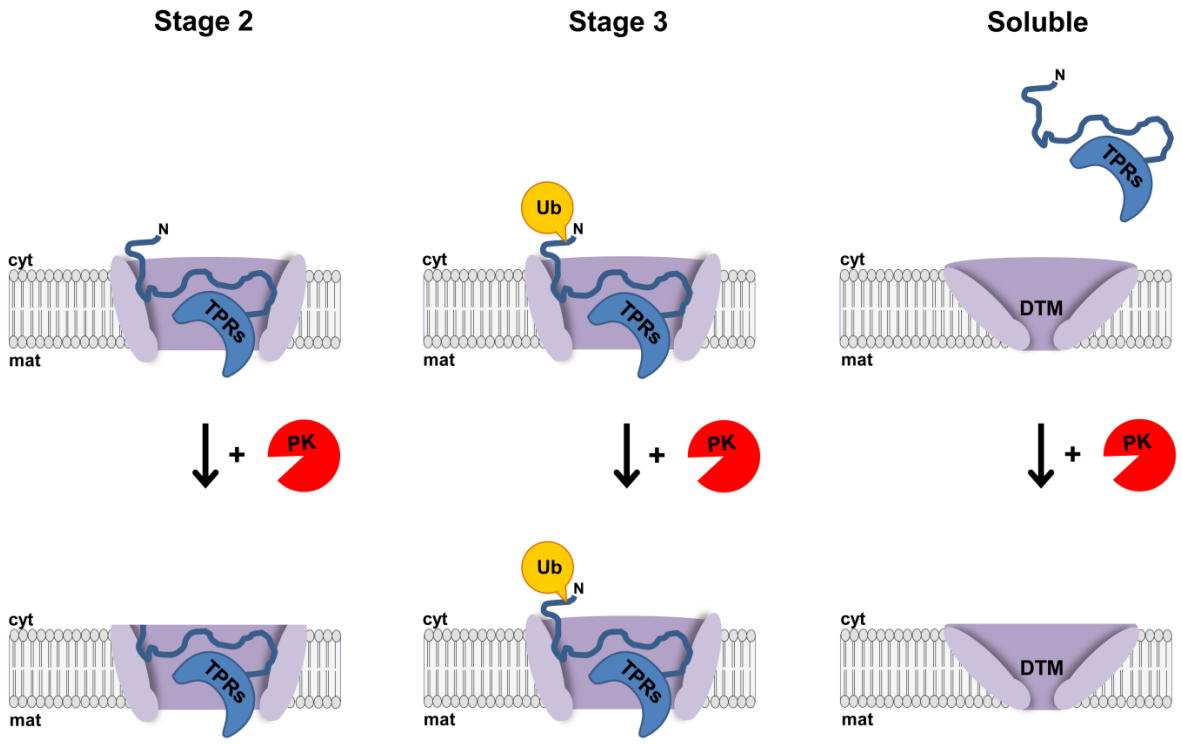

Figure 9. PK as a tool to assess the insertion of PEX5 into the peroxisomal membrane in PNS-based *in vitro* assays. Both stage 2 and stage 3 PEX5 are resistant to PK-treatment. But, while stage 2 PEX5 is partially accessible and the small fragment of its N-terminus that is exposed into the cytosol is cleaved by PK, stage 3 PEX5 is completely resistant to PK. Possibly the ubiquitin moiety (or even the REM) protects Ub-PEX5 from the PK. Soluble PEX5 is extremely sensitive to PK-treatment and is completely degraded by the protease. Abbreviations used: cyt, cytosol; mat, peroxisomal matrix; TPRs, tetratricopeptide repeats domain of PEX5; PK, proteinase K; Ub, ubiquitin; DTM, docking/translocation module.

Initially, we asked whether or not full-length PEX5 and shorter, C-terminally truncated, versions of PEX5 can interact with the peroxisomal membrane with the same stoichiometry. To ensure the saturation of PEX5-binding sites at the peroxisomal membrane, mutant PEX5 proteins, all with the cysteine at position 11 replaced by an alanine (C11A), were used in these experiments. This C11A mutation results in the accumulation of PEX5 into the DTM because the alanine residue cannot be ubiquitinated, and thus, PEX5 is not dislocated back into the cytosol (180). In addition to full-length PEX5 (PEX5(C11A)), two different C-terminally truncated PEX5 proteins were used in these experiments, that is, PEX5(1-324;C11A) and PEX5(1-197;C11A), comprising the first 324 and 197 amino acid residues of PEX5, respectively (see Figure 10A). All proteins were synthesized *in vitro* from pET-28-derived plasmids because the synthesis yields from these plasmids were significantly larger than those achieved with pGEM-4-derived plasmids, used in previous works. Consequently, all ^{35}S-labeled PEX5 proteins have a histidine tag at their N-termini (see Figure 10B).

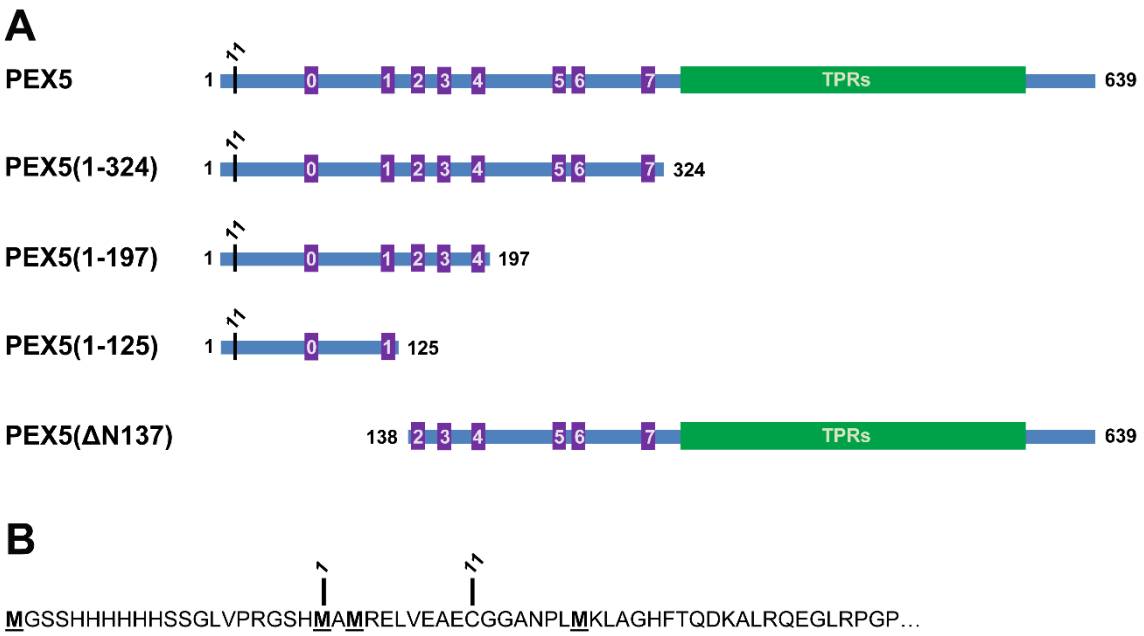

Figure 10. PEX5 molecules used in this study. A, full-length and truncated versions of the large isoform of human PEX5 are schematically represented. The conserved cysteine residue at position 11 (black), which was replaced by an alanine or a lysine in many of the proteins used in this study, the eight pentapeptide motifs responsible for the interaction with PEX13 and PEX14 (numbered from 0 to 7, purple bars) and the structured C-terminal half comprising seven tetratricopeptide repeats (TPRs, green box) are indicated. **B,** N-terminal sequence of the histidine-tagged PEX5 proteins used in this study.

The *in vitro* assays were performed at 37 ºC in the presence of ATP. Under these conditions, peroxisome-associated endogenous PEX5 is exported back into the soluble fraction of PNS, being the occupation of DTMs by the endogenous PEX5 largely decreased

(see Figure 11, compare lanes 2 and 4). Therefore, almost all the DTMs in the PNS are available to bind the ^{35}S-labeled PEX5 protein.

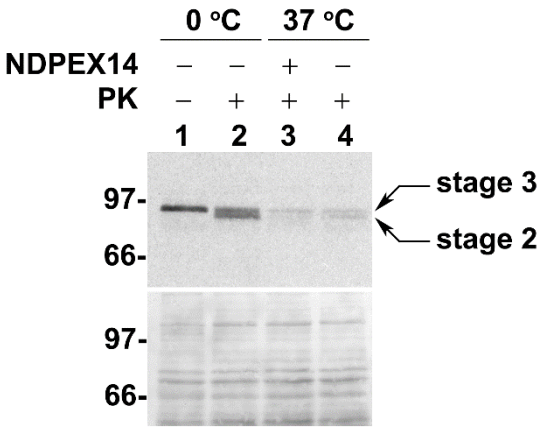

Figure 11. The amount of organelle-associated PK-protected endogenous PEX5 is largely decreased upon incubation at 37 ºC in the presence of ATP. A rat liver PNS in ATP-containing import buffer was incubated at 0 or 37 ºC in the absence (lanes 1, 2 and 4) or presence (lane 3) of 10 µM recombinant NDPEX14. After incubation, samples were treated (+) or not (–) with PK, as indicated. Organelles were then isolated and subjected to reducing SDS-PAGE/western-blotting. Endogenous rat PEX5 was detected by blot-overlay using ^{35}S-PEX14. Stage 2 and stage 3, DTM-embedded non-ubiquitinated and monoubiquitinated PEX5 species, respectively. Note that the Ub-PEX5 thioester conjugate is destroyed under reducing conditions. Thus, only the full-length PEX5 protein is detected in reducing gels (147). The autoradiograph (upper panel) and the corresponding Ponceau S-stained membrane (lower panel) are shown. Numbers to the left indicate the molecular weight (kDa) of protein standards.

The results in Figure 12 show that saturation or near-saturation conditions were reached for many of the PK-resistant species detected in these assays (a densitometric analysis of the data is shown below).

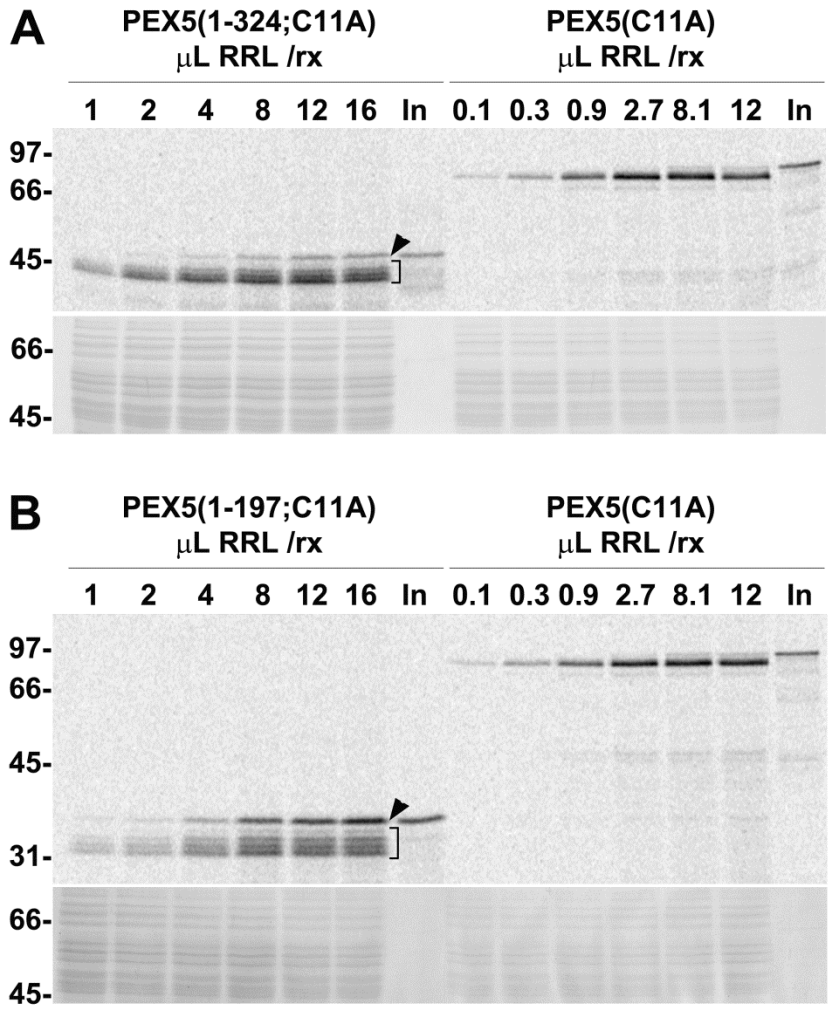

Figure 12. The DTM can accommodate more PEX5(1-197;C11A) molecules than full-length PEX5(C11A). A, increasing volumes of rabbit reticulocyte lysates (RRL; volumes in µL indicated at the top of each lane) containing either PEX5(1-324;C11A) or PEX5(C11A) were used in PNS-based *in vitro* reactions ("rx") performed at 37 ºC in the presence of ATP for 45 min. Organelle suspensions were then treated with PK, organelles were isolated and analyzed by SDS-PAGE/storage phosphor screen autoradiography. Total organelle samples (PEX5(1-324;C11A)) or one third of them (PEX5(C11A)) were loaded onto the gel. The phosphor image (upper panel), and a section of the corresponding Coomassie blue-stained gel (lower panel) are shown. Numbers to the left indicate the molecular weight (kDa) of protein standards. **B,** exactly as in A but using PEX5(1-197;C11A) and PEX5(C11A). In A and B, lanes In, RRL containing the indicated ^{35}S-labeled protein. Brackets and arrow heads indicate the PK-cleaved and intact ^{35}S-labeled proteins, respectively.

To confirm that the saturation observed reflects the occupation of PEX5-binding sites at the peroxisomal membrane, and not the titration of some soluble factor in the PNS, the import-competence of organelles pre-incubated with wild-type PEX5 or PEX5(C11A) was compared. While PEX5 cycles between peroxisomes and the soluble fraction of PNS, the C11A mutant accumulates into the DTM. As shown in Figure 13, the amount of PK-resistant PEX5(1-197;C11A) observed in organelles pre-incubated with PEX5(C11A) is lower than that

observed in organelles pre-incubated with PEX5. So, the saturation conditions observed in Figure 12 reflect occupation of PEX5-binding sites at the peroxisomal membrane.

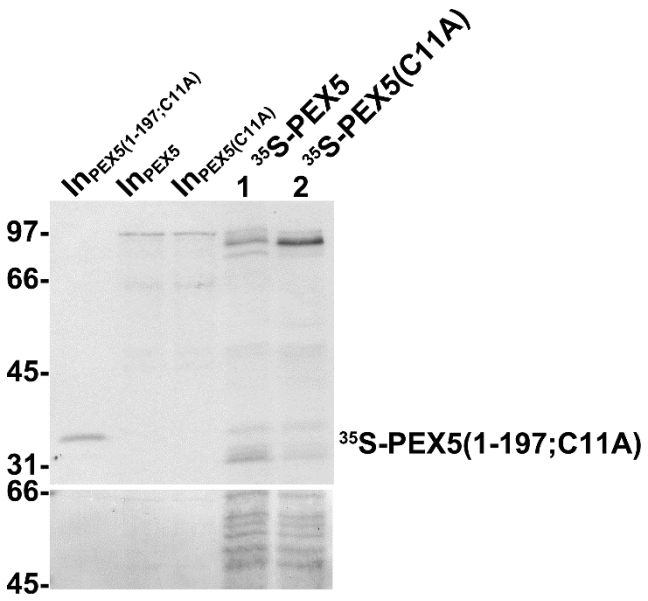

Figure 13. The import-competence of organelles pre-incubated with PEX5(C11A) is largely decreased. PEX5 and PEX5(C11A) were subjected to a PNS-based *in vitro* assay in the presence of ATP. After 30 min at 37 ºC, both reactions received PEX5(1-197;C11A) and were further incubated for 10 min at 37 ºC. After PK treatment, organelles were isolated by centrifugation and analyzed by SDS-PAGE/autoradiography. The RRLs containing radiolabeled PEX5(1-197;C11A) (lane $In_{PEX5(1-197;C11A)}$, input of lanes 1 and 2), wild-type PEX5 (lane In_{PEX5}; input of lane 1) and PEX5(C11A) (lane $In_{PEX5(C11A)}$; input of lane 2) were also analyzed. The autoradiograph (upper panel) and a portion of the Ponceau S-stained membrane (lower panel) are shown. Numbers to the left indicate the molecular weight (kDa) of protein standards.

Interestingly, for both PEX5(1-324;C11A) and PEX5(1-197;C11A), the PK-resistant species exhibited an unexpected heterogeneity; besides a set of partially cleaved species, a protein band corresponding to intact protein was also detected (indicated with brackets and arrow heads, respectively, in Figure 12), particularly in the PEX5(1-197;C11A) assays.

In order to know if all the partially cleaved species correspond to membrane-embedded molecules exposing their N-termini into the cytosol, *i.e.*, if all represent stage 2 PEX5, PK-treated organelles from an *in vitro* assay programmed with radiolabeled PEX5(1-197;C11A) were solubilized with detergent and digested with Genenase I. Genenase I is a protease that cleaves PEX5 only once near its N-terminus ((151); see also section IV-2.5.). As shown in Figure 14A, the PK-resistant PEX5(1-197;C11A) species were converted, by Genenase I, into a single 31-kDa protein, which co-migrates with the smallest PEX5(1-197;C11A) fragment generated by PK (compare lanes 3 and 4). Thus, all the partially cleaved species detected for PEX5(1-197;C11A) correspond to stage 2 PEX5.

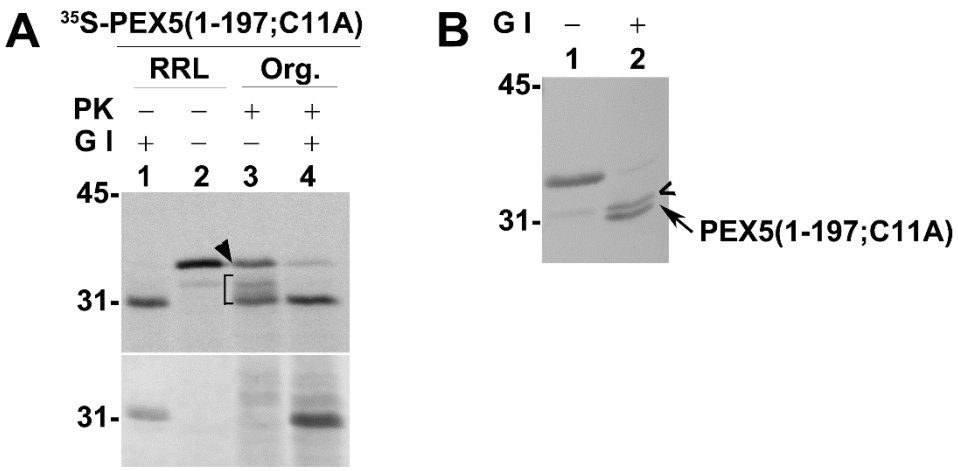

Figure 14. Characterization of PK-resistant, partially cleaved, PEX5(1-197;C11A) species. A, RRL containing PEX5(1-197;C11A) (lanes 1 and 2) or PK-treated organelles (Org.) from a PNS-based *in vitro* assay programmed with PEX5(1-197;C11A) (lanes 3 and 4) were incubated (+) or not (–) with Genenase I (G I) for 30 min at 23 ºC, as indicated. Samples were analyzed by SDS-PAGE/autoradiography. Autoradiograph (upper panel) and the corresponding Ponceau S-stained membrane (lower panel) are shown. Bracket and arrow head indicate the PK-cleaved and intact ^{35}S-labeled proteins, respectively. **B,** recombinant histidine-tagged PEX5(1-197;C11A) was incubated in the absence (–) or presence (+) of Genenase I (G I) for 3 h 30 min at 23 ºC, as indicated. Samples were analyzed by SDS-PAGE/Coomassie blue staining. The "<" symbol indicates Genenase I. In A and B, numbers to the left indicate the molecular weight (kDa) of protein standards.

The heterogeneity of the peroxisomal PK-cleaved PEX5 species observed for the C-terminally truncated versions of PEX5 (see Figure 12), together with the distribution of methionine residues at the N-terminus of PEX5 (see Figure 4A), raises some uncertainty in the determination of stoichiometries of DTM-bound PEX5 molecules. Thus, three different possibilities were considered (see Figure 15A). The most likely possibility (scenario #1) assumes, for the C-terminally truncated versions of PEX5, that: 1) the smallest PK-resistant PEX5 species (peak I, see also Figure 4E) has the same size, and therefore the same number of methionines, of Genenase I-cleaved PEX5 species (see Figure 14A); 2) the largest PK-cleaved PEX5 species (peak IV, see also Figure 4E) is larger than the corresponding untagged PEX5 species (see below); and 3) the difference in size between any two adjacent PK-resistant species in the SDS-gel is approximately 1 kDa (see Figure 12). The other two possibilities assume that: 1) band/peak IV is larger than the untagged protein (see below); and 2) all the other PK-cleaved species contain either the minimum (scenario #2) or the maximum (scenario #3) number of possible methionines.

The results of these analyses are shown in Figure 15B. Considering the most likely distribution of PK-cleavage sites in the PEX5 molecules (scenario #1), at saturation conditions, the estimated molar ratios of DTM-bound PEX5(1-197;C11A), PEX5(1-324;C11A), and PEX5(C11A) were 2.5:1.2:1, respectively. The other two possibilities assume PK-cleavage sites that result in the largest (scenario #2) and smallest (scenario #3)

molar ratios of DTM-bound PEX5(1-197;C11A):PEX5(1-324;C11A):PEX5(C11A) – estimated values of 3.2:1.4:1 and 1.8:1:1 were obtained, respectively. Thus, the results clearly indicate that the DTM can accommodate more PEX5(1-197;C11A) molecules than full-length PEX5(C11A). In fact, these ratios are probably larger because intact PK-resistant PEX5(1-197;C11A) is also specifically bound to peroxisomes, as shown below.

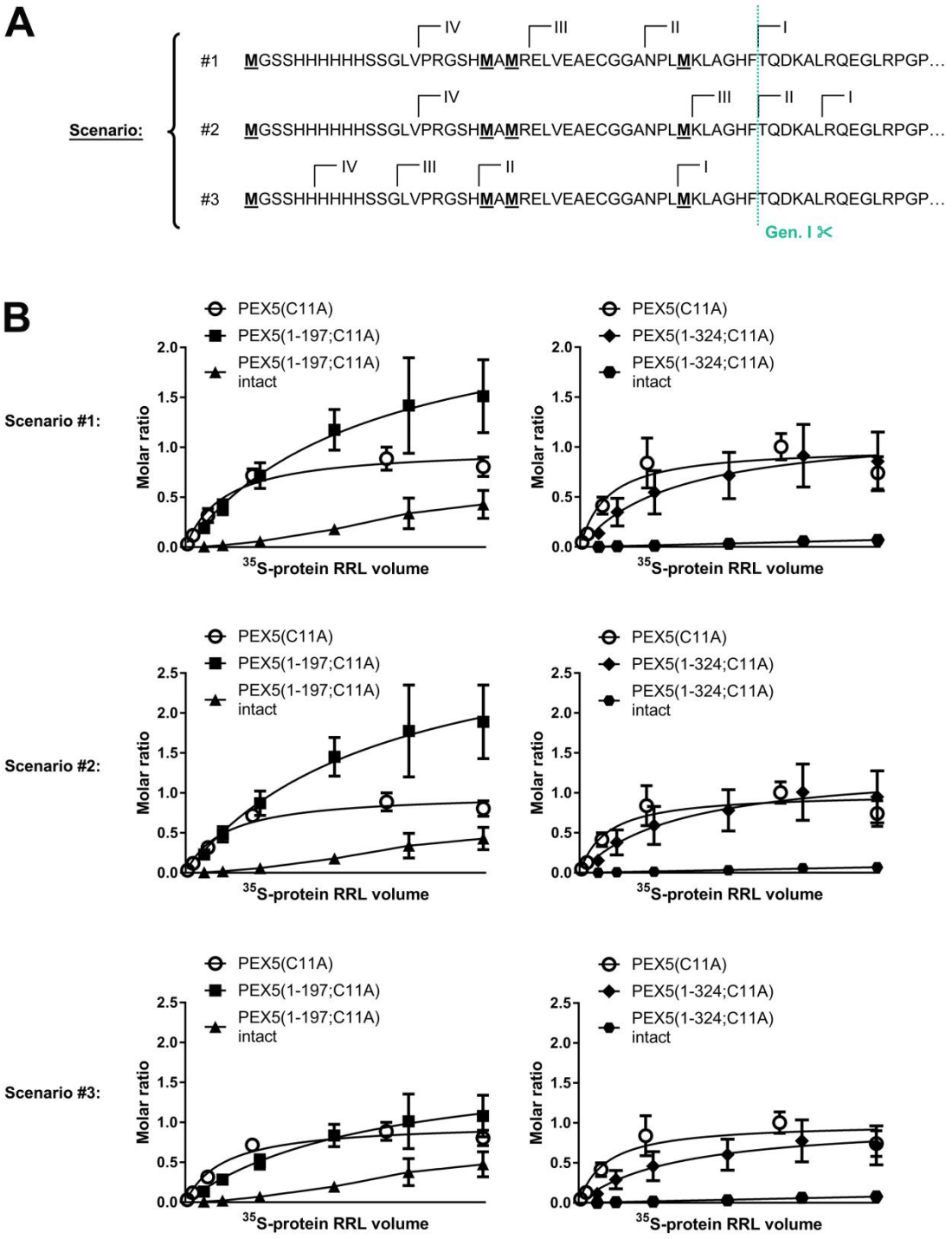

Figure 15. Molar ratios of DTM-bound PEX5(1-324;C11A) or PEX5(1-197;C11A) to PEX5(C11A), considering three different scenarios. A, different possibilities (scenario #1, #2 and #3) for the distribution of

PK-cleavage sites in the N-termini of truncated versions of PEX5, that results in peaks I to IV (see Figure 4). **B,** molar ratios of DTM-bound PEX5(1-324;C11A) or PEX5(1-197;C11A) to PEX5(C11A). Averages and standard deviations from four replicates are shown. Signal intensities from the quantitative analysis of the phosphor images were normalized for protein loads and for the methionine number in each radiolabeled protein, fitted to a dose response one-site specific binding curve, and divided by the Bmax value obtained for full-length PEX5(C11A). In scenario #1, Bmax values for PEX5(1-197;C11A) and PEX5(C11A) are 2.52 (95% confidence interval (CI) = 1.82-4.46) and 1.00 (95% CI = 0.90-1.11), respectively (left panel); and Bmax values for PEX5(1-324;C11A) and PEX5(C11A) are 1.21 (95% CI = 0.88-1.99) and 1.00 (95% CI = 0.85-1.18), respectively (right panel). In scenario #2, Bmax values for PEX5(1-197;C11A) and PEX5(C11A) are 3.24 (95% CI = 2.32-5.87) and 1.00 (95% CI = 0.90-1.11), respectively (left panel); and Bmax values for PEX5(1-324;C11A) and PEX5(C11A) are 1.35 (95% CI = 0.97-2.28) and 1.00 (95% CI = 0.85-1.18), respectively (right panel). In scenario #3, Bmax values for PEX5(1-197;C11A) and PEX5(C11A) are 1.82 (95% CI = 1.31-3.24) and 1.00 (95% CI = 0.90-1.11), respectively (left panel); and Bmax values for PEX5(1-324;C11A) and PEX5(C11A) are 1.02 (95% CI = 0.75-1.69) and 1.00 (95% CI = 0.85-1.18), respectively (right panel). Note that intact PEX5(1-324;C11A) and intact PEX5(1-197;C11A) data cannot be fitted to the same dose response curve ("ambiguous fit"); in these cases the lines simply connect averages. Note that the abscissa scale is different for the two radiolabeled proteins. Note also that for some points the error bars are shorter than the height of the symbols.

2.2.1. Characterization of intact PK-resistant PEX5(1-197;C11A) species

The existence of a PK-resistant species corresponding to intact protein in the saturation binding experiments described above was particularly striking. These assays were performed with non-ubiquitinatable PEX5 molecules and, to date, only DTM-embedded Ub-PEX5 (stage 3) was known to display this behavior. Thus, the properties of this species were analyzed in detail.

Since unusual large amounts of radiolabeled proteins were used in these assays, the possibility of intact PK-resistant species might be a consequence of some non-specific event (*e.g.*, encapsulation of a small fraction of the radiolabeled protein into some membrane vesicles during sample processing) was considered. In order to know if the intact PK-resistant species is localized at the peroxisomes, a PK-treated PNS-based *in vitro* reaction programmed with radiolabeled PEX5(1-197;C11A) was loaded onto the top of a Histodenz™ step gradient and centrifuged. Twelve fractions were collected from the bottom of the gradient and subjected to SDS-PAGE/western-blotting/autoradiography (see Figure 16A). This method takes advantage of the high density of peroxisomes compared with the other organelles present in the PNS (233). The distribution of mitochondria and endoplasmic reticulum was assessed with antibodies directed to cytochrome *c* and the retention signal KDEL, respectively; both were found in fractions 7-12. Only peroxisomes were found near the bottom of the gradient, as assessed using an antibody directed to PEX14. Importantly, intact PK-resistant PEX5(1-197;C11A) co-purified with peroxisomes, as did stage 2 PEX5(1-197;C11A). Moreover, as shown in Figure 16B, intact PK-resistant PEX5(1-197;C11A) was not extracted from the peroxisomal membrane by sonication in a low ionic-strength buffer,

similarly to stage 2 species. Under these conditions, the peroxisomal matrix protein catalase was released and found in the soluble fraction, as expected. Therefore, intact PK-resistant PEX5(1-197;C11A) represents a peroxisome membrane-bound species.

To evaluate the specificity of its association with peroxisomes, radiolabeled PEX5(1-197;C11A) was subjected to a PNS-based *in vitro* reaction in the presence of NDPEX14. As previously mentioned, the N-terminal domain of PEX14 binds with high affinity to the pentapeptide motifs present in the N-terminal half of PEX5 (142, 143, 146), and as a result, blocks the insertion of the receptor into the peroxisomal membrane (87, 152). As shown in Figure 16C, no PK-resistant species were detected in this assay, indicating that the association of intact PK-resistant PEX5(1-197;C11A) with peroxisomes is as specific as that yielding stage 2 PEX5(1-197;C11A).

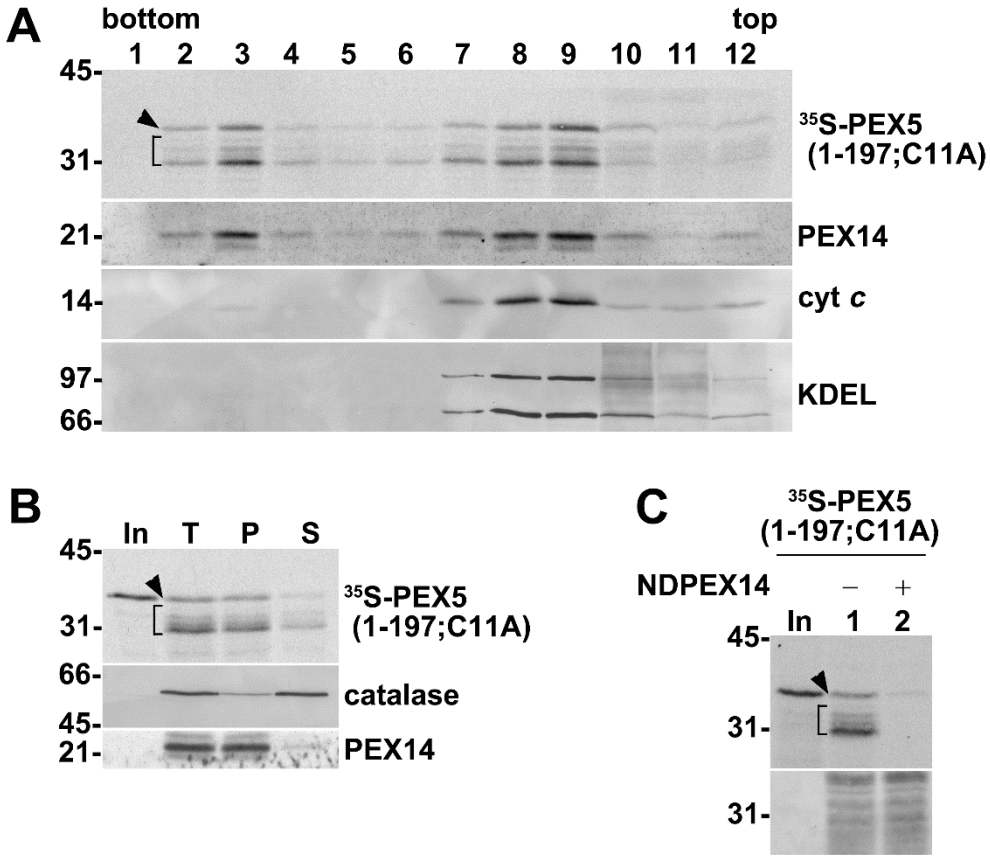

Figure 16. Characterization of intact PK-resistant PEX5(1-197;C11A) species. A, a PK-treated PNS-based *in vitro* reaction performed with PEX5(1-197;C11A) was loaded onto the top of a Histodenz™ gradient and centrifuged. Twelve fractions were then collected from the bottom of the gradient and analyzed by SDS-PAGE/western-blotting/autoradiography. An autoradiograph (upper panel) showing the distribution of PK-resistant PEX5(1-197;C11A) species, and western-blots probed with antibodies directed to PEX14 (peroxisomes), cytochrome *c* (cyt *c*; mitochondria) and the retention signal KDEL (endoplasmic reticulum) are presented. Note that PEX14 is converted into a small fragment upon PK digestion (153). **B,** PK-treated organelles from an *in vitro* assay programmed with PEX5(1-197;C11A) were disrupted by sonication. Half of the sample was kept on ice (lane T), and the other was centrifuged to separate membrane (lane P) and soluble (lane S) fractions. Samples

were analyzed by SDS-PAGE/western-blotting/autoradiography. The autoradiograph (upper panel) showing PK-resistant PEX5(1-197;C11A) species, and blots showing the distribution of catalase (a peroxisomal matrix protein) and PEX14 (an intrinsic membrane protein) are presented. **C,** PEX5(1-197;C11A) was subjected to a PNS-based *in vitro* assay in the absence (lane 1) or presence (lane 2) of 10 µM recombinant NDPEX14. PK-treated organelles were analyzed by SDS-PAGE/autoradiography. The autoradiograph (upper panel) and the corresponding Ponceau S-stained membrane (lower panel) are shown. In B and C, lanes In, RRL containing ^{35}S-labeled PEX5(1-197;C11A). In A to C, brackets and arrow heads indicate the PK-cleaved and intact ^{35}S-labeled PEX5(1-197;C11A), respectively. Numbers to the left indicate the molecular weight (kDa) of protein standards.

Furthermore, the amount of intact PK-resistant PEX5(1-197;C11A) was largely decreased when the *in vitro* assays were performed in the presence of recombinant full-length PEX5(C11A) (see Figure 17, compare lanes 4 and 5). Conversely, recombinant PEX5(1-197;C11A) prevented the insertion of PEX5(C11A) into the peroxisomal membrane (compare lanes 7 and 8). Taken together, the results strongly suggest that both truncated and full-length PEX5 molecules compete for the same PEX5-binding sites at the organelle membrane.

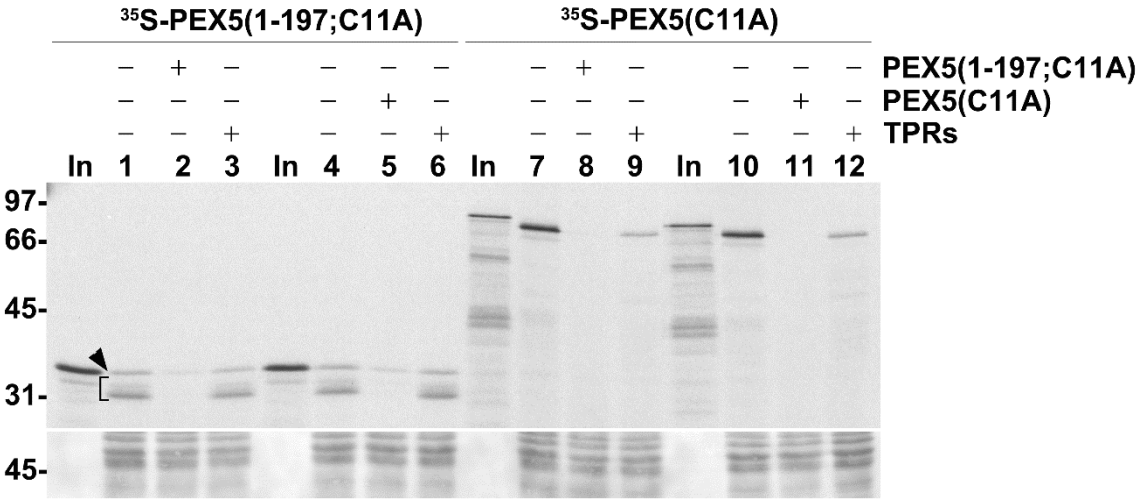

Figure 17. PEX5(1-197;C11A) and PEX5(C11A) compete for the same PEX5-binding sites at the peroxisomal membrane. PNS in import buffer containing ATP was pre-incubated for 5 min at 37 ºC in the absence (–) or presence (+) of the indicated recombinant proteins (15 µg each of PEX5(1-197;C11A), or PEX5(C11A), or TPRs). Radiolabeled PEX5(1-197;C11A) and PEX5(C11A) were then added, as specified, and the reactions were incubated for 30 min. PK-treated organelles were then subjected to SDS-PAGE/ autoradiography. The autoradiograph (upper panel) and a portion of the Ponceau S-stained membrane (lower panel) are shown. Lanes In, RRL containing radiolabeled PEX5(1-197;C11A) and PEX5(C11A), as indicated. Stage 2 PEX5(1-197;C11A) (bracket) and intact PK-resistant PEX5(1-197;C11A) (arrow head) are also indicated. Numbers to the left indicate the molecular weight (kDa) of protein standards.

As stated above, all the PEX5 molecules used in these assays have a histidine tag at their N-termini. For full-length PEX5(C11A), the histidine tag does not change its behavior

during PK digestion; essentially all the peroxisome-associated PEX5(C11A) was degraded by PK into a slightly shorter protein (see Figure 12), as observed before for the untagged PEX5 (*e.g.*, see figure 1 in (147)). To determine whether or not the unexpected heterogeneity observed for the peroxisome-associated C-terminally truncated versions of PEX5, upon PK digestion, results from the presence of the histidine tag in an artificially truncated PEX5 protein, a very large volume of an *in vitro* synthesized untagged version of PEX5(1-197;C11A) was used in an *in vitro* assay. Similar PK-resistant species were detected with the untagged protein (see Figure 18, compare lanes 2 and 3). Seemingly, intact PK-resistant species are observed in these assays as a result of the large amount of C-terminally truncated PEX5 molecules used in the *in vitro* reactions.

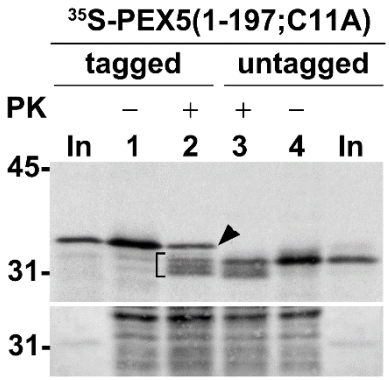

Figure 18. PEX5(1-197;C11A) without a N-terminal histidine tag behaves similarly to PEX5(1-197;C11A) in PNS-based *in vitro* assays. RRL (16 µL) containing untagged PEX5(1-197;C11A) was used in a PNS-based *in vitro* assay, the reaction was divided into two halves (lanes 3 and 4) and one half was treated with PK, as indicated. For comparison, an identical assay performed with the histidine-tagged PEX5(1-197;C11A) (lanes 1 and 2) is also shown. Organelle pellets were then subjected to SDS-PAGE/autoradiography. The autoradiograph (upper panel) and a portion of the Ponceau S-stained membrane (lower panel) are shown. Lanes In, RRL containing ^{35}S-labeled histidine-tagged or untagged PEX5(1-197;C11A). Stage 2 (bracket) and intact PK-resistant (arrow head) species from histidine-tagged PEX5(1-197;C11A) are indicated. Numbers to the left indicate the molecular weight (kDa) of protein standards.

To better understand the nature of the intact PK-resistant PEX5(1-197;C11A), the radiolabeled protein was subjected to a PNS-based *in vitro* reaction, aliquots were taken at different time points, and digested with PK. The isolated organelles were analyzed by SDS-PAGE/storage phosphor screen autoradiography. As shown in Figure 19, the intact PK-resistant species displays a slower kinetics than partially cleaved species. Apparently, the PEX5-binding site occupied by this abnormal PEX5 population is kinetically different from the one occupied by the partially cleaved species. The saturation-binding experiments presented in Figure 12B might already suggest this.

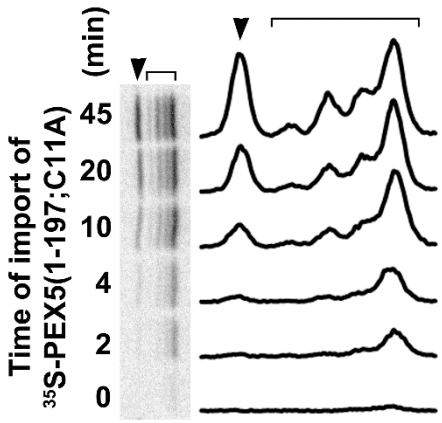

Figure 19. Peroxisome-membrane binding kinetics of intact PK-resistant PEX5(1-197;C11A). RRL containing PEX5(1-197;C11A) was incubated with a PNS in import buffer containing ATP. At the indicated time points, aliquots were withdrawn, treated with PK and the organelles were isolated and analyzed by SDS-PAGE/storage phosphor screen autoradiography. The brackets and arrow heads indicate PK-cleaved and intact PK-resistant PEX5(1-197;C11A), respectively. An intensity profile of each lane is shown.

In summary, the results obtained suggest that PEX5(1-197;C11A) and PEX5(C11A) bind to the same PEX5-binding sites at the peroxisomal membrane, but interact with the DTM with different stoichiometries. Seemingly, many of the sites available to bind a full-length PEX5(C11A) molecule can accommodate more than one truncated PEX5(1-197;C11A) molecule.

2.3. DTM-bound PEX5(1-125;C11A/K) is accessible to PK

When radiolabeled PEX5(1-125;C11A) – a protein comprising only the first 125 amino acid residues of PEX5 (see Figure 10A) – is subjected to a PNS-based *in vitro* assay, PK-resistant species are not observed (see Figure 20, compare lanes 3 and 4 with lanes 7 and 8). In principle, this might suggest that the protein is not associated with the peroxisomes. However, when radiolabeled PEX5(1-125;C11K) – a protein also comprising only the first 125 amino acid residues of PEX5 but with a lysine at position 11 (C11K) – is incubated with a primed PNS in the presence of AMP-PNP (a non-hydrolysable ATP analog that can be used by the ubiquitin-conjugating cascade but not by the REM, (86)), and the PK treatment is omitted, a monoubiquitinated species is clearly detected (see Figure 20, compare lanes 1 and 5). Also, Ub-PEX5(1-125;C11K) is accessible to PK (see Figure 20, compare lanes 1 and 2 with lanes 5 and 6), similarly to PEX5(1-125;C11A). Thus, the protein comprising the first 125 amino acid residues of PEX5 associates with the peroxisome, and is a substrate for the DTM RING finger peroxins, but remains accessible to PK.

Note that the replacement of the cysteine 11 by a lysine results in a functional PEX5 protein that behaves as the wild-type both in *in vitro* and in *in vivo* assays, *i.e.*, it is inserted into the DTM, monoubiquitinated and extracted to the cytosol in an efficient manner (180).

However, while the thioester bond between ubiquitin and the cysteine from PEX5 wild-type is quite labile and tends to hydrolyze during non-reducing SDS-PAGE, the isopeptidic bond linking ubiquitin to PEX5(C11K) species is not. Therefore, the use of C11K mutants is experimentally advantageous because SDS-PAGE can be done under reducing conditions.

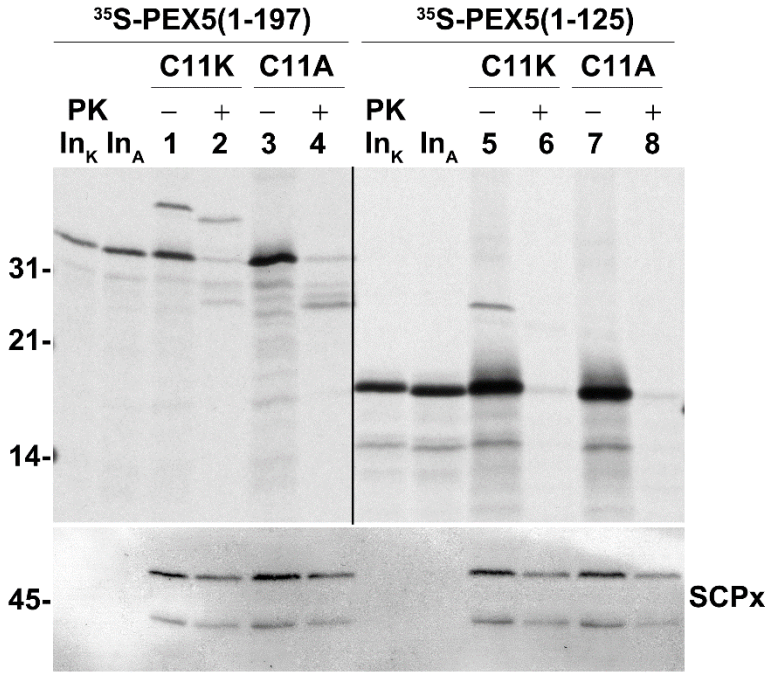

Figure 20. PEX5(1-125;C11K) is correctly monoubiquitinated but does not acquire a PK-protected status. A primed PNS was used in AMP-PNP-supplemented *in vitro* assays programmed with PEX5(1-197;C11K) (lanes 1 and 2; "C11K"), or PEX5(1-197;C11A) (lanes 3 and 4; "C11A"), or PEX5(1-125;C11K) (lanes 5 and 6; "C11K"), or PEX5(1-125;C11A) (lanes 7 and 8; "C11A"). One half of each reaction was treated with PK, as indicated. Organelle fractions were analyzed by SDS-PAGE/western-blotting/autoradiography. The autoradiograph (upper panel) and the corresponding nitrocellulose membrane probed with an antibody directed to SCPx (lower panel), to assess intactness of peroxisomes (224), are shown. The exposure time of the PEX5(1-125;C11K/A) panel was 4-fold larger than the one of PEX5(1-197;C11K/A) to obtain identical intensities of the ubiquitinated species. Note that PEX5(1-197;C11K/A) and PEX5(1-125;C11K/A) have the same number of methionines. Lanes In_K and In_A, RRL containing the C11K and C11A versions of the indicated ^{35}S-labeled proteins, respectively. Numbers to the left indicate the molecular weight (kDa) of protein standards.

The interaction between PEX5 and the DTM happens in two steps: a reversible docking, in which PEX5 remains at the organelle surface and protease-accessible (152), followed by the irreversible (in the absence of ATP) insertion of PEX5 into the DTM, where PEX5 remains protease-resistant (151). One possible explanation for the results presented in Figure 20 is that PEX5(1-125;C11A/K) is unable to enter the DTM remaining trapped at the docking step and, therefore, PK-accessible. To test this hypothesis, organelles isolated from a PNS-based *in vitro* reaction performed with radiolabeled PEX5(1-125;C11K) in the presence of AMP-PNP were resuspended in import buffer and incubated with either

recombinant PEX5(1-324) or PEX19. PEX5(1-324) interacts with the DTM and competes with PEX5 at the docking step (152), whereas PEX19 is a protein involved in a different aspect of peroxisomal biogenesis and was used here as a negative control (66). Organelle-associated proteins and soluble proteins were then separated by centrifugation and subjected to SDS-PAGE/autoradiography. Because protease-treatment cannot be done in this type of experiments, the radiolabeled protein that remains non-specifically adsorbed to the organelles is not degraded, explaining the relatively large background observed (see (152)). As shown in Figure 21, a fraction of the non-ubiquitinated PEX5(1-125;C11K) was specifically extracted from the organelles upon incubation with recombinant PEX5(1-324), indicating that the protein was specifically adsorbed to peroxisomes, as expected for a PEX5 molecule at the docking step (152). On the contrary, all the Ub-PEX5(1-125;C11K) remained in the organelle pellet upon incubation with recombinant PEX5(1-324). Seemingly, Ub-PEX5(1-125;C11K) is beyond the docking step.

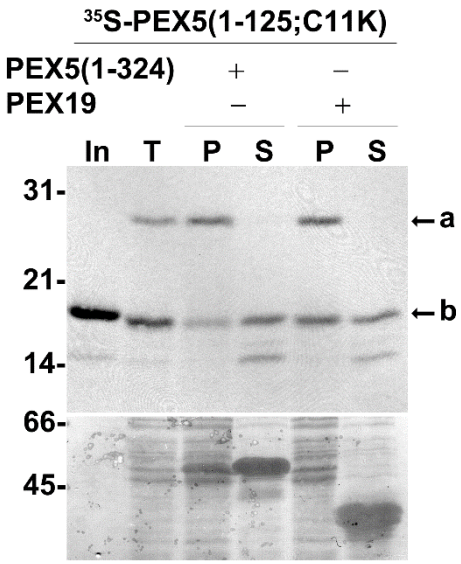

Figure 21. Ub-PEX5(1-125;C11K), but not PEX5(1-125;C11K), is tightly bound to organelles. PEX5(1-125;C11K) was incubated with a primed PNS in AMP-PNP-containing import buffer for 30 min. The organelles were then recovered by centrifugation, resuspended in import buffer and divided into three tubes. One tube was kept on ice (lane T), and the other two were incubated for 15 min at 37 ºC in the presence of 10 µg of either recombinant PEX5(1-324) or PEX19, as indicated. Organelles (P) and the corresponding supernatants (S) were separated by centrifugation and analyzed by SDS-PAGE/autoradiography. The autoradiograph (upper panel) and a portion of the corresponding Ponceau S-stained membrane (lower panel) are shown. Lane In, RRL containing the ^{35}S-labeled PEX5(1-125;C11K). The a and b indicate monoubiquitinated and non-ubiquitinated PEX5 species, respectively. Numbers to the left indicate the molecular weight (kDa) of protein standards.

We next subjected PEX5(1-125;C11K) to a two-step import-export experiment (86), aiming at determining whether this truncated PEX5 species is also a substrate for the REM. Succinctly, radiolabeled PEX5(1-125;C11K) was incubated with a primed PNS in the

presence of AMP-PNP (to accumulate Ub-PEX5(1-125;C11K) at the DTM), then the isolated organelles were resuspended in import buffer and incubated with either AMP-PNP (to maintain the block of the REM) or ATP (to activate the REM). Organelle-associated and soluble proteins were analyzed by SDS-PAGE/western-blotting/autoradiography. As shown in Figure 22 (right panel), in the export reaction containing AMP-PNP, Ub-PEX5(1-125;C11K) remained in the organelle fraction, as expected. In the ATP-containing export reaction, on the contrary, a large fraction of Ub-PEX5(1-125;C11K) was released into the supernatant. The same results were obtained with PEX5(1-197;C11K), used here as a positive control (Figure 22 (left panel)). Thus, Ub-PEX5(1-125;C11K) is a substrate for the REM. Similar results had been previously observed in our laboratory for the untagged version of this protein (215).

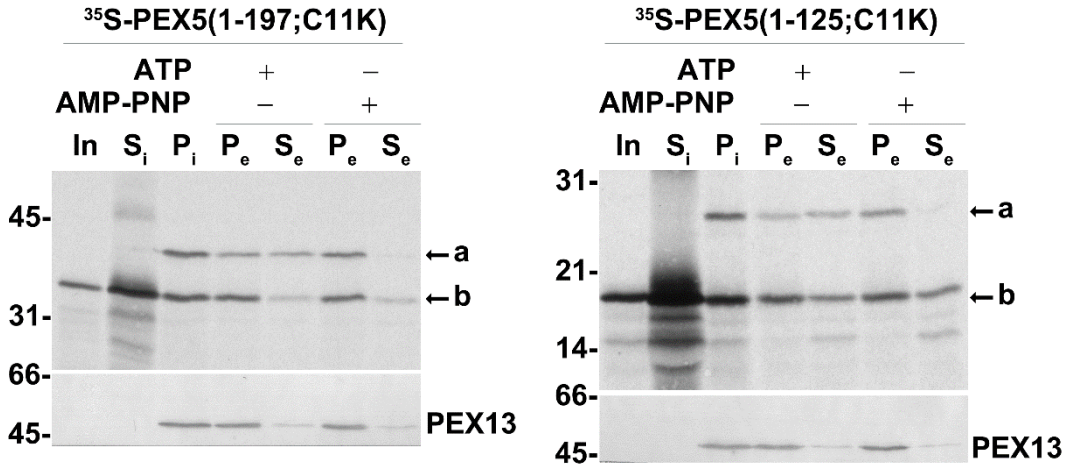

Figure 22. Ub-PEX5(1-125;C11K) is a substrate for the REM. PEX5(1-197;C11K) (left panels) or PEX5(1-125;C11K) (right panels) were incubated with a primed PNS in import buffer supplemented with ubiquitin aldehyde and AMP-PNP. The reactions were then centrifuged to separate supernatant fraction (Si) from organelles (Pi). The organelles were resuspended in an ATP- or AMP-PNP-containing import buffer, and further incubated for 15 min at 37 ºC. The organelle suspensions were again centrifuged to obtain a supernatant (Se) and an organelle pellet (Pe). Samples were analyzed by SDS-PAGE/western-blotting/autoradiography. The autoradiographs (upper panels) and the behavior of endogenous PEX13 (lower panels) are shown. Si, equivalent to 50 µg of PNS; Pi, Pe and Se, equivalent to 600 µg of PNS. Lanes In, RRL containing radiolabeled PEX5(1-197;C11K) and PEX5(1-125;C11K), as indicated. The a and b indicate monoubiquitinated and non-ubiquitinated PEX5 species, respectively. Numbers to the left indicate the molecular weight (kDa) of protein standards.

As previously mentioned, DTM-embedded PEX5 displays a transmembrane topology, exposing most of its polypeptide chain into the peroxisomal matrix (211). To determine whether or not PEX5(1-125;C11K) also acquires a transmembrane topology during its passage through the DTM, we employed a strategy previously used to show that a portion of the polypeptide chains of PEX5 and PEX7 reach the peroxisomal matrix (186, 214). Specifically, two almost identical PEX5(1-125;C11K) proteins, both having at their C-termini an extension of about 5 kDa, were synthesized. In one of these proteins, called PEX5(1-

125;C11K)-clv, the extension comprises a cleavable, but otherwise non-functional, PTS2 derived from pre-thiolase pre-sequence (214), followed by 19 amino acid residues corresponding to the N-terminus of human sterol carrier protein-2; the other protein, named PEX5(1-125;C11K)-nclv, is identical to PEX5(1-125;C11K)-clv with the exception that it lacks the last two residues of the non-functional pre-thiolase pre-sequence (see Experimental Procedures for details). This deletion was designed based on the observation that a similar deletion in pre-phytanoyl CoA hydroxylase dramatically decreased its processing efficiency at the peroxisomal matrix (116). The PTS2-containing proteins are processed upon import, in the peroxisomal matrix, by Tysnd1 (97). Thus, if the C-terminus of PEX5(1-125;C11K)-clv becomes exposed into the peroxisomal matrix, a 2-kDa shorter protein should be generated by the action of Tysnd1. In contrast, no or very little cleavage should be observed for PEX5(1-125;C11K)-nclv.

Both radiolabeled proteins were subjected to PNS-based *in vitro* assays performed in the presence of AMP-PNP, and organelle-bound and soluble proteins were analyzed by SDS-PAGE/autoradiography. The results in Figure 23 show that a small fraction of PEX5(1-125;C11K)-clv was converted into a smaller protein (indicated by an arrow head). Thus, at least a fraction of PEX5(1-125;C11K)-clv acquires a transmembrane topology during its transient passage through the DTM.

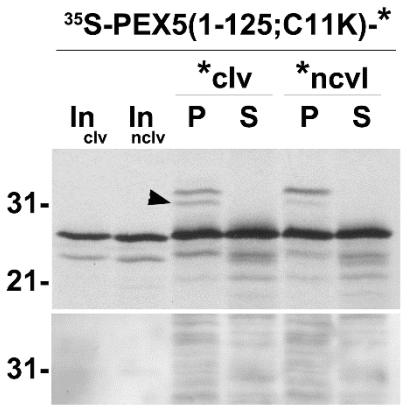

Figure 23. PEX5(1-125;C11K)-clv is partially processed in the PNS-based *in vitro* assay. PEX5(1-125;C11K)-clv and PEX5(1-125;C11K)-nclv were subjected to PNS-based *in vitro* assays in the presence of AMP-PNP for 60 min. The reactions were then centrifuged to separate organelles (lanes P) from soluble proteins (lanes S). Organelles and soluble fractions from 600 µg and 100 µg of PNS, respectively, were subjected to SDS-PAGE/ autoradiography. Lanes Inclv and Innclv, RRL containing the indicated ^{35}S-labeled proteins. The autoradiograph (upper panel) and the corresponding Ponceau S-stained membrane (lower panel) are shown. The cleaved species is indicated by an arrow head. Numbers to the left indicate the molecular weight (kDa) of protein standards.

In summary, the results obtained suggest that a small protein containing only the first 125 amino acid residues of PEX5 can enter the DTM, yielding a correct substrate for the RING finger peroxins and for the REM, and yet remains largely accessible to PK added from the cytosolic side of the peroxisomal membrane.

2.4. Two non-overlapping PEX5 fragments interact with the DTM in a competitive manner

In addition to the PEX5 molecules previously mentioned, a N-terminal truncated molecule comprising the amino acid residues 138 to 639 of PEX5 (PEX5(ΔN137)) was used in this study (see Figure 10A). It was already shown that PEX5(ΔN137) can still become inserted into the DTM in a cargo-dependent manner (215). Importantly, this protein shows no sequence overlap with PEX5(1-125).

To determine whether or not both PEX5(ΔN137) and PEX5(1-125) compete for insertion into the DTM, PNS-based *in vitro* assays were programmed with radiolabeled PEX5(1-125;C11K) in the presence of AMP-PNP and recombinant PEX5(ΔN137) or TPRs. TPRs lack the PEX5 domain required for a productive interaction with the DTM and was used as a negative control. Organelles were then isolated and analyzed by SDS-PAGE/autoradiography. The results in Figure 24 show that the amount of Ub-PEX5(1-125;C11K) was largely decreased when PEX5(ΔN137) was added to the reaction (lanes 4-6). The same result was observed for PEX5(1-197;C11K) (lanes 1-3), a protein that shares some DTM-interacting regions with PEX5(ΔN137) (see Figure 10A). So, the two proteins compete for insertion into the DTM.

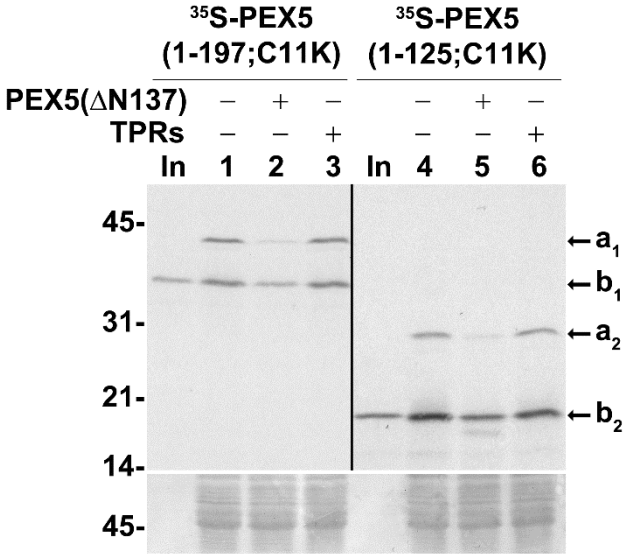

Figure 24. Two non-overlapping PEX5 fragments interact with the DTM in a competitive manner. PEX5(1-197;C11K) and PEX5(1-125;C11K) were subjected to PNS-based *in vitro* assays in the presence of AMP-PNP and in the absence (–) or presence (+) of 1 µM of recombinant PEX5(ΔN137) or TPRs, as indicated. Organelle

fractions were analyzed by SDS-PAGE/autoradiography. The autoradiograph (upper panel) and a portion of the corresponding Ponceau S-stained membrane (lower panel) are shown. The exposure time of the PEX5(1-125;C11K) panel was 4-fold larger than that of PEX5(1-197;C11K). Lanes In, RRL containing the indicated ^{35}S-labeled proteins. The a and b indicate monoubiquitinated and non-ubiquitinated PEX5 species, respectively. Numbers to the left indicate the molecular weight (kDa) of protein standards.

To clarify if the competition between PEX5(ΔN137) and PEX5(1-125;C11K) is occurring at the docking step or only at the insertion step, the experiment presented in Figure 21 was repeated but this time using recombinant PEX5(ΔN137) as a competitor of organelle-associated PEX5(1-125;C11K). As shown in Figure 25, a fraction of the non-ubiquitinated PEX5(1-125;C11K) was specifically extracted from the organelles upon incubation with recombinant PEX5(ΔN137), suggesting that PEX5(ΔN137) competes with PEX5(1-125;C11K) at the docking step.

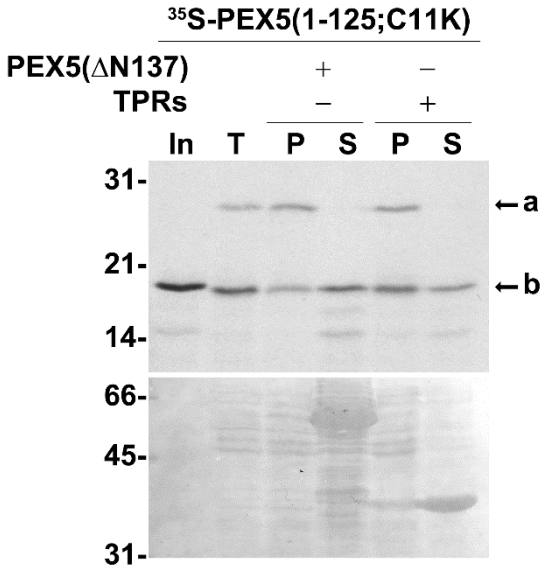

Figure 25. PEX5(ΔN137) competes with PEX5(1-125;C11K) at the docking step. PEX5(1-125;C11K) was incubated with a primed PNS in AMP-PNP-containing import buffer for 30 min. The organelles were then isolated by centrifugation, resuspended in import buffer and divided into three tubes. One tube remained on ice (lane T). The others were incubated for 15 min at 37 ºC in the presence 10 µg of either recombinant PEX5(ΔN137) or TPRs, as indicated. Organelle (P) and soluble proteins (S) were separated by centrifugation and analyzed by SDS-PAGE/autoradiography. The autoradiograph (upper panel) and a portion of the corresponding Ponceau S-stained membrane (lower panel) are shown. Lane In, RRL containing ^{35}S-labeled PEX5(1-125;C11K). The a and b indicate monoubiquitinated and non-ubiquitinated PEX5 species, respectively. Numbers to the left indicate the molecular weight (kDa) of protein standards.

2.5. Supplemental results – Mapping of the Genenase I-cleavage site in PEX5

Genenase I is an engineered protease, a variant of the subtilisin from *Bacillus amyloliquefaciens*, in which the catalytic histidine was replaced by an alanine. This protease works by "substrate-assisted catalysis": a histidine from the substrate substitutes the mutated catalytic residue and contributes to the catalysis (220). It is described that Genenase I cleaves particularly well at sites possessing a histidine at the P2 position and a phenylalanine or a tyrosine at the P1 position (220). Two such sequences exist in human PEX5 – His23Phe24 and His578Phe579 – but previous work suggests that only the first is cleaved by Genenase I (151). To confirm the exact cleavage site of Genenase I in PEX5, intact and Genenase I-cleaved recombinant histidine-tagged PEX5(1-197;C11A) (see Figure 14B) were analyzed by mass spectrometry in the reflectron mode at i3S Proteomics Core Facility. Note that residues His23Phe24 of human PEX5 correspond to residues His43Phe44 of the histidine-tagged PEX5(1-197;C11A). For the intact protein, no small peptides were found (see Figure 26A), while for the Genenase I-cleaved protein, five major small peptides were detected (see Figure 26B). Importantly, all map to the 1-44 amino acid region of histidine-tagged PEX5(1-197;C11A) (see Figure 26C).

The same protein samples were also analyzed by mass spectrometry in the linear mode. Masses of 23963.6 Da (MH+) for the intact protein (theoretical mass 23961.172 Da (MH+), excluding the initial methionine) and 19405.6 Da for the Genenase I-cleaved protein were determined (see Figure 27A and B). This suggests that Genenase I removes a region of 4576 Da from PEX5(1-197;C11A), in good agreement with the theoretical molecular mass of 4576.13 Da for a peptide comprising amino acid residues 2-44 of the protein. Collectively, the results from mass spectrometry show that Genenase I cleaves PEX5 immediately after Phe24.

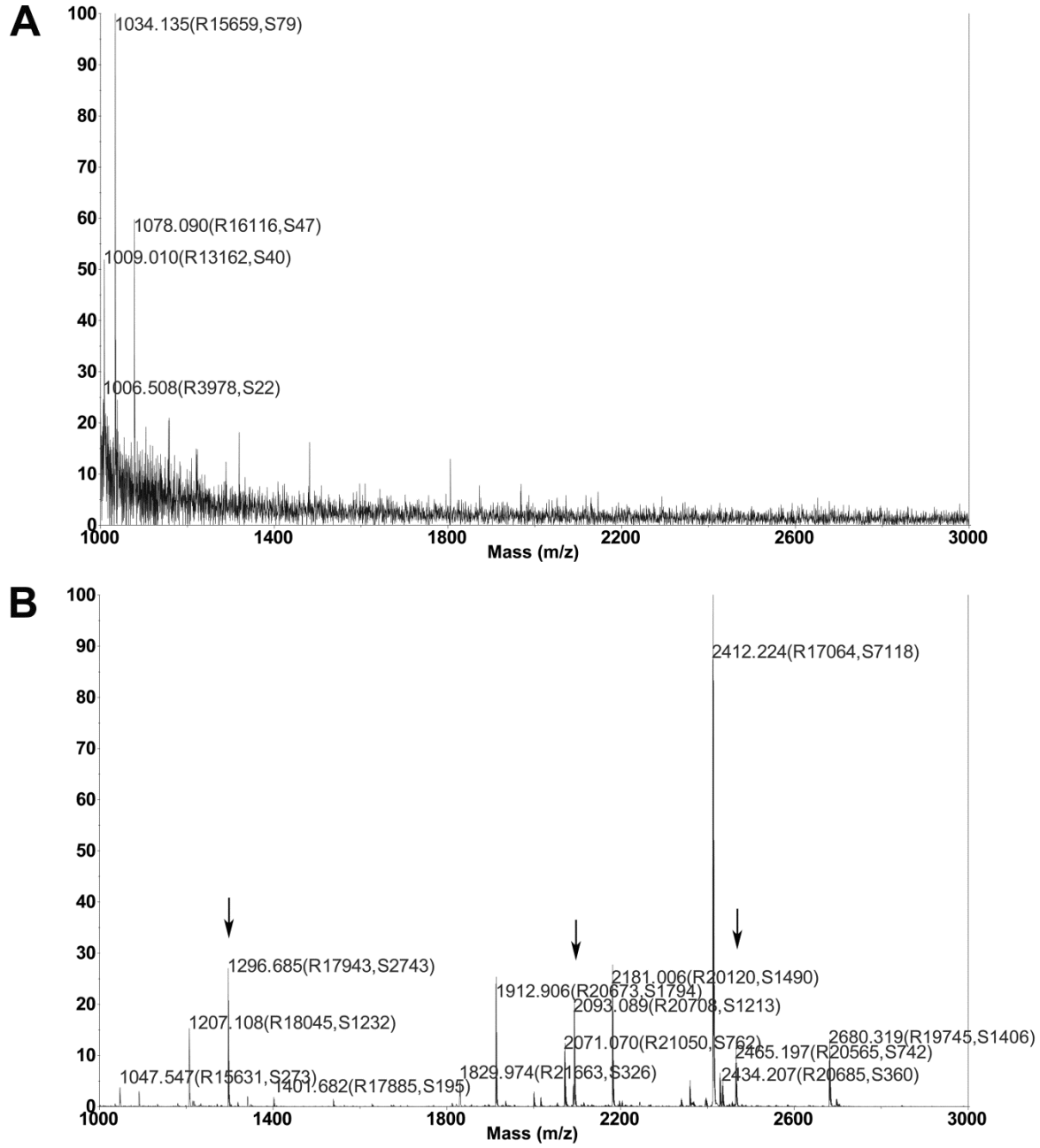

C **FindPept output.**

Experimental mass (Da)	Theoretical mass (Da)	Δmass (ppm)	Peptide	Position
1912.906	1912.902	-2.000	(M)GSSHHHHHHSSGLVPRGS(H)	2-19
2071.070	2071.067	-1.200	(M)AMRELVEAEAGGANPLMKLA(G)	22-41
2181.006	2181.002	-2.000	(M)GSSHHHHHHSSGLVPRGSHM(A)	2-21
2181.006	2181.002	-2.000	MGSSHHHHHHSSGLVPRGSH(M)	1-20
2412.224	2412.216	-3.200	(M)AMRELVEAEAGGANPLMKLAGHF(T)	22-44
2680.319	2680.316	-1.200	(S)HMAMRELVEAEAGGANPLMKLAGHF(T)	20-44

Figure 26. Mass spectrometry analyses of intact and Genenase I-cleaved recombinant histidine-tagged PEX5(1-197;C11A) in the reflectron positive mode. A, intact histidine-tagged PEX5(1-197;C11A). **B,** Genenase I-cleaved histidine-tagged PEX5(1-197;C11A). Arrows indicate the internal standards added to the sample. **C,** FindPept software (221) output for the five major peptides observed in the panel B ("unspecific cleavage" option and mass tolerance of 10 ppm).

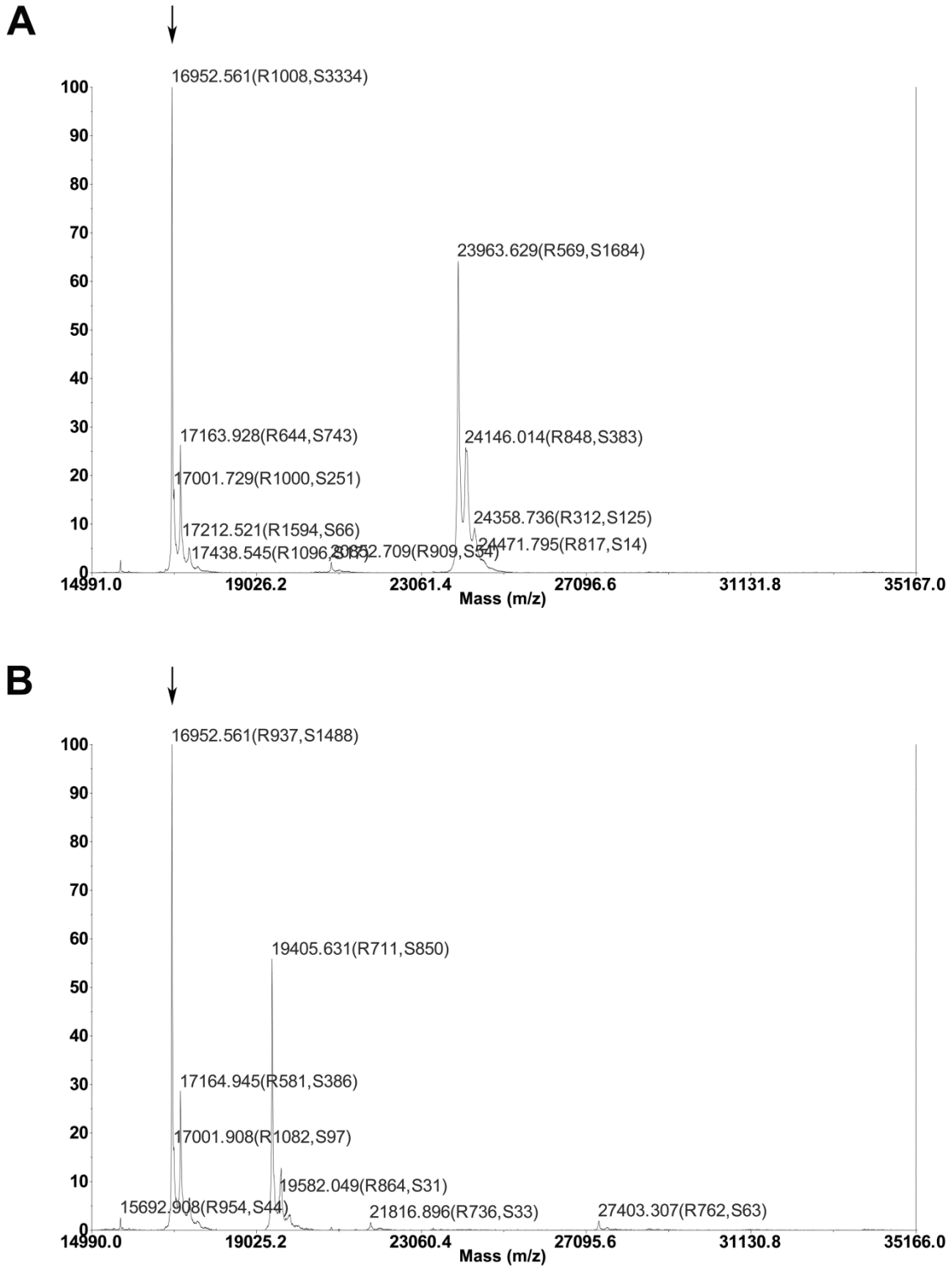

Figure 27. Mass spectrometry analyses of intact and Genenase I-cleaved recombinant histidine-tagged PEX5(1-197;C11A) in the linear positive mode. A, intact histidine-tagged PEX5(1-197;C11A). **B,** Genenase I-cleaved histidine-tagged PEX5(1-197;C11A). In A and B, the arrow indicates the internal mass standard horse myoglobin.

V - DISCUSSION

PEX5 is essential for the peroxisome biogenesis, as it is involved in all stages of the peroxisomal matrix protein import pathway. Our group proposed that PEX5, in addition to a receptor and translocator for peroxisomal matrix proteins, is also a holdase-like protein that binds its newly synthesized cargo proteins into the cytosol, preventing premature or incorrect interactions (107). In this study, several strategies were used to explore the role of PEX5 as a holdase-like protein. The thermal-induced aggregation of malate dehydrogenase and inactivation of citrate synthase were both prevented by the N-terminal half of PEX5, suggesting that PEX5 can act as a holdase-like protein.

As already mentioned, the monomeric versions of catalase, ACOX and UOX, display hydrodynamic properties compatible with a globular conformation. However, in contrast to the corresponding oligomeric native forms, these monomeric proteins are extremely sensitive to proteases. Interestingly, this protease-sensitivity is maintained when they interact with PEX5, suggesting that PTS1-containing molten globules are the *bona fide* substrates of the PIM. If true, then even peroxisomal proteins that are monomeric in their native state might be kept in a molten globule conformation by PEX5, prior to the import step. This mechanism was appealing to us for two reasons: 1) it would provide a simple way to maintain newly synthesized peroxisomal matrix proteins in an inactive state during their transit through the cytosol, thus avoiding undesirable reactions in the cytosol (*e.g.*, the generation of H_2O_2); 2) it would suggest that, although fully folded and even oligomeric proteins can be substrates for the PIM, this machinery might function even better with molten globule substrates, which are much more flexible than already folded proteins. To test this hypothesis, we asked whether the presence of recombinant human PEX5 during the *in vitro* synthesis of firefly luciferase would block/retard the folding of this enzyme. Unfortunately, the results were negative. Thus, either the initial hypothesis is wrong (*i.e.*, the PIM does not discriminate between folded monomeric proteins and monomeric molten globules), or this phenomenon is difficult to capture *in vitro*. The fact that PEX5 proteins from human and insect are rather different (particularly at their N-terminal half) might also explain this negative result. Thus, it is clear that additional work has to be done to clarify this issue.

The ability to accept already folded proteins as substrates is not an exclusive property of the peroxisomal matrix protein import machinery. In fact, in both eukaryotes and prokaryotes, several protein transport systems have this capacity. Examples include the nuclear pore complex, some bacterial secretion systems, the twin-arginine translocation system, and the pore-forming proteins. Although these protein transport systems present an overwhelming diversity of compositions and architectures, they can be coarsely grouped into three mechanistic classes. First, those that comprise a gated pore of fixed composition and geometry that enables the transport of folded and soluble cargo proteins across a membrane (*e.g.* the nuclear pore complex and the bacterial type II and IV secretion systems (234–236)).

Second, those that comprise membrane proteins with the ability to assemble into an appropriately sized transient channel every time a cargo protein has to be transported (*i.e.*, the Tat system (237)). Finally, those where initially soluble proteins undergo oligomerization and major conformational changes enabling them to insert into a membrane creating pores of variable dimensions (pore-forming proteins (238)). An important question in the field of peroxisome biogenesis is which of these three mechanisms, if any, best describes the PIM.

Several years ago our research group proposed that newly synthesized folded matrix proteins are translocated through the peroxisomal membrane by PEX5 itself, when PEX5 becomes inserted into the DTM (151, 161, 211). This model postulates that the soluble receptor-cargo complex is recruited into a gated proteinaceous pore/channel formed by DTM components. The striking resistance of peroxisome-associated PEX5 to alkaline extraction (211), has been interpreted within the context of all the other PEX5 data (151), as probably meaning that there is some unusually strong protein-protein interaction involving PEX5 and components of the DTM (99, 166, 211, 225).

A different perspective is presented in the “transient pore model”, which uses the alkaline-resistance of peroxisomal PEX5 as its main supporting fact (212). We note that, in its essence, this model is a derivative of the one described above, *i.e.*, it also proposes that cargo proteins are pushed through the peroxisomal membrane by PEX5 itself, when the receptor interacts with the DTM. However, it introduces the novelty that the protein translocation pore is formed by a combination of PEX5 molecules and DTM components (*e.g.*, PEX14), all of them interacting directly with the lipid bilayer of the peroxisomal membrane, and all together creating the hydrophilic pore that allows the translocation of cargo proteins through the membrane (212, 213).

The results obtained in this study show that in the absence of membrane lipids the PEX5-PEX14 interaction is resistant to alkaline pH and, thus, clarify the discrepancies between the biochemical behavior of DTM-embedded PEX5 and the primary structure and biochemical properties of the N-terminal domain of PEX5, which were never entirely explained by the transient pore model. Clearly, there is no need to assume that PEX5 is a pore-forming protein because alkaline-resistance of peroxisomal PEX5 has now a much simpler explanation – the PEX5-PEX14 is alkaline-resistant.

Although additional biochemical work and detailed structural data will be necessary to understand the mechanism and architecture of the PIM, the results obtained in this study with the PEX5 truncated molecules can be used to infer some of its properties.

Interestingly, the saturation-binding experiments revealed that PEX5(C11A) and PEX5(1-197;C11A) interact with the peroxisomal membrane with different stoichiometries (see Figure 28). Apparently, several of the sites available to bind a single full-length PEX5(C11A) protein can accommodate more than one truncated PEX5(1-197;C11A) protein.

This finding suggests that each site at the DTM that is occupied by a single full-length PEX5 protein comprises more than one PEX5-interacting domain. Moreover, at least some of these PEX5-interacting domains are most likely equivalent, *i.e.*, they can bind to the same PEX5 sequence(s).

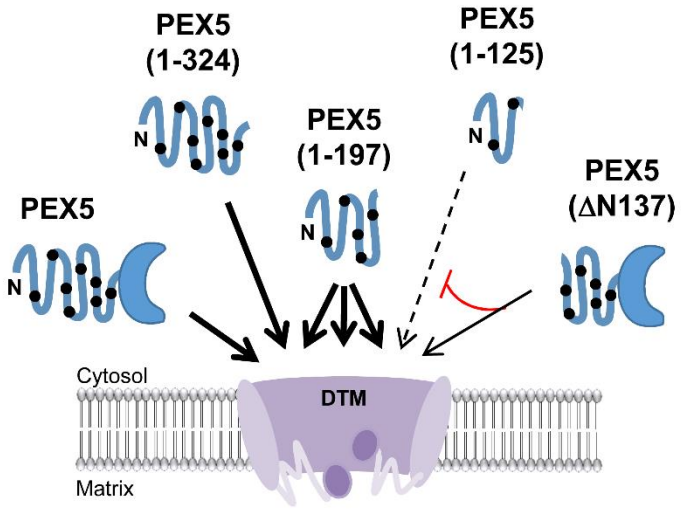

Figure 28. Model of the peroxisomal matrix protein translocon (DTM). The DTM, comprising the transmembrane proteins PEX14, PEX13 and RING finger PEX2, PEX10 and PEX12, is a large cavity-forming protein assembly into which soluble PEX5 enters to release its cargo. Each site at the DTM available to bind one full-length PEX5 molecule can accommodate one PEX5(1-324) molecule or 2-3 PEX5(1-197) molecules (thick arrows). The small PEX5(1-125) species also interacts correctly with DTM, albeit with low efficiency (dashed arrow); interestingly, it remains largely accessible to proteinase K added from the cytosolic side of the membrane. Furthermore, PEX5(ΔN137) competes with PEX5(1-125) in the interaction with the DTM (red line), a finding suggesting that the DTM can recruit cytosolic PEX5 through different pentapeptide motifs. The putative disorder of DTM components (purple ovals with wavy lines) might contribute to this interaction flexibility. The C-shaped form and the thick blue line represent the PTS1-binding domain and the intrinsically disordered N-terminal half of PEX5, respectively. The black dots indicate the pentapeptide motifs involved in the interactions with PEX14 and PEX13.

The finding that PEX5(ΔN137) competes with PEX5(1-125;C11K) for insertion into the DTM is also interesting. Currently, we do not know if this competition is due to steric hindrance or if the two proteins bind the same DTM component(s). However, the fact that two PEX5 proteins showing no sequence overlap can enter into the DTM suggests that this complex can interact with PEX5 using alternative binding paths. In other words, during the docking and insertion steps, it is possible that the initial interactions that occur between a single PEX5 protein and the DTM, most of them probably involving PEX14 (107, 156), do not necessarily involve a well-defined order of events. If true, this would suggest that at least some of the interactions established between PEX5 and the DTM are polymorphic, and most likely better described by the principles that rule fuzzy protein-protein interactions (see (239,

240)). The data discussed above for PEX5(1-197), the fact that the N-terminal half of PEX5 is a natively unfolded domain interacting with DTM components mainly (if not exclusively) through several small motifs, together with an abundance of intrinsic disorder in many DTM components, such as PEX13 and PEX14 (see Figure 29), are surely compatible with this idea.

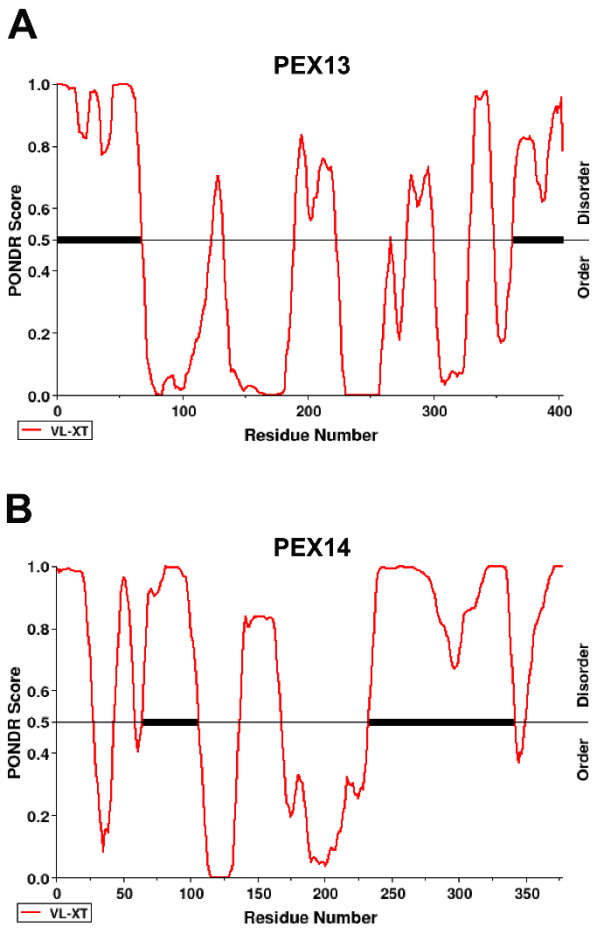

Figure 29. *In silico* prediction of PEX13 and PEX14 disorder using the Predictor of Natural Disordered Regions (PONDR®)-VLXT algorithm (241)**.** About 40% and 60% of human PEX13 and PEX14 sequences, respectively, are predicted to be intrinsically disordered.

The results showing that PEX5(1-125;C11K) is a correct substrate for the RING finger peroxins and for the REM indicate that the amino acid residues 126 to 639 of PEX5 do not contain crucial information to the ubiquitination and export components of the PIM. Importantly, peroxisome-associated PEX5(1-125;C11K) is largely accessible to PK added from the cytosolic side of the peroxisomal membrane. This might suggest that PEX5(1-125;C11K) remains trapped at the docking step and that docking is enough to position this PEX5 molecule in the correct orientation to be monoubiquitinated at the DTM and exported by the REM. However, the interaction of Ub-PEX5(1-125;C11K) with the DTM is irreversible, contrary to the PEX5-DTM interaction at the docking step. Moreover, at least a fraction of

PEX5(1-125;C11K)-clv acquires a transmembrane topology and exposes its C-terminus into the peroxisomal matrix. So, it is more likely that PEX5(1-125) becomes inserted into the DTM, as all the other PEX5 proteins used in this study do, but that due to its small size there is still sufficient space inside the DTM to provide access to PK.

In summary, the data presented in this study reveal novel aspects of the PEX5-DTM interaction and provide additional evidence to support the idea that the DTM comprises the transmembrane hydrophilic channel in which soluble PEX5 enters to deliver its cargoes into the peroxisomal matrix.

VI - REFERENCES

1. Rhodin, J. (1954) *Correlation of ultrastructural organization and function in normal and experimentally changed proximal convoluted tubule cells of the mouse kidney*. Ph.D. thesis, Karolinska Institutet, Aktiebolaget Godvil, Stockholm, Sweden
2. De Duve, C. (1965) Functions of microbodies (peroxisomes). *J. Cell Biol.* **27**, 25A
3. De Duve, C., and Baudhuin, P. (1966) Peroxisomes (microbodies and related particles). *Physiol. Rev.* **46**, 323–357
4. Lazarow, P., and Fujiki, Y. (1985) Biogenesis of peroxisomes. *Ann. Rev. Cell Biol*. **1**, 489–530
5. Völkl, A., Baumgart, E., and Fahimi, H. D. (1988) Localization of urate oxidase in the crystalline cores of rat liver peroxisomes by immunocytochemistry and immunoblotting. *J. Histochem. Cytochem. Off. J. Histochem. Soc.* **36**, 329–336
6. Douglass, S. A., Criddle, R. S., and Breidenbach, R. W. (1973) Characterization of deoxyribonucleic acid species from castor bean endosperm: inability to detect a unique deoxyribonucleic acid species associated with glyoxysomes. *Plant Physiol.* **51**, 902–906
7. Kamiryo, T., Abe, M., Okazaki, K., Kato, S., and Shimamoto, N. (1982) Absence of DNA in peroxisomes of Candida tropicalis. *J. Bacteriol.* **152**, 269–274
8. Schrader, M., Burkhardt, J. K., Baumgart, E., Luers, G., Volkl, A., and Fahimi, H. D. (1996) The Importance of Microtubules in Determination of Shape and Intracellular Distribution of Peroxisomes. *Ann. N. Y. Acad. Sci.* **804**, 669–671
9. Islinger, M., Grille, S., Fahimi, H. D., and Schrader, M. (2012) The peroxisome: an update on mysteries. *Histochem. Cell Biol.* **137**, 547–574
10. Fransen, M., Nordgren, M., Wang, B., and Apanasets, O. (2012) Role of peroxisomes in ROS/RNS-metabolism: Implications for human disease. *Biochim. Biophys. Acta - Mol. Basis Dis.* **1822**, 1363–1373
11. Wanders, R. J. A., and Waterham, H. R. (2006) Biochemistry of mammalian peroxisomes revisited. *Annu. Rev. Biochem.* **75**, 295–332
12. Smith, J. J., and Aitchison, J. D. (2013) Peroxisomes take shape. *Nat. Rev. Mol. Cell Biol.* **14**, 803–817
13. Schrader, M., and Fahimi, H. D. (2006) Peroxisomes and oxidative stress. *Biochim. Biophys. Acta - Mol. Cell Res.* **1763**, 1755–1766
14. Fidaleo, M. (2010) Peroxisomes and peroxisomal disorders: The main facts. *Exp. Toxicol. Pathol.* **62**, 615–625
15. Wanders, R. J. A. (2014) Metabolic functions of peroxisomes in health and disease. *Biochimie*. **98**, 36–44
16. Opperdoes, F. R., and Borst, P. (1977) Localization of nine glycolytic enzymes in a microbody-like organelle in Trypanosoma brucei: The glycosome. *FEBS Lett.* **80**, 360–

364

17. Haanstra, J. R., González-Marcano, E. B., Gualdrón-López, M., and Michels, P. A. M. (2016) Biogenesis, maintenance and dynamics of glycosomes in trypanosomatid parasites. *Biochim. Biophys. Acta - Mol. Cell Res.* **1863**, 1038–1048
18. Olsen, L. J. (1998) The surprising complexity of peroxisome biogenesis. *Plant Mol. Biol.* **38**, 163–189
19. Waterham, H. R., Ferdinandusse, S., and Wanders, R. J. A. (2016) Human disorders of peroxisome metabolism and biogenesis. *Biochim. Biophys. Acta - Mol. Cell Res.* **1863**, 922–933
20. Wanders, R., and Waterham, H. (2006) Peroxisomal disorders: The single peroxisomal enzyme deficiencies. *Biochim. Biophys. Acta - Mol. Cell Res.* **1763**, 1707–1720
21. Wiesinger, C., Eichler, F. S., and Berger, J. (2015) The genetic landscape of X-linked adrenoleukodystrophy: inheritance, mutations, modifier genes, and diagnosis. *Appl. Clin. Genet.* **8**, 109–121
22. Engelen, M., Kemp, S., and Poll-The, B.-T. (2014) X-Linked Adrenoleukodystrophy: Pathogenesis and Treatment. *Curr. Neurol. Neurosci. Rep.* **14**, 486
23. Wanders, R. J. A., Waterham, H. R., and Ferdinandusse, S. (2016) Metabolic Interplay between Peroxisomes and Other Subcellular Organelles Including Mitochondria and the Endoplasmic Reticulum. *Front. cell Dev. Biol.* **3**, 83
24. Vilarinho, S., Sari, S., Mazzacuva, F., Bilgüvar, K., Esendagli-Yilmaz, G., Jain, D., Akyol, G., Dalgiç, B., Günel, M., Clayton, P. T., and Lifton, R. P. (2016) ACOX2 deficiency: A disorder of bile acid synthesis with transaminase elevation, liver fibrosis, ataxia, and cognitive impairment. *Proc. Natl. Acad. Sci.* **113**, 11289–11293
25. Wanders, R., and Waterham, H. (2004) Peroxisomal disorders I: Biochemistry and genetics of peroxisome biogenesis disorders. *Clin. Genet.* **67**, 107–133
26. Ratbi, I., Falkenberg, K. D., Sommen, M., Al-Sheqaih, N., Guaoua, S., Vandeweyer, G., Urquhart, J. E., Chandler, K. E., Williams, S. G., Roberts, N. A., El Alloussi, M., Black, G. C., Ferdinandusse, S., Ramdi, H., Heimler, A., Fryer, A., Lynch, S. A., Cooper, N., Ong, K. R., Smith, C. E. L., Inglehearn, C. F., Mighell, A. J., Elcock, C., Poulter, J. A., Tischkowitz, M., Davies, S. J., Sefiani, A., Mironov, A. A., Newman, W. G., Waterham, H. R., and Van Camp, G. (2015) Heimler Syndrome Is Caused by Hypomorphic Mutations in the Peroxisome-Biogenesis Genes PEX1 and PEX6. *Am. J. Hum. Genet.* **97**, 535–545
27. Goldfischer, S., Johnson, A. B., Moore, C., Essner, E., and Ritch, R. H. (1973) Peroxisomal abnormalities in metabolic diseases. *J. Histochem. Cytochem.* **21**, 972–977

28. Brown, F. R., McAdams, A. J., Cummins, J. W., Konkol, R., Singh, I., Moser, A. B., and Moser, H. W. (1982) Cerebro-hepato-renal (Zellweger) syndrome and neonatal adrenoleukodystrophy: similarities in phenotype and accumulation of very long chain fatty acids. *Johns Hopkins Med. J.* **151**, 344–351
29. Barøy, T., Koster, J., Strømme, P., Ebberink, M. S., Misceo, D., Ferdinandusse, S., Holmgren, A., Hughes, T., Merckoll, E., Westvik, J., Woldseth, B., Walter, J., Wood, N., Tvedt, B., Stadskleiv, K., Wanders, R. J. A., Waterham, H. R., and Frengen, E. (2015) A novel type of rhizomelic chondrodysplasia punctata, RCDP5, is caused by loss of the PEX5 long isoform. *Hum. Mol. Genet.* **24**, 5845–5854
30. Braverman, N., Steel, G., Obie, C., Moser, A., Moser, H., Gould, S. J., and Valle, D. (1997) Human PEX7 encodes the peroxisomal PTS2 receptor and is responsible for rhizomelic chondrodysplasia punctata. *Nat. Genet.* **15**, 369–376
31. Purdue, P. E., Zhang, J. W., Skoneczny, M., and Lazarow, P. B. (1997) Rhizomelic chondrodysplasia punctata is caused by deficiency of human PEX7, a homologue of the yeast PTS2 receptor. *Nat. Genet.* **15**, 381–384
32. Motley, A. M., Hettema, E. H., Hogenhout, E. M., Brites, P., ten Asbroek, A. L., Wijburg, F. A., Baas, F., Heijmans, H. S., Tabak, H. F., Wanders, R. J., and Distel, B. (1997) Rhizomelic chondrodysplasia punctata is a peroxisomal protein targeting disease caused by a non-functional PTS2 receptor. *Nat. Genet.* **15**, 377–380
33. Braverman, N., Chen, L., Lin, P., Obie, C., Steel, G., Douglas, P., Chakraborty, P. K., Clarke, J. T. R., Boneh, A., Moser, A., Moser, H., and Valle, D. (2002) Mutation analysis of PEX7 in 60 probands with rhizomelic chondrodysplasia punctata and functional correlations of genotype with phenotype. *Hum. Mutat.* **20**, 284–297
34. Santos, M. J., Imanaka, T., Shio, H., Small, G. M., and Lazarow, P. B. (1988) Peroxisomal membrane ghosts in Zellweger syndrome--aberrant organelle assembly. *Science (80-.).* **239**, 1536–1538
35. Santos, M. J., Imanaka, T., Shio, H., and Lazarow, P. B. (1988) Peroxisomal integral membrane proteins in control and Zellweger fibroblasts. *J. Biol. Chem.* **263**, 10502–10509
36. Muntau, A. C., Mayerhofer, P. U., Paton, B. C., Kammerer, S., and Roscher, A. A. (2000) Defective peroxisome membrane synthesis due to mutations in human PEX3 causes Zellweger syndrome, complementation group G. *Am. J. Hum. Genet.* **67**, 967–975
37. Shimozawa, N., Suzuki, Y., Zhang, Z., Imamura, A., Ghaedi, K., Fujiki, Y., and Kondo, N. (2000) Identification of PEX3 as the gene mutated in a Zellweger syndrome patient lacking peroxisomal remnant structures. *Hum. Mol. Genet.* **9**, 1995–1999
38. Honsho, M., Tamura, S., Shimozawa, N., Suzuki, Y., Kondo, N., and Fujiki, Y. (1998)

Mutation in PEX16 is causal in the peroxisome-deficient Zellweger syndrome of complementation group D. *Am J Hum Genet*. **63**, 1622–1630

39. South, S. T., and Gould, S. J. (1999) Peroxisome synthesis in the absence of preexisting peroxisomes. *J. Cell Biol.* **144**, 255–266
40. Matsuzono, Y., Kinoshita, N., Tamura, S., Shimozawa, N., Hamasaki, M., Ghaedi, K., Wanders, R. J., Suzuki, Y., Kondo, N., and Fujiki, Y. (1999) Human PEX19: cDNA cloning by functional complementation, mutation analysis in a patient with Zellweger syndrome, and potential role in peroxisomal membrane assembly. *Proc. Natl. Acad. Sci.* **96**, 2116–2121
41. Ebberink, M. S., Koster, J., Visser, G., Spronsen, F. van, Stolte-Dijkstra, I., Smit, G. P. A., Fock, J. M., Kemp, S., Wanders, R. J. A., and Waterham, H. R. (2012) A novel defect of peroxisome division due to a homozygous non-sense mutation in the PEX11β gene. *J. Med. Genet.* **49**, 307–313
42. Kiel, J. A. K. W., Veenhuis, M., and van der Klei, I. J. (2006) PEX genes in fungal genomes: Common, rare or redundant. *Traffic*. **7**, 1291–1303
43. Cross, L. L., Ebeed, H. T., and Baker, A. (2016) Peroxisome biogenesis, protein targeting mechanisms and PEX gene functions in plants. *Biochim. Biophys. Acta*. **1863**, 850–862
44. Schluter, A., Fourcade, S., Ripp, R., Mandel, J. L., Poch, O., and Pujol, A. (2006) The Evolutionary Origin of Peroxisomes: An ER-Peroxisome Connection. *Mol. Biol. Evol.* **23**, 838–845
45. Platta, H. W., Brinkmeier, R., Reidick, C., Galiani, S., Clausen, M. P., and Eggeling, C. (2016) Regulation of peroxisomal matrix protein import by ubiquitination. *Biochim. Biophys. Acta - Mol. Cell Res.* **1863**, 838–849
46. Yofe, I., Soliman, K., Chuartzman, S. G., Morgan, B., Weill, U., Yifrach, E., Dick, T. P., Cooper, S. J., Ejsing, C. S., Schuldiner, M., Zalckvar, E., and Thoms, S. (2017) Pex35 is a regulator of peroxisome abundance. *J. Cell Sci.* **130**, 791–804
47. Fujiki, Y., Okumoto, K., Mukai, S., Honsho, M., and Tamura, S. (2014) Peroxisome biogenesis in mammalian cells. *Front. Physiol.* **5**, 1–8
48. Yifrach, E., Chuartzman, S. G., Dahan, N., Maskit, S., Zada, L., Weill, U., Yofe, I., Olender, T., Schuldiner, M., and Zalckvar, E. (2016) Characterization of proteome dynamics during growth in oleate reveals a new peroxisome-targeting receptor. *J. Cell Sci.* **129**, 4067–4075
49. Goldman, B. M., and Blobel, G. (1978) Biogenesis of peroxisomes: intracellular site of synthesis of catalase and uricase. *Proc. Natl. Acad. Sci.* **75**, 5066–5070
50. Fujiki, Y., Rachubinski, R. A., and Lazarow, P. B. (1984) Synthesis of a major integral membrane polypeptide of rat liver peroxisomes on free polysomes. *Proc. Natl. Acad.*

Sci. **81**, 7127–7131

51. Miura, S., Mori, M., Takiguchi, M., Tatibana, M., Furuta, S., Miyazawa, S., and Hashimoto, T. (1984) Biosynthesis and intracellular transport of enzymes of peroxisomal beta-oxidation. *J. Biol. Chem.* **259**, 6397–6402
52. Imanaka, T., Shiina, Y., Takano, T., Hashimoto, T., and Osumi, T. (1996) Insertion of the 70-kDa peroxisomal membrane protein into peroxisomal membranes in vivo and in vitro. *J. Biol. Chem.* **271**, 3706–3713
53. Lazarow, P. B. (2003) Peroxisome biogenesis: Advances and conundrums. *Curr. Opin. Cell Biol.* **15**, 489–497
54. Tabak, H. F., Hoepfner, D., Zand, A. v d, Geuze, H. J., Braakman, I., and Huynen, M. A. (2006) Formation of peroxisomes: Present and past. *Biochim. Biophys. Acta - Mol. Cell Res.* **1763**, 1647–1654
55. Hua, R., and Kim, P. K. (2016) Multiple paths to peroxisomes: Mechanism of peroxisome maintenance in mammals. *Biochim. Biophys. Acta - Mol. Cell Res.* **1863**, 881–891
56. Hettema, E. H., and Gould, S. J. (2017) Organelle formation from scratch. *Nature*. **542**, 174–175
57. Knoops, K., Manivannan, S., Cepińska, M. N., Krikken, A. M., Kram, A. M., Veenhuis, M., and van der Klei, I. J. (2014) Preperoxisomal vesicles can form in the absence of Pex3. *J. Cell Biol.* **204**, 659–668
58. Sugiura, A., Mattie, S., Prudent, J., and McBride, H. M. (2017) Newly born peroxisomes are a hybrid of mitochondrial and ER-derived pre-peroxisomes. *Nature*. **542**, 251–254
59. Raychaudhuri, S., and Prinz, W. a (2008) Nonvesicular phospholipid transfer between peroxisomes and the endoplasmic reticulum. *Proc. Natl. Acad. Sci.* **105**, 15785–15790
60. Rosenberger, S., Connerth, M., Zellnig, G., and Daum, G. (2009) Phosphatidylethanolamine synthesized by three different pathways is supplied to peroxisomes of the yeast Saccharomyces cerevisiae. *Biochim. Biophys. Acta*. **1791**, 379–387
61. Lev, S. (2012) Nonvesicular lipid transfer from the endoplasmic reticulum. *Cold Spring Harb. Perspect. Biol.* **4**, a013300
62. Van Ael, E., and Fransen, M. (2006) Targeting signals in peroxisomal membrane proteins. *Biochim. Biophys. Acta - Mol. Cell Res.* **1763**, 1629–1638
63. Sacksteder, K. A., Jones, J. M., South, S. T., Li, X., Liu, Y., and Gould, S. J. (2000) Pex19 Binds Multiple Peroxisomal Membrane Proteins, Is Predominantly Cytoplasmic, and Is Required for Peroxisome Membrane Synthesis. *J. Cell Biol.* **148**, 931–944
64. Jones, J. M., Morrell, J. C., and Gould, S. J. (2004) PEX19 is a predominantly

cytosolic chaperone and import receptor for class 1 peroxisomal membrane proteins. *J. Cell Biol.* **164**, 57–67

65. Shibata, H., Kashiwayama, Y., Imanaka, T., and Kato, H. (2004) Domain architecture and activity of human Pex19p, a chaperone-like protein for intracellular trafficking of peroxisomal membrane proteins. *J. Biol. Chem.* **279**, 38486–38494
66. Fujiki, Y., Matsuzono, Y., Matsuzaki, T., and Fransen, M. (2006) Import of peroxisomal membrane proteins: The interplay of Pex3p- and Pex19p-mediated interactions. *Biochim. Biophys. Acta - Mol. Cell Res.* **1763**, 1639–1646
67. Matsuzono, Y., and Fujiki, Y. (2006) In vitro transport of membrane proteins to peroxisomes by shuttling receptor Pex19p. *J. Biol. Chem.* **281**, 36–42
68. Pinto, M. P., Grou, C. P., Alencastre, I. S., Oliveira, M. E., Sá-Miranda, C., Fransen, M., and Azevedo, J. E. (2006) The Import Competence of a Peroxisomal Membrane Protein Is Determined by Pex19p before the Docking Step. *J. Biol. Chem.* **281**, 34492–34502
69. Fang, Y., Morrell, J. C., Jones, J. M., and Gould, S. J. (2004) PEX3 functions as a PEX19 docking factor in the import of class I peroxisomal membrane proteins. *J. Cell Biol.* **164**, 863–875
70. Diestelkötter, P., and Just, W. W. (1993) In vitro insertion of the 22-kD peroxisomal membrane protein into isolated rat liver peroxisomes. *J. Cell Biol.* **123**, 1717–25
71. Pinto, M. P., Grou, C. P., Fransen, M., Sá-Miranda, C., and Azevedo, J. E. (2009) The cytosolic domain of PEX3, a protein involved in the biogenesis of peroxisomes, binds membrane lipids. *Biochim. Biophys. Acta - Mol. Cell Res.* **1793**, 1669–1675
72. Chen, Y., Pieuchot, L., Loh, R. A., Yang, J., Kari, T. M. A., Wong, J. Y., and Jedd, G. (2014) Hydrophobic handoff for direct delivery of peroxisome tail-anchored proteins. *Nat. Commun.* **5**, 5790
73. Kim, P. K., and Mullen, R. T. (2013) PEX16: A multifaceted regulator of peroxisome biogenesis. *Front. Physiol.* **4**, 1–6
74. Liu, Y., Yagita, Y., and Fujiki, Y. (2016) Assembly of Peroxisomal Membrane Proteins via the Direct Pex19p-Pex3p Pathway. *Traffic*. **17**, 433–455
75. Fakieh, M. H., Drake, P. J. M., Lacey, J., Munck, J. M., Motley, A. M., and Hettema, E. H. (2013) Intra-ER sorting of the peroxisomal membrane protein Pex3 relies on its luminal domain. *Biol. Open*. **2**, 829–837
76. Mayerhofer, P. U., Bañó-Polo, M., Mingarro, I., and Johnson, A. E. (2016) Human Peroxin PEX3 Is Co-translationally Integrated into the ER and Exits the ER in Budding Vesicles. *Traffic*. **17**, 117–130
77. Dodt, G., Braverman, N., Wong, C., Moser, A., Moser, H. W., Watkins, P., Valle, D., and Gould, S. J. (1995) Mutations in the PTS1 receptor gene, PXR1, define

complementation group 2 of the peroxisome biogenesis disorders. *Nat. Genet.* **9**, 115–125

78. Fransen M, Brees C, Baumgart E, Vanhooren JC, Baes M, Mannaerts GP, V. V. P. (1995) Identification and characterization of the putative human peroxisomal C-terminal targeting signal import receptor. *J. Biol. Chem.* **270**, 7731–7736
79. Agne, B., Meindl, N. M., Niederhoff, K., Einwächter, H., Rehling, P., Sickmann, A., Meyer, H. E., Girzalsky, W., and Kunau, W. H. (2003) Pex8p: An intraperoxisomal organizer of the peroxisomal import machinery. *Mol. Cell*. **11**, 635–646
80. Oeljeklaus, S., Reinartz, B. S., Wolf, J., Wiese, S., Tonillo, J., Podwojski, K., Kuhlmann, K., Stephan, C., Meyer, H. E., Schliebs, W., Brocard, C., Erdmann, R., and Warscheid, B. (2012) Identification of core components and transient interactors of the peroxisomal importomer by dual-track stable isotope labeling with amino acids in cell culture analysis. *J. Proteome Res.* **11**, 2567–2580
81. Reguenga, C., Oliveira, M. E. M., Gouveia, A. M. M., Sá-Miranda, C., and Azevedo, J. E. (2001) Characterization of the mammalian peroxisomal import machinery. Pex2p, Pex5p, Pex12p, and Pex14p are subunits of the same protein assembly. *J. Biol. Chem.* **276**, 29935–29942
82. Matsumoto, N., Tamura, S., and Fujiki, Y. (2003) The pathogenic peroxin Pex26p recruits the Pex1p-Pex6p AAA ATPase complexes to peroxisomes. *Nat. Cell Biol.* **5**, 454–460
83. Miyata, N., and Fujiki, Y. (2005) Shuttling mechanism of peroxisome targeting signal type 1 receptor Pex5: ATP-independent import and ATP-dependent export. *Mol. Cell. Biol.* **25**, 10822–10832
84. Platta, H. W., Grunau, S., Rosenkranz, K., Girzalsky, W., and Erdmann, R. (2005) Functional role of the AAA peroxins in dislocation of the cycling PTS1 receptor back to the cytosol. *Nat. Cell Biol.* **7**, 817–822
85. Grou, C. P., Carvalho, A. F., Pinto, M. P., Wiese, S., Piechura, H., Meyer, H. E., Warscheid, B., Sá-Miranda, C., and Azevedo, J. E. (2008) Members of the E2D (UbcH5) Family Mediate the Ubiquitination of the Conserved Cysteine of Pex5p, the Peroxisomal Import Receptor. *J. Biol. Chem.* **283**, 14190–14197
86. Grou, C. P., Francisco, T., Rodrigues, T. A., Freitas, M. O., Pinto, M. P., Carvalho, A. F., Domingues, P., Wood, S. A., Rodríguez-Borges, J. E., Sá-Miranda, C., Fransen, M., and Azevedo, J. E. (2012) Identification of ubiquitin-specific protease 9X (USP9X) as a deubiquitinase acting on ubiquitin-peroxin 5 (PEX5) thioester conjugate. *J. Biol. Chem.* **287**, 12815–12827
87. Rodrigues, T. A., Francisco, T., Dias, A. F., Pedrosa, A. G., Grou, C. P., and Azevedo, J. E. (2016) A cell-free organelle-based in vitro system for studying the peroxisomal

protein import machinery. *Nat. Protoc.* **11**, 2454–2469

88. Gould, S. J., Keller, G. a, and Subramani, S. (1987) Identification of a peroxisomal targeting signal at the carboxyl terminus of firefly luciferase. *J. Cell Biol.* **105**, 2923–2931
89. Gould, S. J., Keller, G. A., Hosken, N., Wilkinson, J., and Subramani, S. (1989) A conserved tripeptide sorts proteins to peroxisomes. *J. Cell Biol.* **108**, 1657–1664
90. Brocard, C., and Hartig, A. (2006) Peroxisome targeting signal 1: Is it really a simple tripeptide? *Biochim. Biophys. Acta - Mol. Cell Res.* **1763**, 1565–1573
91. Lametschwandtner, G., Brocard, C., Fransen, M., Van Veldhoven, P., Berger, J., and Hartig, A. (1998) The difference in recognition of terminal tripeptides as peroxisomal targeting signal 1 between yeast and human is due to different affinities of their receptor Pex5p to the cognate signal and to residues adjacent to it. *J. Biol. Chem.* **273**, 33635–33643
92. Maynard, E. L., Gatto, G. J., and Berg, J. M. (2004) Pex5p binding affinities for canonical and noncanonical PTS1 peptides. *Proteins Struct. Funct. Bioinforma.* **55**, 856–861
93. Chowdhary, G., Kataya, A. R., Lingner, T., and Reumann, S. (2012) Non-canonical peroxisome targeting signals: identification of novel PTS1 tripeptides and characterization of enhancer elements by computational permutation analysis. *BMC Plant Biol.* **12**, 142
94. Swinkels, B. W., Gould, S. J., Bodnar, A. G., Rachubinski, R. A., and Subramani, S. (1991) A novel, cleavable peroxisomal targeting signal at the amino-terminus of the rat 3-ketoacyl-CoA thiolase. *EMBO J.* **10**, 3255–3262
95. Osumi, T., Tsukamoto, T., Hata, S., Yokota, S., Miura, S., Fujiki, Y., Hijikata, M., Miyazawa, S., and Hashimoto, T. (1991) Amino-terminal presequence of the precursor of peroxisomal 3-ketoacyl-CoA thiolase is a cleavable signal peptide for peroxisomal targeting. *Biochem. Biophys. Res. Commun.* **181**, 947–954
96. Petriv, O. I., Tang, L., Titorenko, V. I., and Rachubinski, R. A. (2004) A new definition for the consensus sequence of the peroxisome targeting signal type 2. *J. Mol. Biol.* **341**, 119–134
97. Kurochkin, I. V, Mizuno, Y., Konagaya, A., Sakaki, Y., Schönbach, C., and Okazaki, Y. (2007) Novel peroxisomal protease Tysnd1 processes PTS1- and PTS2-containing enzymes involved in beta-oxidation of fatty acids. *EMBO J.* **26**, 835–845
98. Lazarow, P. B. (2006) The import receptor Pex7p and the PTS2 targeting sequence. *Biochim. Biophys. Acta - Mol. Cell Res.* **1763**, 1599–1604
99. Terlecky, S. R., Nuttley, W. M., McCollum, D., Sock, E., and Subramani, S. (1995) The Pichia pastoris peroxisomal protein PAS8p is the receptor for the C-terminal tripeptide

peroxisomal targeting signal. *EMBO J.* **14**, 3627–3634

100. Dodt, G., and Gould, S. J. (1996) Multiple PEX genes are required for proper subcellular distribution and stability of Pex5p, the PTS1 receptor: Evidence that PTS1 protein import is mediated by a cycling receptor. *J. Cell Biol.* **135**, 1763–1774
101. Gatto, G. J., Geisbrecht, B. V., Gould, S. J., and Berg, J. M. (2000) A proposed model for the PEX5-peroxisomal targeting signal-1 recognition complex. *Proteins Struct. Funct. Genet.* **38**, 241–246
102. Gatto, G. J., Geisbrecht, B. V, Gould, S. J., and Berg, J. M. (2000) Peroxisomal targeting signal-1 recognition by the TPR domains of human PEX5. *Nat. Struct. Biol.* **7**, 1091–1095
103. Klein, A. T. J., Barnett, P., Bottger, G., Konings, D., Tabak, H. F., and Distel, B. (2001) Recognition of Peroxisomal Targeting Signal Type 1 by the Import Receptor Pex5p. *J. Biol. Chem.* **276**, 15034–15041
104. Klein, A. T. J., Van Den Berg, M. V., Bottger, G., Tabak, H. F., and Distel, B. (2002) Saccharomyces cerevisiae acyl-CoA oxidase follows a novel, non-PTS1, import pathway into peroxisomes that is dependent on Pex5p. *J. Biol. Chem.* **277**, 25011–25019
105. Gunkel, K., van Dijk, R., Veenhuis, M., and van der Klei, I. (2004) Routing of Hansenula polymorpha Alcohol Oxidase: An Alternative Peroxisomal Protein-sorting Machinery. *Mol. Biol. Cell*. **15**, 1347–1355
106. Oshima, Y., Kamigaki, A., Nakamori, C., Mano, S., Hayashi, M., Nishimura, M., and Esaka, M. (2008) Plant catalase is imported into peroxisomes by Pex5p but is distinct from typical PTS1 import. *Plant Cell Physiol.* **49**, 671–677
107. Freitas, M. O., Francisco, T., Rodrigues, T. A., Alencastre, I. S., Pinto, M. P., Grou, C. P., Carvalho, A. F., Fransen, M., Sa-Miranda, C., and Azevedo, J. E. (2011) PEX5 Protein Binds Monomeric Catalase Blocking Its Tetramerization and Releases It upon Binding the N-terminal Domain of PEX14. *J. Biol. Chem.* **286**, 40509–40519
108. Marzioch, M., Erdmann, R., Veenhuis, M., and Kunau, W. H. (1994) PAS7 encodes a novel yeast member of the WD-40 protein family essential for import of 3-oxoacyl-CoA thiolase, a PTS2-containing protein, into peroxisomes. *EMBO J.* **13**, 4908–4918
109. Rehling, P., Marzioch, M., Niesen, F., Wittke, E., Veenhuis, M., and Kunau, W. H. (1996) The import receptor for the peroxisomal targeting signal 2 (PTS2) in Saccharomyces cerevisiae is encoded by the PAS7 gene. *EMBO J.* **15**, 2901–2913
110. Zhang, J. W., and Lazarow, P. B. (1996) Peb1p (Pas7p) is an intraperoxisomal receptor for the NH2-terminal, type 2, peroxisomal targeting sequence of thiolase: Peb1p itself is targeted to peroxisomes by an NH2-terminal peptide. *J. Cell Biol.* **132**, 325–334

111. Braverman, N., Dodt, G., Gould, S. J., and Valle, D. (1998) An isoform of pex5p, the human PTS1 receptor, is required for the import of PTS2 proteins into peroxisomes. *Hum. Mol. Genet.* **7**, 1195–1205
112. Otera, H., Okumoto, K., Tateishi, K., Ikoma, Y., Matsuda, E., Nishimura, M., Tsukamoto, T., Osumi, T., Ohashi, K., Higuchi, O., and Fujiki, Y. (1998) Peroxisome Targeting Signal Type 1 (PTS1) Receptor Is Involved in Import of Both PTS1 and PTS2: Studies with PEX5-Defective CHO Cell Mutants. *Mol. Cell. Biol.* **18**, 388–399
113. Woodward, A. W., and Bartel, B. (2005) The Arabidopsis peroxisomal targeting signal type 2 receptor PEX7 is necessary for peroxisome function and dependent on PEX5. *Mol. Biol. Cell*. **16**, 573–583
114. Pan, D., Nakatsu, T., and Kato, H. (2013) Crystal structure of peroxisomal targeting signal-2 bound to its receptor complex Pex7p–Pex21p. *Nat. Struct. Mol. Biol.* **20**, 1–9
115. Kunze, M., Malkani, N., Maurer-Stroh, S., Wiesinger, C., Schmid, J. A., and Berger, J. (2015) Mechanistic insights into PTS2-mediated peroxisomal protein import: The co-receptor PEX5L drastically increases the interaction strength between the cargo protein and the receptor PEX7. *J. Biol. Chem.* **290**, 4928–4940
116. Rodrigues, T. A., Grou, C. P., and Azevedo, J. E. (2015) Revisiting the intraperoxisomal pathway of mammalian PEX7. *Sci. Rep.* **5**, 11806
117. Purdue, P. E., Yang, X., and Lazarow, P. B. (1998) Pex18p and Pex21p, a Novel Pair of Related Peroxins Essential for Peroxisomal Targeting by the PTS2 Pathway. *J. Cell Biol.* **143**, 1859–1869
118. Titorenko, V. I., Smith, J. J., Szilard, R. K., and Rachubinski, R. A. (1998) Pex20p of the yeast Yarrowia lipolytica is required for the oligomerization of thiolase in the cytosol and for its targeting to the peroxisome. *J. Cell Biol.* **142**, 403–420
119. Dodt, G., Warren, D., Becker, E., Rehling, P., and Gould, S. J. (2001) Domain Mapping of Human PEX5 Reveals Functional and Structural Similarities to Saccharomyces cerevisiae Pex18p and Pex21p. *J. Biol. Chem.* **276**, 41769–41781
120. Einwächter, H., Sowinski, S., Kunau, W. H., and Schliebs, W. (2001) Yarrowia lipolytica Pex20p, Saccharomyces cerevisiae Pex18p/Pex21p and mammalian Pex5pL fulfil a common function in the early steps of the peroxisomal PTS2 import pathway. *EMBO Rep.* **2**, 1035–1039
121. Islinger, M., Li, K. W., Seitz, J., Völkl, A., and Lüers, G. H. (2009) Hitchhiking of Cu/Zn superoxide dismutase to peroxisomes--evidence for a natural piggyback import mechanism in mammals. *Traffic*. **10**, 1711–1721
122. Schueren, F., Lingner, T., George, R., Hofhuis, J., Dickel, C., Gärtner, J., and Thoms, S. (2014) Peroxisomal lactate dehydrogenase is generated by translational readthrough in mammals. *Elife*. **3**, e03640

123. Effelsberg, D., Cruz-Zaragoza, L. D., Tonillo, J., Schliebs, W., and Erdmann, R. (2015) Role of Pex21p for Piggyback Import of Gpd1p and Pnc1p into Peroxisomes of Saccharomyces cerevisiae. *J. Biol. Chem.* **290**, 25333–25342
124. Elgersma, Y., Elgersma-Hooisma, M., Wenzel, T., McCaffery, J. M., Farquhar, M. G., and Subramani, S. (1998) A mobile PTS2 receptor for peroxisomal protein import in Pichia pastoris. *J. Cell Biol.* **140**, 807–820
125. Mukai, S., Ghaedi, K., and Fujiki, Y. (2002) Intracellular localization, function, and dysfunction of the peroxisome-targeting signal type 2 receptor, Pex7p, in mammalian cells. *J. Biol. Chem.* **277**, 9548–9561
126. Léon, S., Goodman, J. M., and Subramani, S. (2006) Uniqueness of the mechanism of protein import into the peroxisome matrix: Transport of folded, co-factor-bound and oligomeric proteins by shuttling receptors. *Biochim. Biophys. Acta - Mol. Cell Res.* **1763**, 1552–1564
127. Gunkel, K., Veenhuis, M., and van der Klei, I. (2005) Protein translocation machineries: How organelles bring in matrix proteins. *FEMS Yeast Res.* **5**, 1037–1045
128. Lazarow, P. B., and de Duve, C. (1973) The synthesis and turnover of rat liver peroxisomes. V. Intracellular pathway of catalase synthesis. *J. Cell Biol.* **59**, 507–524
129. Goodman, J. M., Scott, C. W., Donahue, P. N., and Atherton, J. P. (1984) Alcohol oxidase assembles post-translationally into the peroxisome of Candida boidinii. *J. Biol. Chem.* **259**, 8485–8493
130. Stewart, M. Q., Esposito, R. D., Gowani, J., and Goodman, J. M. (2001) Alcohol oxidase and dihydroxyacetone synthase, the abundant peroxisomal proteins of methylotrophic yeasts, assemble in different cellular compartments. *J. Cell Sci.* **114**, 2863–2868
131. Crookes, W. J., and Olsen, L. J. (1998) The effects of chaperones and the influence of protein assembly on peroxisomal protein import. *J. Biol. Chem.* **273**, 17236–17242
132. Freitas, M. O., Francisco, T., Rodrigues, T. A., Lismont, C., Domingues, P., Pinto, M. P., Grou, C. P., Fransen, M., and Azevedo, J. E. (2015) The peroxisomal protein import machinery displays a preference for monomeric substrates. *Open Biol.* **5**, 140236
133. Tanaka, N., Aoki, K. ichi, Ishikura, S., Nagano, M., Imamura, Y., Hara, A., and Nakamura, K. T. (2008) Molecular Basis for Peroxisomal Localization of Tetrameric Carbonyl Reductase. *Structure*. **16**, 388–397
134. Luo, B., Norris, C., Bolstad, E. S. D., Knecht, D. A., and Grant, D. F. (2008) Protein Quaternary Structure and Expression Levels Contribute to Peroxisomal-Targeting-Sequence-1-Mediated Peroxisomal Import of Human Soluble Epoxide Hydrolase. *J. Mol. Biol.* **380**, 31–41

135. Faber, K. N., van Dijk, R., Keizer-Gunnink, I., Koek, A., van der Klei, I. J., and Veenhuis, M. (2002) Import of assembled PTS1 proteins into peroxisomes of the yeast Hansenula polymorpha: Yes and No! *Biochim. Biophys. Acta - Mol. Cell Res.* **1591**, 157–162
136. McCollum, D., Monosov, E., and Subramani, S. (1993) The pas8 mutant of Pichia pastoris exhibits the peroxisomal protein import deficiencies of Zellweger syndrome cells--the PAS8 protein binds to the COOH-terminal tripeptide peroxisomal targeting signal, and is a member of the TPR protein family. *J. Cell Biol.* **121**, 761–774
137. Van Der Leij, I., Franse, M. M., Elgersma, Y., Distel, B., and Tabak, H. F. (1993) PAS10 is a tetratricopeptide-repeat protein that is essential for the import of most matrix proteins into peroxisomes of Saccharomyces cerevisiae. *Proc. Natl. Acad. Sci.* **90**, 11782–11786
138. Costa-Rodrigues, J., Carvalho, A. F., Fransen, M., Hambruch, E., Schliebs, W., Sá-Miranda, C., and Azevedo, J. E. (2005) Pex5p, the Peroxisomal Cycling Receptor, Is a Monomeric Non-globular Protein. *J. Biol. Chem.* **280**, 24404–24411
139. Stanley, W. A., Filipp, F. V., Kursula, P., Schüller, N., Erdmann, R., Schliebs, W., Sattler, M., and Wilmanns, M. (2006) Recognition of a Functional Peroxisome Type 1 Target by the Dynamic Import Receptor Pex5p. *Mol. Cell*. **24**, 653–663
140. Carvalho, A. F., Costa-Rodrigues, J., Correia, I., Costa Pessoa, J., Faria, T. Q., Martins, C. L., Fransen, M., Sá-Miranda, C., and Azevedo, J. E. (2006) The N-terminal Half of the Peroxisomal Cycling Receptor Pex5p is a Natively Unfolded Domain. *J. Mol. Biol.* **356**, 864–875
141. Nito, K., Hayashi, M., and Nishimura, M. (2002) Direct interaction and determination of binding domains among peroxisomal import factors in Arabidopsis thaliana. *Plant Cell Physiol.* **43**, 355–266
142. Saidowsky, J., Dodt, G., Kirchberg, K., Wegner, A., Nastainezyk, W., Kunau, W. H., and Schliebs, W. (2001) The Di-aromatic Pentapeptide Repeats of the Human Peroxisome Import Receptor PEX5 Are Separate High Affinity Binding Sites for the Peroxisomal Membrane Protein PEX14. *J. Biol. Chem.* **276**, 34524–34529
143. Schliebs, W., Saidowsky, J., Agianian, B., Dodt, G., Herberg, F., and Kunau, W.-H. (1999) Recombinant human peroxisomal targeting signal receptor PEX5 Structural basis for interaction of PEX5 with PEX14. *J. Biol. Chem.* **274**, 5666–5673
144. Fransen, M., Brees, C., Ghys, K., Amery, L., Mannaerts, G. P., Ladant, D., and Van Veldhoven, P. P. (2002) Analysis of mammalian peroxin interactions using a non-transcription-based bacterial two-hybrid assay. *Mol. Cell. proteomics*. **1**, 243–252
145. Otera, H., Setoguchi, K., Hamasaki, M., Kumashiro, T., Shimizu, N., and Fujiki, Y. (2002) Peroxisomal targeting signal receptor Pex5p interacts with cargoes and import

machinery components in a spatiotemporally differentiated manner: conserved Pex5p WXXXF/Y motifs are critical for matrix protein import. *Mol. Cell. Biol.* **22**, 1639–1655

146. Neuhaus, A., Kooshapur, H., Wolf, J., Helge Meyer, N., Madl, T., Saidowsky, J., Hambruch, E., Lazam, A., Jung, M., Sattler, M., Schliebs, W., and Erdmann, R. (2014) A novel Pex14 protein-interacting site of human Pex5 is critical for matrix protein import into peroxisomes. *J. Biol. Chem.* **289**, 437–448
147. Carvalho, A. F., Pinto, M. P., Grou, C. P., Alencastre, I. S., Fransen, M., Sá-Miranda, C., and Azevedo, J. E. (2007) Ubiquitination of mammalian Pex5p, the peroxisomal import receptor. *J. Biol. Chem.* **282**, 31267–31272
148. Williams, C., Van Den Berg, M., Sprenger, R. R., and Distel, B. (2007) A conserved cysteine is essential for Pex4p-dependent ubiquitination of the peroxisomal import receptor Pex5p. *J. Biol. Chem.* **282**, 22534–22543
149. Kragler, F., Lametschwandtner, G., Christmann, J., Hartig, A., and Harada, J. J. (1998) Identification and analysis of the plant peroxisomal targeting signal 1 receptor NtPEX5. *Proc. Natl. Acad. Sci.* **95**, 13336–13341
150. Gouveia, A. M., Guimarães, C. P., Oliveira, M. E., Sá-Miranda, C., and Azevedo, J. E. (2003) Insertion of Pex5p into the peroxisomal membrane is cargo protein-dependent. *J. Biol. Chem.* **278**, 4389–4392
151. Gouveia, A. M., Guimarães, C. P., Oliveira, M. E., Reguenga, C., Sá-Miranda, C., and Azevedo, J. E. (2003) Characterization of the peroxisomal cycling receptor, Pex5p, using a cell-free in vitro import system. *J. Biol. Chem.* **278**, 226–232
152. Francisco, T., Rodrigues, T. A., Freitas, M. O., Grou, C. P., Carvalho, A. F., Sá-Miranda, C., Pinto, M. P., and Azevedo, J. E. (2013) A cargo-centered perspective on the PEX5 receptor-mediated peroxisomal protein import pathway. *J. Biol. Chem.* **288**, 29151–29159
153. Oliveira, M. E. M., Reguenga, C., Gouveia, A. M. M., Guimarães, C. P., Schliebs, W., Kunau, W. H., Silva, M. T., Sá-Miranda, C., and Azevedo, J. E. (2002) Mammalian Pex14p: Membrane topology and characterisation of the Pex14p-Pex14p interaction. *Biochim. Biophys. Acta - Biomembr.* **1567**, 13–22
154. Itoh, R., and Fujiki, Y. (2006) Functional domains and dynamic assembly of the peroxin Pex14p, the entry site of matrix proteins. *J. Biol. Chem.* **281**, 10196–10205
155. Krause, C., Rosewich, H., Woehler, A., and Gartner, J. (2013) Functional analysis of PEX13 mutation in a Zellweger syndrome spectrum patient reveals novel homooligomerization of PEX13 and its role in human peroxisome biogenesis. *Hum. Mol. Genet.* **22**, 3844–3857
156. Azevedo, J. E., and Schliebs, W. (2006) Pex14p, more than just a docking protein. *Biochim. Biophys. Acta - Mol. Cell Res.* **1763**, 1574–1584

157. Williams, C., and Distel, B. (2006) Pex13p: Docking or cargo handling protein? *Biochim. Biophys. Acta - Mol. Cell Res.* **1763**, 1585–1591
158. Costa-Rodrigues, J., Carvalho, A. F., Gouveia, A. M., Fransen, M., Sá-Miranda, C., and Azevedo, J. E. (2004) The N Terminus of the Peroxisomal Cycling Receptor, Pex5p, Is Required for Redirecting the Peroxisome-associated Peroxin Back to the Cytosol. *J. Biol. Chem.* **279**, 46573–46579
159. Carvalho, A. F., Grou, C. P., Pinto, M. P., Alencastre, I. S., Costa-Rodrigues, J., Fransen, M., Sá-Miranda, C., and Azevedo, J. E. (2007) Functional characterization of two missense mutations in Pex5p-C11S and N526K. *Biochim. Biophys. Acta - Mol. Cell Res.* **1773**, 1141–1148
160. Francisco, T., Rodrigues, T. A., Dias, A. F., Barros-Barbosa, A., Bicho, D., and Azevedo, J. E. (2017) Protein transport into peroxisomes: Knowns and unknowns. *BioEssays*. 10.1002/bies.201700047
161. Azevedo, J. E., Costa-Rodrigues, J., Guimarães, C. P., Oliveira, M. E., and Sá-Miranda, C. (2004) Protein translocation across the peroxisomal membrane. *Cell Biochem. Biophys.* **41**, 451–468
162. Oliveira, M. E., Gouveia, A. M., Pinto, R. A., Sá-Miranda, C., and Azevedo, J. E. (2003) The energetics of Pex5p-mediated peroxisomal protein import. *J. Biol. Chem.* **278**, 39483–39488
163. Alencastre, I. S., Rodrigues, T. A., Grou, C. P., Fransen, M., Sá-Miranda, C., and Azevedo, J. E. (2009) Mapping the Cargo Protein Membrane Translocation Step into the PEX5 Cycling Pathway. *J. Biol. Chem.* **284**, 27243–27251
164. Imanaka, T., Small, G. M., and Lazarow, P. B. (1987) Translocation of acyl-CoA oxidase into peroxisomes requires ATP hydrolysis but not a membrane potential. *J. Cell Biol.* **105**, 2915–2922
165. Wendland, M., and Subramani, S. (1993) Cytosol-dependent peroxisomal protein import in a permeabilized cell system. *J. Cell Biol.* **120**, 675–685
166. Grou, C. P., Carvalho, A. F., Pinto, M. P., Alencastre, I. S., Rodrigues, T. A., Freitas, M. O., Francisco, T., Sá-Miranda, C., and Azevedo, J. E. (2009) The peroxisomal protein import machinery - A case report of transient ubiquitination with a new flavor. *Cell. Mol. Life Sci.* **66**, 254–262
167. Lanyon-Hogg, T., Hooper, J., Gunn, S., Warriner, S. L., and Baker, A. (2014) PEX14 binding to Arabidopsis PEX5 has differential effects on PTS1 and PTS2 cargo occupancy of the receptor. *FEBS Lett.* **588**, 2223–2229
168. McDowell, G. S., and Philpott, A. (2013) Non-canonical ubiquitylation: Mechanisms and consequences. *Int. J. Biochem. Cell Biol.* **45**, 1833–1842
169. Gonen, H., Bercovich, B., Orian, A., Carrano, A., Takizawa, C., Yamanaka, K.,

Pagano, M., Iwai, K., and Ciechanover, A. (1999) Identification of the ubiquitin carrier proteins, E2s, involved in signal-induced conjugation and subsequent degradation of IkappaBalpha. *J. Biol. Chem.* **274**, 14823–14830

170. Saville, M. K., Sparks, A., Xirodimas, D. P., Wardrop, J., Stevenson, L. F., Bourdon, J.-C., Woods, Y. L., and Lane, D. P. (2004) Regulation of p53 by the ubiquitin-conjugating enzymes UbcH5B/C in vivo. *J. Biol. Chem.* **279**, 42169–42181
171. Wiebel, F. F., and Kunau, W. H. (1992) The Pas2 protein essential for peroxisome biogenesis is related to ubiquitin-conjugating enzymes. *Nature*. **359**, 73–76
172. Crane, D. I., Kalish, J. E., and Gould, S. J. (1994) The Pichia pastoris PAS4 gene encodes a ubiquitin-conjugating enzyme required for peroxisome assembly. *J. Biol. Chem.* **269**, 21835–21844
173. Koller, A., Snyder, W. B., Faber, K. N., Wenzel, T. J., Rangell, L., Keller, G. A., and Subramani, S. (1999) Pex22p of Pichia pastoris, Essential for Peroxisomal Matrix Protein Import, Anchors the Ubiquitin-Conjugating Enzyme, Pex4p, on the Peroxisomal Membrane. *J. Cell Biol.* **146**, 99–112
174. Zolman, B. K., Monroe-Augustus, M., Silva, I. D., and Bartel, B. (2005) Identification and functional characterization of Arabidopsis PEROXIN4 and the interacting protein PEROXIN22. *Plant Cell*. **17**, 3422–3435
175. Williams, C., van den Berg, M., Geers, E., and Distel, B. (2008) Pex10p functions as an E3 ligase for the Ubc4p-dependent ubiquitination of Pex5p. *Biochem. Biophys. Res. Commun.* **374**, 620–624
176. Platta, H. W., El Magraoui, F., Bäumer, B. E., Schlee, D., Girzalsky, W., and Erdmann, R. (2009) Pex2 and pex12 function as protein-ubiquitin ligases in peroxisomal protein import. *Mol. Cell. Biol.* **29**, 5505–5516
177. Kaur, N., Zhao, Q., Xie, Q., and Hu, J. (2013) Arabidopsis RING Peroxins are E3 Ubiquitin Ligases that Interact with Two Homologous Ubiquitin Receptor Proteins. *J. Integr. Plant Biol.* **55**, 108–120
178. Okumoto, K., Noda, H., and Fujiki, Y. (2014) Distinct modes of ubiquitination of peroxisome-targeting signal type 1 (PTS1) receptor Pex5p regulate PTS1 protein import. *J. Biol. Chem.* **289**, 14089–14108
179. Joazeiro, C. A., and Weissman, A. M. (2000) RING finger proteins: mediators of ubiquitin ligase activity. *Cell*. **102**, 549–552
180. Grou, C. P., Carvalho, A. F., Pinto, M. P., Huybrechts, S. J., Sá-Miranda, C., Fransen, M., and Azevedo, J. E. (2009) Properties of the Ubiquitin-Pex5p Thiol Ester Conjugate. *J. Biol. Chem.* **284**, 10504–10513
181. Apanasets, O., Grou, C. P., Van Veldhoven, P. P., Brees, C., Wang, B., Nordgren, M., Dodt, G., Azevedo, J. E., and Fransen, M. (2014) PEX5, the Shuttling Import Receptor

for Peroxisomal Matrix Proteins, Is a Redox-Sensitive Protein. *Traffic*. **15**, 94–103

182. Walton, P. A., Brees, C., Lismont, C., Apanasets, O., and Fransen, M. (2017) The peroxisomal import receptor PEX5 functions as a stress sensor, retaining catalase in the cytosol in times of oxidative stress. *Biochim. Biophys. Acta - Mol. Cell Res.* **1864**, 1833–1843
183. Schwartzkopff, B., Platta, H. W., Hasan, S., Girzalsky, W., and Erdmann, R. (2015) Cystein-specific ubiquitination protects the peroxisomal import receptor Pex5p against proteasomal degradation. *Biosci. Rep.* **35**, e00215
184. Platta, H. W., El Magraoui, F., Schlee, D., Grunau, S., Girzalsky, W., and Erdmann, R. (2007) Ubiquitination of the peroxisomal import receptor Pex5p is required for its recycling. *J. Cell Biol.* **177**, 197–204
185. Miyata, N., Okumoto, K., Mukai, S., Noguchi, M., and Fujiki, Y. (2012) AWP1/ZFAND6 functions in Pex5 export by interacting with cys-monoubiquitinated Pex5 and Pex6 AAA ATPase. *Traffic*. **13**, 168–183
186. Rodrigues, T. A., Alencastre, I. S., Francisco, T., Brites, P., Fransen, M., Grou, C. P., and Azevedo, J. E. (2014) A PEX7-centered perspective on the peroxisomal targeting signal type 2-mediated protein import pathway. *Mol. Cell. Biol.* **34**, 2917–2928
187. Tamura, S., Matsumoto, N., Takeba, R., and Fujiki, Y. (2014) AAA peroxins and their recruiter Pex26p modulate the interactions of peroxins involved in peroxisomal protein import. *J. Biol. Chem.* **289**, 24336–24346
188. Blok, N. B., Tan, D., Wang, R. Y.-R., Penczek, P. A., Baker, D., DiMaio, F., Rapoport, T. A., and Walz, T. (2015) Unique double-ring structure of the peroxisomal Pex1/Pex6 ATPase complex revealed by cryo-electron microscopy. *Proc. Natl. Acad. Sci.* **112**, E4017–E4025
189. Ciniawsky, S., Grimm, I., Saffian, D., Girzalsky, W., Erdmann, R., and Wendler, P. (2015) Molecular snapshots of the Pex1/6 AAA+ complex in action. *Nat. Commun.* **6**, 7331
190. Gardner, B. M., Chowdhury, S., Lander, G. C., and Martin, A. (2015) The Pex1/Pex6 complex is a heterohexameric AAA+ motor with alternating and highly coordinated subunits. *J. Mol. Biol.* **427**, 1375–1388
191. Tan, D., Blok, N. B., Rapoport, T. A., and Walz, T. (2016) Structures of the double-ring AAA ATPase Pex1-Pex6 involved in peroxisome biogenesis. *FEBS J.* **283**, 986–992
192. Nordgren, M., Francisco, T., Lismont, C., Hennebel, L., Brees, C., Wang, B., Veldhoven, P. P. Van, Azevedo, J. E., and Fransen, M. (2015) Export-deficient monoubiquitinated PEX5 triggers peroxisome removal in SV40 large T antigen-transformed mouse embryonic fibroblasts. *Autophagy*. **11**, 1326–1340
193. Schulz, C., Schendzielorz, A., and Rehling, P. (2015) Unlocking the presequence

import pathway. *Trends Cell Biol.* **25**, 265–275

194. Bölter, B., and Soll, J. (2016) Once upon a Time - Chloroplast Protein Import Research from Infancy to Future Challenges. *Mol. Plant*. **9**, 798–812
195. Nordgren, M., Wang, B., Apanasets, O., and Fransen, M. (2013) Peroxisome degradation in mammals: mechanisms of action, recent advances, and perspectives. *Front. Physiol.* **4**, 145
196. Honsho, M., Yamashita, S. ichi, and Fujiki, Y. (2016) Peroxisome homeostasis: Mechanisms of division and selective degradation of peroxisomes in mammals. *Biochim. Biophys. Acta - Mol. Cell Res.* **1863**, 984–991
197. Schrader, M., Costello, J. L., Godinho, L. F., Azadi, A. S., and Islinger, M. (2016) Proliferation and fission of peroxisomes - An update. *Biochim. Biophys. Acta - Mol. Cell Res.* **1863**, 971–983
198. Schrader, M., Reuber, B. E., Morrell, J. C., Jimenez-Sanchez, G., Obie, C., Stroh, T. A., Valle, D., Schroer, T. A., and Gould, S. J. (1998) Expression of PEX11 Mediates Peroxisome Proliferation in the Absence of Extracellular Stimuli. *J. Biol. Chem.* **273**, 29607–29614
199. Abe, I., and Fujiki, Y. (1998) cDNA Cloning and Characterization of a Constitutively Expressed Isoform of the Human Peroxin Pex11p. *Biochem. Biophys. Res. Commun.* **252**, 529–533
200. Li, X., Baumgart, E., Dong, G.-X., Morrell, J. C., Jimenez-Sanchez, G., Valle, D., Smith, K. D., and Gould, S. J. (2002) PEX11alpha is required for peroxisome proliferation in response to 4-phenylbutyrate but is dispensable for peroxisome proliferator-activated receptor alpha-mediated peroxisome proliferation. *Mol. Cell. Biol.* **22**, 8226–8240
201. Tanaka, A., Okumoto, K., and Fujiki, Y. (2003) cDNA cloning and characterization of the third isoform of human peroxin Pex11p. *Biochem. Biophys. Res. Commun.* **300**, 819–823
202. Schrader, M., Bonekamp, N. A., and Islinger, M. (2012) Fission and proliferation of peroxisomes. *Biochim. Biophys. Acta - Mol. Basis Dis.* **1822**, 1343–1357
203. Mizushima, N., and Komatsu, M. (2011) Autophagy: Renovation of Cells and Tissues. *Cell*. **147**, 728–741
204. Kim, P. K., Hailey, D. W., Mullen, R. T., and Lippincott-Schwartz, J. (2008) Ubiquitin signals autophagic degradation of cytosolic proteins and peroxisomes. *Proc. Natl. Acad. Sci.* **105**, 20567–20574
205. Deosaran, E., Larsen, K. B., Hua, R., Sargent, G., Wang, Y., Kim, S., Lamark, T., Jauregui, M., Law, K., Lippincott-Schwartz, J., Brech, A., Johansen, T., and Kim, P. K. (2013) NBR1 acts as an autophagy receptor for peroxisomes. *J. Cell Sci.* **126**, 939–

952

206. Rogov, V., Dötsch, V., Johansen, T., and Kirkin, V. (2014) Interactions between autophagy receptors and ubiquitin-like proteins form the molecular basis for selective autophagy. *Mol. Cell*. **53**, 167–178
207. Yamashita, S., Abe, K., Tatemichi, Y., and Fujiki, Y. (2014) The membrane peroxin PEX3 induces peroxisome-ubiquitination-linked pexophagy. *Autophagy*. **10**, 1549–1564
208. Nuttall, J. M., Motley, A. M., and Hettema, E. H. (2014) Deficiency of the exportomer components Pex1, Pex6, and Pex15 causes enhanced pexophagy in Saccharomyces cerevisiae. *Autophagy*. **10**, 835–845
209. Law, K. B., Bronte-Tinkew, D., Di Pietro, E., Snowden, A., Jones, R. O., Moser, A., Brumell, J. H., Braverman, N., and Kim, P. K. (2017) The Peroxisomal AAA ATPase Complex Prevents Pexophagy and Development of Peroxisome Biogenesis Disorders. *Autophagy*. **13**, 868–884
210. McNew, J. A., and Goodman, J. M. (1994) An oligomeric protein is imported into peroxisomes in vivo. *J. Cell Biol.* **127**, 1245–1257
211. Gouveia, A. M. M., Reguenga, C., Oliveira, M. E. M., Sa-Miranda, C., and Azevedo, J. E. (2000) Characterization of peroxisomal Pex5p from rat liver: Pex5p in the Pex5p-Pex14p membrane complex is a transmembrane protein. *J. Biol. Chem.* **275**, 32444–32451
212. Erdmann, R., and Schliebs, W. (2005) Peroxisomal matrix protein import: the transient pore model. *Nat. Rev. Mol. cell Biol.* **6**, 738–742
213. Meinecke, M., Bartsch, P., and Wagner, R. (2016) Peroxisomal protein import pores. *Biochim. Biophys. Acta - Mol. Cell Res.* **1863**, 821–827
214. Dammai, V., and Subramani, S. (2001) The human peroxisomal targeting signal receptor, Pex5p, is translocated into the peroxisomal matrix and recycled to the cytosol. *Cell*. **105**, 187–196
215. Pedrosa, A. G. (2016) *The peroxisomal protein import machinery: a functional study of the N-terminal half of PEX5*. Ph.D. thesis, Universidade do Porto
216. Sanz-Barrio, R., Fernández-San Millán, A., Carballeda, J., Corral-Martínez, P., Seguí-Simarro, J. M., and Farran, I. (2012) Chaperone-like properties of tobacco plastid thioredoxins f and m. *J. Exp. Bot.* **63**, 365–379
217. Buchner, J., Grallert, H., and Jakob, U. (1998) Analysis of chaperone function using citrate synthase as nonnative substrate protein. *Methods Enzymol.* **290**, 323–338
218. Kolb, V. A., Makeyev, E. V, and Spirin, A. S. (1994) Folding of firefly luciferase during translation in a cell-free system. *EMBO J.* **13**, 3631–3637
219. Hershko, A., and Rose, I. A. (1987) Ubiquitin-aldehyde: a general inhibitor of ubiquitin-

recycling processes. *Proc. Natl. Acad. Sci.* **84**, 1829–33

220. Carter, P., Nilsson, B., Burnier, J. P., Burdick, D., and Wells, J. A. (1989) Engineering subtilisin BPN' for site-specific proteolysis. *Proteins*. **6**, 240–248
221. Gattiker, A., Bienvenut, W. V., Bairoch, A., and Gasteiger, E. (2002) FindPept, a tool to identify unmatched masses in peptide mass fingerprinting protein identification. *Proteomics*. **2**, 1435–1444
222. Wojdyr, M. (2010) Fityk: a general-purpose peak fitting program. *J. Appl. Crystallogr.* **43**, 1126–1128
223. Hartl, F. U., Bracher, A., and Hayer-Hartl, M. (2011) Molecular chaperones in protein folding and proteostasis. *Nature*. **475**, 324–332
224. Francisco, T., Dias, A. F., Pedrosa, A. G., Grou, C. P., Rodrigues, T. A., and Azevedo, J. E. (2017) Determining the Topology of Peroxisomal Proteins Using Protease Protection Assays. in *Methods in molecular biology (Clifton, N.J.)*, pp. 27–35, **1595**, 27–35
225. Wiemer, E. A., Nuttley, W. M., Bertolaet, B. L., Li, X., Francke, U., Wheelock, M. J., Anné, U. K., Johnson, K. R., and Subramani, S. (1995) Human peroxisomal targeting signal-1 receptor restores peroxisomal protein import in cells from patients with fatal peroxisomal disorders. *J. Cell Biol.* **130**, 51–65
226. Kerssen, D., Hambruch, E., Klaas, W., Platta, H. W., de Kruijff, B., Erdmann, R., Kunau, W.-H., and Schliebs, W. (2006) Membrane Association of the Cycling Peroxisome Import Receptor Pex5p. *J. Biol. Chem.* **281**, 27003–27015
227. Bottger, G., Barnett, P., Klein, A. T., Kragt, A., Tabak, H. F., and Distel, B. (2000) Saccharomyces cerevisiae PTS1 receptor Pex5p interacts with the SH3 domain of the peroxisomal membrane protein Pex13p in an unconventional, non-PXXP-related manner. *Mol. Biol. Cell*. **11**, 3963–3976
228. Fransen, M., Terlecky, S. R., and Subramani, S. (1998) Identification of a human PTS1 receptor docking protein directly required for peroxisomal protein import. *Proc. Natl. Acad. Sci.* **95**, 8087–8092
229. Urquhart, A. J., Kennedy, D., Gould, S. J., and Crane, D. I. (2000) Interaction of Pex5p, the type 1 peroxisome targeting signal receptor, with the peroxisomal membrane proteins Pex14p and Pex13p. *J. Biol. Chem.* **275**, 4127–4136
230. Will, G. K., Soukupova, M., Hong, X., Erdmann, K. S., Kiel, J. A., Dodt, G., Kunau, W. H., and Erdmann, R. (1999) Identification and characterization of the human orthologue of yeast Pex14p. *Mol. Cell. Biol.* **19**, 2265–2277
231. Fujiki, Y., Hubbard, A. L., Fowler, S., and Lazarow, P. B. (1982) Isolation of intracellular membranes by means of sodium carbonate treatment: application to endoplasmic reticulum. *J. Cell Biol.* **93**, 97–102

232. Celedon, J. M., and Cline, K. (2012) Stoichiometry for binding and transport by the twin arginine translocation system. *J. Cell Biol.* **197**, 523–534
233. Hartl, F. U., Just, W. W., Köster, A., and Schimassek, H. (1985) Improved isolation and purification of rat liver peroxisomes by combined rate zonal and equilibrium density centrifugation. *Arch. Biochem. Biophys.* **237**, 124–134
234. Beck, M., and Hurt, E. (2017) The nuclear pore complex: understanding its function through structural insight. *Nat. Rev. Mol. Cell Biol.* **18**, 73–89
235. Korotkov, K. V, Sandkvist, M., and Hol, W. G. J. (2012) The type II secretion system: biogenesis, molecular architecture and mechanism. *Nat. Rev. Microbiol.* **10**, 336–351
236. Fronzes, R., Christie, P. J., and Waksman, G. (2009) The structural biology of type IV secretion systems. *Nat. Rev. Microbiol.* **7**, 703–714
237. Berks, B. C. (2015) The twin-arginine protein translocation pathway. *Annu. Rev. Biochem.* **84**, 843–864
238. Dal Peraro, M., and van der Goot, F. G. (2016) Pore-forming toxins: ancient, but never really out of fashion. *Nat. Rev. Microbiol.* **14**, 77–92
239. Tompa, P., and Fuxreiter, M. (2008) Fuzzy complexes: polymorphism and structural disorder in protein-protein interactions. *Trends Biochem. Sci.* **33**, 2–8
240. Sharma, R., Raduly, Z., Miskei, M., and Fuxreiter, M. (2015) Fuzzy complexes: Specific binding without complete folding. *FEBS Lett.* **589**, 2533–2542
241. Li, Romero, Rani, Dunker, and Obradovic (1999) Predicting Protein Disorder for N-, C-, and Internal Regions. *Genome Inform. Ser. Workshop Genome Inform.* **10**, 30–40